DEVELOPMENT OF AN ACCELERATED

STRESS-CORROSION TEST FOR

FERROUS AND NICKEL ALLOYS

NOR 68-58

FINAL SUMMARY REPORT
Covering the Period March 1966 to March 1968

APRIL 1968

Prepared for

NATIONAL AERONAUTICS AND SPACE ADMINISTRATION
GEORGE C. MARSHALL SPACE FLIGHT CENTER
HUNTSVILLE, ALABAMA 35812

CONTRACT NUMBER NAS 8-20333

CONTROL NUMBER DCM 1-7-54-20097(1F)

Northrop Corporation, Norair Division
3901 West Broadway,
Hawthorne, California 90250
Research and Technology Section
A. H. Freedman (Author)

COPY NO 17

DEVELOPMENT OF AN ACCELERATED

STRESS-CORROSION TEST FOR

FERROUS AND NICKEL ALLOYS

NOR 68-58

FINAL SUMMARY REPORT
Covering the Period March 1966 to March 1968

APRIL 1968

Prepared for

NATIONAL AERONAUTICS AND SPACE ADMINISTRATION
GEORGE C. MARSHALL SPACE FLIGHT CENTER
HUNTSVILLE, ALABAMA 35812

CONTRACT NUMBER NAS 8-20333

CONTROL NUMBER DCM 1-7-54-20097(1F)

Northrop Corporation, Norair Division
3901 West Broadway,
Hawthorne, California 90250
Research and Technology Section
A. H. Freedman (Author)

FOREWORD

This report was prepared by Northrop Norair under Contract NAS 8-20333, Development of an Accelerated Stress-Corrosion Test for Ferrous and Nickel Alloys, for the George C. Marshall Space Flight Center of the National Aeronautics and Space Administration. The work was administered under the technical direction of the Propulsion and Vehicle Engineering Laboratory, Materials Division of the George C. Marshall Space Flight Center, with Mr. T. S. Humphries acting as Project Manager.

This program was performed at Northrop Norair during the period March 1966 to March 1968. Mr. A. H. Freedman served as Principal Investigator, except for a period from 17 March through 31 October 1967 when Mr. L. H. Stone served as Principal Investigator. Additional Northrop personnel who made contributions to the effort described in this report include Messrs. H. E. Langman, H. R. Miller, R. E. Herfert, G. A. Blake, H. B. Howell, K. C. Wu, T. A. Krinke, J. Lewis, W. E. Nordling, and F. O. Flower; Dr. R. E. Lowrie and Mr. B. G. Calfin assisted in preparing the report.

This report has been assigned Northrop number NOR-68-58 for internal control.

This annual summary report has been reviewed and is approved.

E. B. Mikus

Dr. E. B. Mikus
Chief, Materials Research Group

ABSTRACT

A simple, accelerated, laboratory test for evaluating the stress-corrosion susceptibility of a ferrous or nickel-base alloy has been developed in this program. Single-edge-notched and fatigue-cracked specimens are tension loaded in a NaCl solution (200gm/liter distilled water), and the threshold stress intensity for stress corrosion (K_{ISCC}) is determined. Identical specimens were tension loaded in racks exposed at the seacoast, and their K_{ISCC} values were measured to act as standards for evaluating the accelerated test.

The materials investigated were Inconel 718 and the following steels in one or more conditions of heat treatment: H-11 (air melted and vacuum melted), 4340, AM355, 18Ni Maraging (250 grade), 410SS, 304SS, and 17-4PH. Weld fusion zones and synthetic heat-affected zones of the 4340, AM355, and 18Ni Maraging steels were also tested. A specimen thickness of 1/4 inch was adequate to maintain plane-strain loading at the threshold stress intensity for stress corrosion except for Inconel 718, 304SS, 17-4PH (H1150), and 410SS (1125F).

The accelerated test requires a maximum test time of 1000 hours. Test times are one to three orders of magnitude shorter than those required for similar specimens in a seacoast environment. The acceleration of test time is produced by the aggressive corrodent, the presence of a crack, and the plane-strain loading conditions.

Twenty of the twenty-three combinations of material, heat treatment, and welding conditions that were tested showed good-to-excellent agreement between the K_{ISCC} values obtained in seacoast and in accelerated tests. For H-11(AM) 1000F and 4340 800F the accelerated test is more severe than seacoast exposure and, therefore, conservative. Only AM355 SCT850(FH) has an appreciably lower K_{ISCC} for seacoast tests than is found by the accelerated test. AM355 in three other conditions of heat treatment gave good-to-excellent agreement between the two types of test.

TABLE OF CONTENTS

LIST OF TABLES

LIST OF ILLUSTRATIONS

LIST OF ILLUSTRATIONS
(Continued)

INTRODUCTION

In general, stress-corrosion susceptibility of ferrous and nickel alloys increases with increasing strength levels. As structural applications for the high-strength alloys increase, greater attention to attendant stress-corrosion problems is needed. Since there presently are no reliable, accelerated, stress-corrosion test methods that correlate laboratory results with the behavior of these materials in a natural atmospheric environment, the purpose of this program was to develop a relatively simple, standard, accelerated laboratory test for evaluating stress corrosion susceptibility of ferrous and nickel alloys in a seacoast environment.

Many stress-corrosion test approaches have used smooth, self-stressed specimens that required long test times and produced test results exhibiting a high degree of scatter. Two prime disadvantages are inherent in these test methods. First, it is difficult to accurately define the stress changes produced during crack initiation and growth in self-stressed specimens. Second, smooth specimens that are stress-corrosion tested to failure provide a conglomerate measurement without distinguishing between the three independent stages of specimen deterioration:

Stage 1 - Crack initiation on the surface through general corrosion, pitting, and/or material defects;
Stage 2 - Crack growth by "environmental cracking;"
Stage 3 - Overload or fast fracture related to the fracture toughness of the specific material.

The initiation of stress corrosion (Stage 1) in a smooth specimen generally requires pit formation. However, Brown[1] has shown that a titanium alloy was immune to surface pitting in salt water and that smooth specimens did not fail by stress corrosion. Introduction of an artificial pit (fatigue crack) produced rapid failure. Thus, in cases where pit formation is required for stress corrosion to initiate, pit formation may be as much as a million times slower than crack growth by environmental cracking. Failure times for smooth-specimen tests, therefore, are highly weighted in terms of pitting susceptibility (Stage 1).

If one alloy exhibits lower toughness than another, a small stress-corrosion crack may cause failure in the lower-toughness material, while a large crack may be required to cause failure in the higher-toughness material. Thus, the tougher alloy may require a longer time to fail - not because of a slower rate of stress-corrosion cracking but because of the ability of the alloy to withstand a longer stress-corrosion crack. Test results based upon failure times of smooth specimens do not differentiate between the combined effects on failure time of fracture toughness and stress-corrosion behavior.

To solve many of these problems, a single-edge-notched and fatigue-cracked coupon was selected as the standard stress-corrosion test specimen for this program. Some work was also performed using a fatigue-cracked wedge-opening-loading (WOL) specimen[2]. In both cases, the presence of a fatigue crack eliminated the time-consuming crack-initiation process (Stage 1) as a dependent variable and also permitted use of fracture mechanics concepts.

The threshold stress intensity (K_{ISCC}) required to produce crack growth by stress corrosion may be determined experimentally. This value, which depends only on Stage 2, is the most meaningful and important because crack growth and fracture will not occur below this value. The stress-corrosion susceptibility can be rated by the ratio of K_{ISCC} to plane-strain fracture toughness (K_{Ic}) to normalize differences in toughness of various alloys. At stress intensities above K_{ISCC}, stress-corrosion crack growth and fracture can occur. However, by relating the applied stress intensity (K_{Ii}) to the plane-strain fracture toughness of each material, differences in toughness of various alloys may be normalized, and Stage 3 is still eliminated as a dependent variable in a stress-corrosion test. In other words, alloys of different fracture toughness will require the same amount of crack growth to produce failure when loaded to the same ratio of K_{Ii}/K_{Ic}. Thus, failure times are a direct measure of stress-corrosion crack growth.

Dead-weight loading was selected (1) to permit accurately defined stresses and (2) to produce increased stress intensities during crack growth, thereby increasing crack-growth rates. A controlled laboratory environment of NaCl solution (200 gm NaCl/liter of distilled water) was used to accelerate stress-corrosion testing in a simulated seacoast environment. This corrodent was selected as most appropriate based on screening tests conducted during the first year of effort[3]. The following alloys and heat treatments were studied:

1. H-11 (Air Melted)

   280-300 ksi (tempered at 1000F)
   220-240 ksi (tempered at 1100F)

2. H-11 (Vacuum Melted)

   280-300 ksi (tempered at 1000F)

3. 4340

   260-280 ksi (tempered at 475F)
   200-220 ksi (tempered at 800F)

4. 18Ni Maraging steel (250 grade)

   Aged at 900F

5. 410SS

   Tempered at 650F
   Tempered at 1125F

6. 17-4PH

   H900
   H1150

7. <u>AM355</u>

SCT850
SCT850 Fully Hardened

SCT1000
SCT1000 Fully Hardened

8. <u>304SS</u>

Annealed
Sensitized 100 hours at 1100F

9. <u>Inconel 718</u>

Solution annealed and aged

Three materials were selected for determining the effect of welding on stress-corrosion susceptibility and the suitability of the accelerated test for evaluating it. These were 4340 tempered at 475F, 18Ni Maraging steel aged at 900F, and AM355 heat treated to the SCT850 (fully hardened) condition. These alloys were selected to represent three distinctly different matrices, each requiring very different welding and heat-treating sequences.

MATERIALS

All of the program alloys except AM355 were procured in the form of 1/4-inch plate. The AM355, which was only available in plate of 1-1/8-inch thickness, was band-sawed to provide 1/4-inch-thick slabs. Vendor-supplied chemical analyses for all materials except AM355 are recorded in Table 1.

The corrodent used in this investigation was prepared from reagent-grade NaCl.

TABLE I

ALLOY CHEMICAL ANALYSES(1)

MATERIAL	PRODUCER	HEAT	ELEMENT - PERCENT									As Noted					
			C	Mn	P	S	Si	Ni	Cr	Cu	Mo						
H-11 (Air Melt)	Vanadium Pacific	34251	0.37	0.30	0.009	0.006	0.91		4.95		1.33					V 0.49	
H-11 (Vacuum Melt)	Vanadium Pacific	02528	0.38	0.36	0.009	0.009	0.92		4.99		1.39					V 0.52	
4340	Armco	59773	0.39	0.75	0.012	0.013	0.35	1.74	0.89		0.26						
18Ni-250	Vanadium Pacific	09821	0.015	0.08	0.004	0.007	0.05	18.10			4.78	Al 0.05	Ti 0.37	Co 7.52	B 0.004	Ca 0.05	Zr 0.013
410 SS	Republic	3330239	0.136	0.53	0.021	0.009	0.39	0.20	12.25	0.19	0.06	Al 0.03	Sn 0.018	N 0.025			
17-4PH	Republic	3343353	0.045	0.04	0.020	0.009	0.60	4.31	15.72	3.40							
304 SS	Republic	3341069	0.067	1.83	0.022	0.007	0.52	9.07	18.26	0.20	0.34			Co 0.14			
Inconel 718	Cameron	50284	0.05	0.11	0.006	0.004	0.20	52.42	18.50	0.04	3.12	Al 0.60	Ti 0.85	Co 0.10	B 0.004		Cb & Ta 5.46

(1) Vendor-supplied.

PROCEDURES

SPECIMEN PREPARATION

Parent Materials

The transverse single-edge-notched and fatigue-cracked tension specimen, shown in Figure 1, was used for stress-corrosion tests. This specimen configuration approximated design recommendations of Srawley and Brown[4] and Payne[5] for plane-strain fracture-toughness tests. Side-notched specimens were employed for materials that exhibited more than approximately 15 percent shear when they were tensile tested without side notches.

Procedures for machining, heat treating, and fatigue cracking these specimens are summarized in Appendix A for each material. All specimens were solvent-degreased before fatiguing, and specimen cleanliness was maintained during operations preceding stress-corrosion testing. Specimens prepared earlier in the program were fatigue cracked on a Baldwin-Sonntag Model SF-4 fatigue machine that operated at 3600 cycles per minute. Later specimens were fatigue cracked on a Baldwin-Sonntag Model SF-1U fatigue machine that operated at 1800 cycles per minute. Slightly different loads were sometimes used for the same material on these two machines for reasons of experimental convenience.

A transit was used to measure fatigue-crack lengths. In the case of the side-notched specimens, it was necessary to sandblast the notches to provide suitable matte surfaces for tracking the fatigue cracks. All fatigue-cracked specimens were stored in a dessicator prior to stress-corrosion testing.

A limited number of stress-corrosion tests were conducted using wedge-opening-loading (WOL) specimens of the IT type. The specimens of AM355 were cut from the same 1 1/8-inch plate from which the 1/4-inch thick, single-edge-notched specimens were machined. The same heat treating parameters were used to attain the SCT1000 condition (Appendix A) except that the thicker WOL blanks were oil-quenched from the austenite conditioning temperature whereas the single-edge-notched specimens were cooled in air or argon.

The WOL specimens were machined to the configuration shown in Figure 2, which closely approximated the specimen configuration developed by Westinghouse Research Laboratories[2], with two exceptions. The slot width was increased from 0.0938 to 0.156 inch, and the notch geometry was modified slightly because of the difficulty in machining AM355.

Transverse tensile specimens were prepared to qualify materials and heat treatments. These specimens were nominally 1/4-inch thick with a gage length of 2 inches and a width of 1/2-inch at the reduced section. The machining and heat treatment procedures for these specimens were the same as outlined in Appendix A for single-edge-notched stress-corrosion specimens.

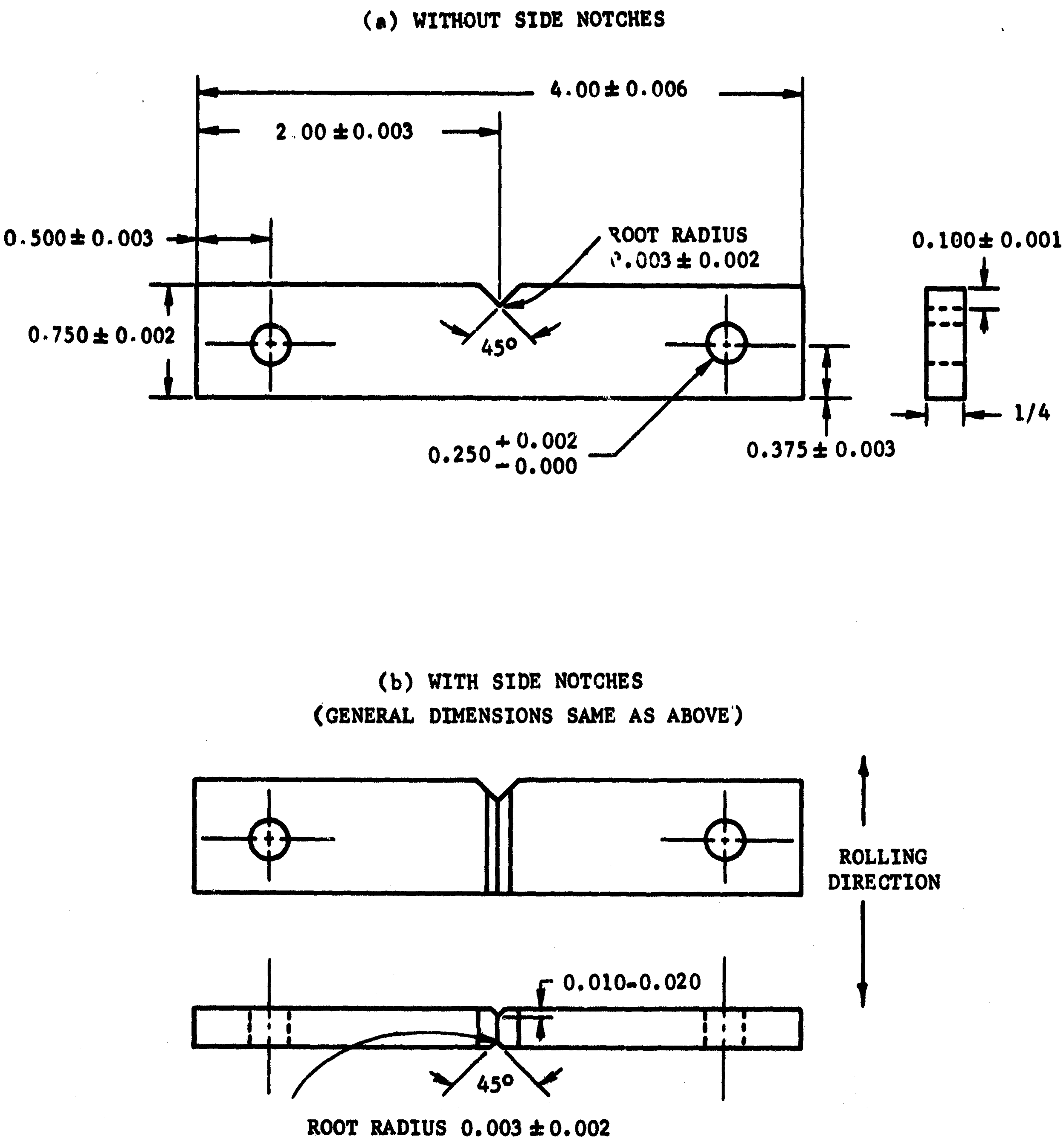

NOTE: ALL DIMENSIONS IN INCHES

FIGURE 1 SINGLE-EDGE-NOTCHED STRESS-CORROSION SPECIMENS

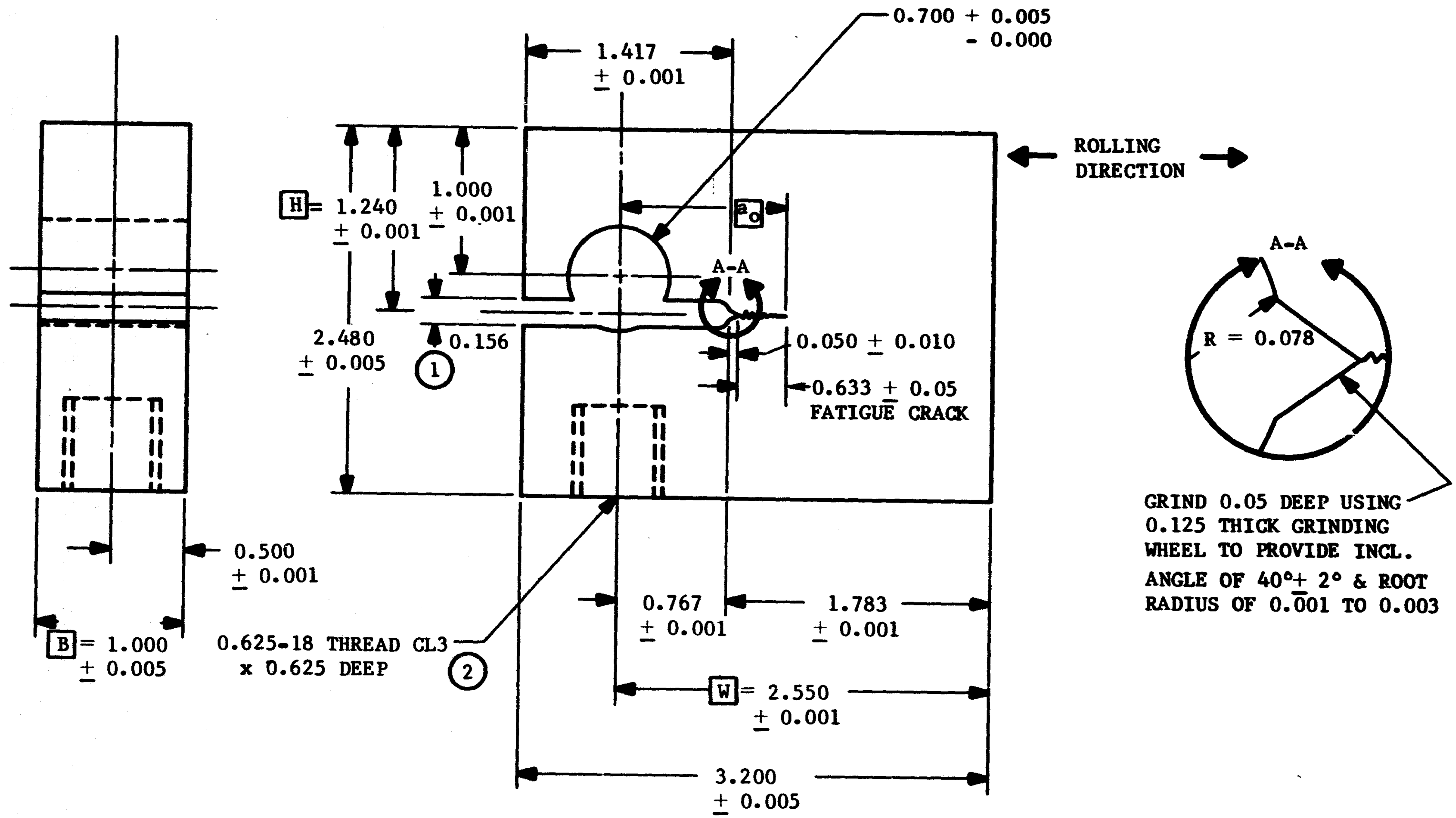

NOTES

1. BORE & SLOT ⊥ TO THREADS AND FACE WITHIN 0.001
2. ℄ OF THREAD MUST COINCIDE WITH ℄ OF BORE WITHIN 0.001

FIGURE 2 1T-TYPE WEDGE-OPENING-LOADING (WOL) SPECIMEN

Weldments

The materials selected for development of an accelerated stress-corrosion test for weldments were 18Ni Maraging steel (aged 3 hours at 900F), 4340 (475F temper), and AM355 (SCT850 fully hardened). Both fusion zones and heat-affected zones were studied. Fusion zones were produced by welding together two plates 16 x 4 x 1/4 inches using the automatic TIG process and the welding parameters shown in Table II. Fusion-zone specimens geometrically identical to parent-material specimens (Figure 1) were cut from the plates after weld quality was established by x-ray. The edge notch on each specimen was located in the center of the fusion zone so that the fatigue crack and subsequent stress-corrosion crack grew in a constant fusion-zone microstructure. Detailed preparation procedures, summarized in Appendix A, closely paralleled those used for parent materials.

Transverse, synthetic, heat-affected-zone specimens were produced using a time-temperature simulator (Gleeble) that could reproduce the time-temperature cycle at any point in a heat-affected zone. Various peak temperatures were produced using heating and cooling rates typical for 3/8-inch-thick plate. The test specimens were geometrically identical to parent-material specimens (Figure 1). The edge notch in each specimen was located in the center of the heat-affected zone so that the fatigue crack and subsequent stress-corrosion crack grew in a region of constant and well-defined microstructure resulting from a known thermal cycle. Detailed preparation procedures, summarized in Appendix A, closely paralleled those used for parent materials and fusion zones.

Charpy Specimens

Sub-size Charpy V-notch blanks of 18Ni Maraging steel, 4340, and AM355 were prepared and thermal cycled in the Gleeble to produce various synthetic-heat-affected zones. Specimen preparation procedures followed those used for stress-corrosion specimens of synthetic, heat-affected zones.

Curves of impact energy versus peak temperature attained in the Gleeble cycle were obtained at room temperature for AM355 SCT850(FH) and 18Ni Maraging steel (aged 3 hours at 900F) and at 320F for 4340 (475F temper). Fractured impact specimens were examined metallographically to reveal the change in microstructure produced by various thermal cycles.

SEACOAST STRESS-CORROSION TESTS

Stress-corrosion tests were conducted in a seacoast environment to provide information for establishing the validity of laboratory test data. The test site was provided by the Los Angeles Department of Water and Power, adjacent to the Scattergood Steam Plant, approximately 100 yards from the Pacific Ocean shoreline at Playa del Rey, California. Tests were conducted in a dead-weight, lever-arm loading fixture employing a lever arm ratio of 24.4 to 1. This fixture, shown in Figure 3, consisted of six load trains, each with a capacity for eight specimens. Strain-gage load-cell calibrations showed that actual loads were within $\pm$ 1.6 percent of calculated loads. All clevises in

TABLE II

AUTOMATIC TIG WELDING PARAMETERS

BASE ALLOY	HEAD TRAVEL (inch per min)	CURRENT (amps)	VOLTAGE	He GAS FLOW (cfh)			ELECTRODE		HOLD DOWN		FILLER WIRE			BACKUP MATERIAL	PREHEAT	POSTHEAT	NUMBER OF PASSES
				TORCH	TRAILING	BACKUP	DIAMETER (inch)	GEOMETRY (inch)	SPACING (inch)	PRESSURE (psi)	TYPE	DIA-METER (inch)	FEED (inch per min)				
18Ni-250	15	315	16.5	60	None	15	1/8	5° Taper 1/16 Radius	0.600	105-110	18Ni	1/16	7.5	Copper	None	None	One/Side
4340	8	280	15	60	None	15	1/8	5° Taper 1/16 Radius	0.600	105-110	4340	1/16	7	Copper	400-500F	700F 1 Hour	One/Side
AM355	6	310	14.5	60	None	15	1/8	5° Taper 1/16 Radius	0.600	105-110	AM355	1/16	4	Copper	None	None	One/Side

JOINT DESIGN:

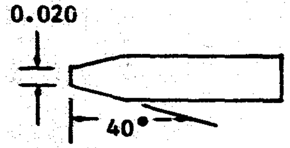

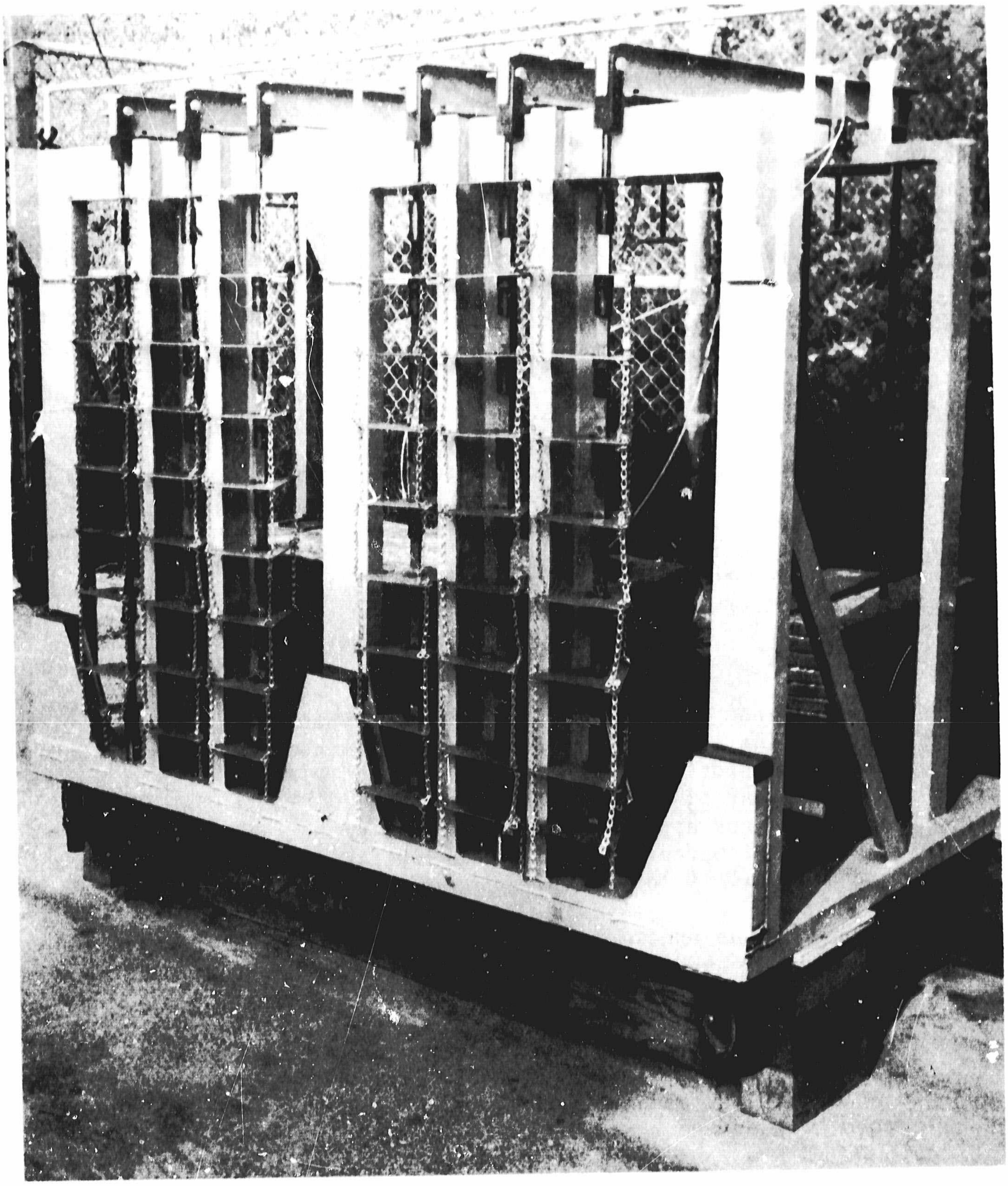

FIGURE 3 LOADING FIXTURE FOR SEACOAST STRESS-CORROSION TESTS

each load train were made of 17-4PH alloy in the H900 condition. Shear pins for holding specimens in the clevices were made of 18Ni Maraging steel (280 grade). Each lever arm was equipped with a timer and microswitch system to record specimen failure time.

The rig was inspected at least weekly. Any broken specimen was removed, and the train that had contained it was reloaded. The time that specimens were not under load was not recorded by the timer. Such time is not believed to have had any effect on the stress-corrosion threshold. A triangular plate of 321 stainless steel was pinned to each clevice, and a chain system connected the plates so that each load train was supported, though unloaded, when a specimen failed. The test rig was positioned so that the front of the unit faced the ocean. Each specimen was positioned within the fixture so that one face was exposed to the ocean.

ACCELERATED STRESS-CORROSION TESTS

A typical specimen-and-corrodent-container assembly for aqueous, accelerated, stress-corrosion tests is shown in Figure 4. The stainless steel container was coated with General Electric RTV-11 silicone rubber cured with Thermolite 12 (dibutyl tin dilaurate) during a cure cycle of two hours at 350F. The coating was applied to prevent galvanic attack as well as stray solution potentials between container and specimen. Some of these containers were equipped with annular immersion heaters and temperature control thermostats, which were also coated.

The bottom of each container was slotted so that the specimen could be extended through the slot for attachment to the loading clevice. Corrodent leakage around the slot was prevented by potting. The potting procedure used during the first year of effort[3] was modified to eliminate bond-line degradation and leakage after approximately 400 hours of test time on specimens of 4340, H-11, and 18Ni Maraging steel. The modified potting technique outlined below worked effectively for all program materials.

1. One end of the specimen was coated with General Electric primer #SS4155 or #SS4004 and air dried for 1.5 hours minimum at room temperature.

2. The coated specimen end was placed in the slot of a can, and a fillet of General Electric RTV-77 resin was applied around the slot area. The assembly was cured for 12 hours at room temperature to bond the specimen firmly to the can.

3. The RTV-77 resin was coated with a thin layer of Turco 4472 neoprene rubber and air dried at room temperature.

Each container was covered with a stainless steel lid, which was sometimes taped to the container. The lid minimized water evaporation and also the splashing of the corrodent when a specimen fractured. Figure 5 shows a typical container assembly positioned in the same type of test fixture as that used for seacoast tests. The triangular stainless steel plate pinned to the clevice supported the container assembly and minimized stresses on the potting compound.

FIGURE 4 CONTAINER ASSEMBLY FOR ACCELERATED STRESS-CORROSION TESTS

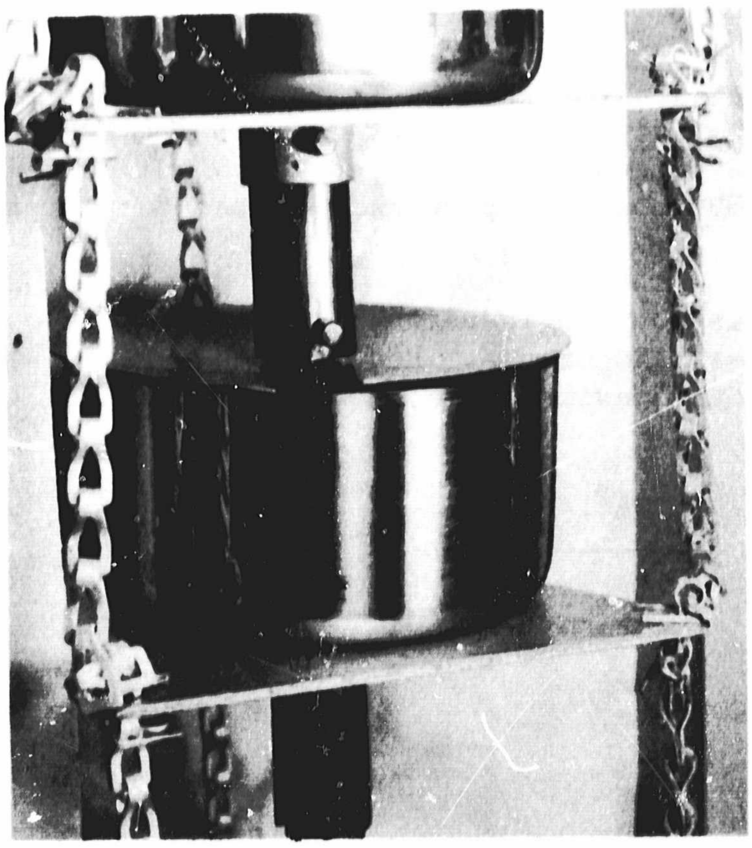

FIGURE 5 CONTAINER ASSEMBLY POSITIONED IN LOADING FIXTURE

During the second year of effort, stress-corrosion testing was conducted using the procedure shown below.

1. The specimen was placed in the stress-corrosion fixture under no-load conditions.

2. An eye-dropper was used to place the NaCl solution in the notch of the specimen.

3. The specimen was loaded to the desired stress or stress intensity.

4. The container was filled with the NaCl solution 10 minutes after Step 3 was completed. The 10-minute delay was necessary to allow the salt-water solution to expel air from the crack.

5. Once each week the corrodent was siphoned from each container and immediately replaced by fresh solution.

This procedure was a modification of the procedure used during the first year of effort[3], where the specimen was stressed before introducing the corrodent. The modified procedure was more desirable because it reduced the possibility of blunting the crack tip by creep, which could increase failure times.

STRESS AND STRESS-INTENSITY CALCULATIONS

The specimen width W and thickness B were measured with a micrometer before testing. Based on these and rough measurements of fatigue-crack length and side-notch depth (when present), specimens were loaded to approximately the desired stress intensity. Initial crack length a_o, final crack length a_f, and net-section thickness B_N for side-notched specimens were measured with a toolmakers' microscope after testing. In cases where a crack front was not perfectly straight, an integrated measurement of crack length was made. These accurately determined dimensions were used to calculate values for stress intensity. An IBM 7090 computer program was used to perform calculations rapidly.

Stress intensities for single-notched specimens were calculated from the data of Srawley, Jones, and Gross[6]. Recommended stress intensities in dimensionless form for smooth specimens are shown in Table III; they are plotted in Figure 6 as:

$$\frac{K_I{}^2 W B^2}{P^2} \text{ versus } \frac{a}{W} \, .$$

TABLE III

STRESS-INTENSITY SOLUTION FOR A SINGLE-EDGE-NOTCHED SPECIMEN
(AFTER SRAWLEY, JONES, AND GROSS)

$\frac{a}{W}$	$\frac{K_I^2 W B^2}{P^2}$	$\frac{a}{W}$	$\frac{K_I^2 W B^2}{P^2}$
0	0		
0.01	0.073	0.26	1.878
.02	.140	.27	2.031
.03	.202	.28	2.198
.04	.260	.29	2.378
.05	.314	.30	2.571
0.06	0.366	0.31	2.780
.07	.415	.32	3.004
.08	.462	.33	3.245
.09	.510	.34	3.501
.10	.556	.35	3.775
0.11	0.605	0.36	4.069
.12	.653	.37	4.380
.13	.705	.38	4.711
.14	.758	.39	5.064
.15	.816	.40	5.436
0.16	0.877	0.41	5.830
.17	.944	.42	6.248
.18	1.016	.43	6.688
.19	1.094	.44	7.153
.20	1.180	.45	7.641
0.21	1.273	0.46	8.155
.22	1.374	.47	8.695
.23	1.484	.48	9.261
.24	1.604	.49	9.855
.25	1.735	.50	10.477

a = crack length (inches)
W = specimen width (inches)
B = specimen thickness (inches)
P = applied load (pounds)
K_I = plane-strain stress intensity (psi$\sqrt{\text{in}}$)

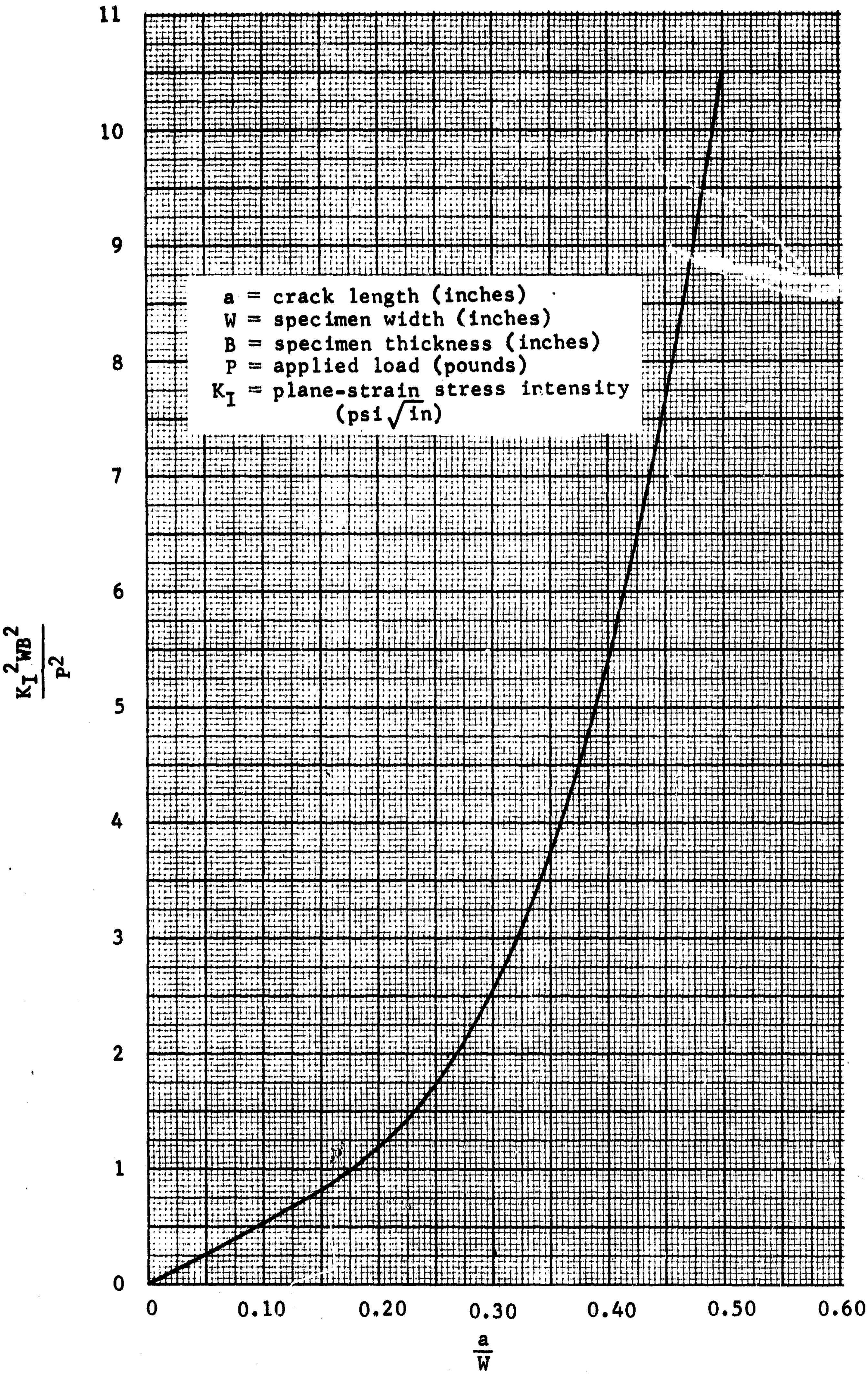

FIGURE 6 STRESS-INTENSITY SOLUTION FOR A SINGLE-EDGE-NOTCHED SPECIMEN (AFTER SRAWLEY, JONES AND GROSS)

Side-notched specimens were treated like smooth specimens to obtain nominal stress intensities (K_{nom}). These values were corrected according to the method of Freed and Kraft[7] as follows:

$$K_I = K_{nom}\left(\frac{B}{B_N}\right)^{0.75} .$$

Since the exponent in this equation may vary between 0.5 and 1.0, depending upon the material, an average of 0.75 was used for this investigation.

Stress intensities for the WOL specimen were calculated from the data of Wilson[8], as shown in Figure 7. It is believed that the modifications in slot width and notch geometry affected the accuracy of this stress-intensity solution by less than five percent.

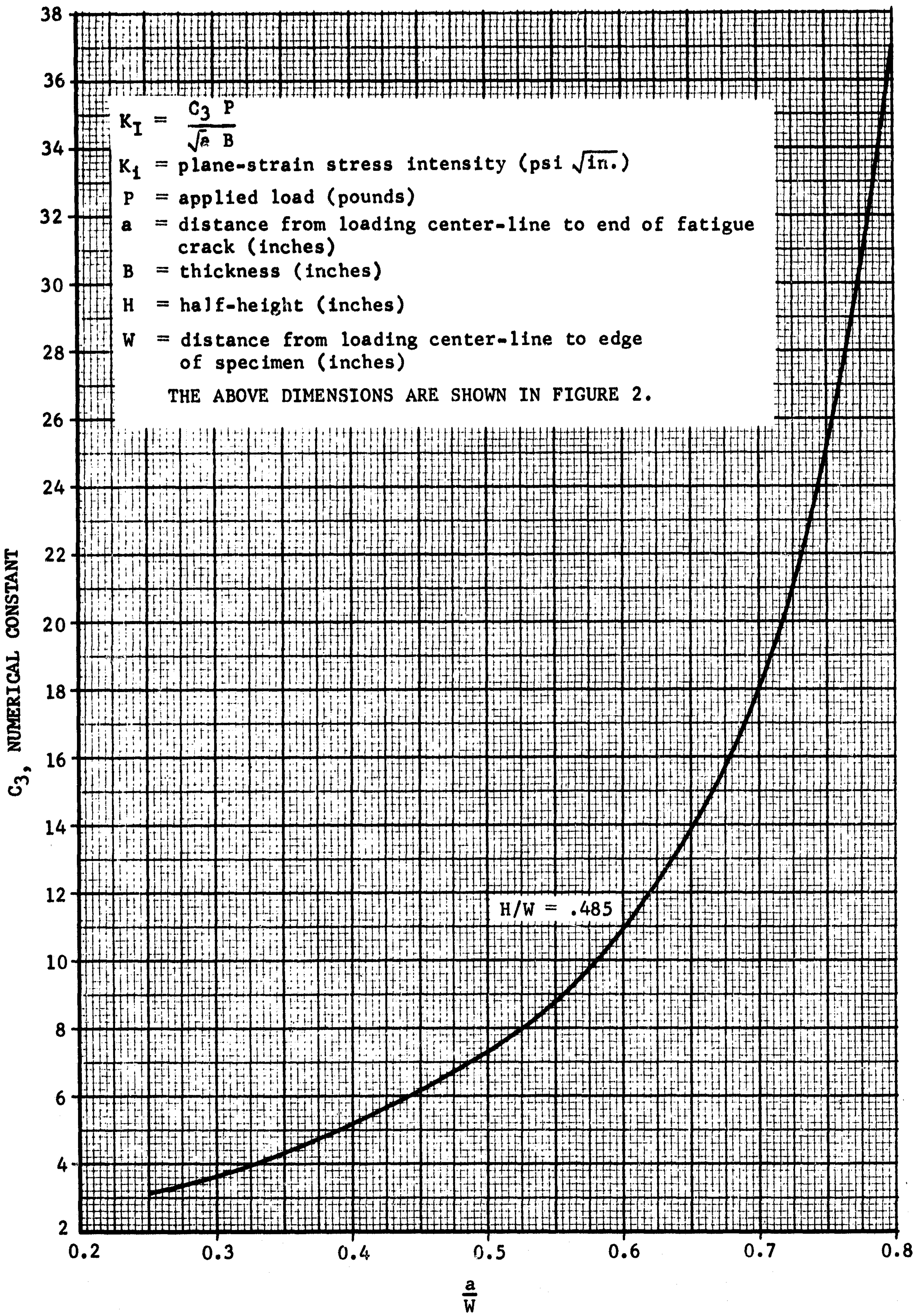

FIGURE 7 STRESS-INTENSITY SOLUTION FOR THE T-TYPE WEDGE-OPENING-LOADING (WOL) SPECIMEN (AFTER WILSON)

RESULTS AND DISCUSSION

MATERIAL QUALIFICATION TESTS

Transverse tensile tests and hardness tests were used to quality most of the materials and heat treatment procedures. As shown in Table IV, results indicated that acceptable mechanical properties were obtained.

DESIGN OF STRESS-CORROSION SPECIMENS

While Brown[1] used a fatigue-cracked cantilever-beam specimen for stress-corrosion testing, a single-edge-notched and fatigue-cracked tension specimen was selected for this program for the following reasons:

1. Tension loading permitted testing of a number of specimens in a single test fixture. The cantilever-beam specimen required a test fixture for each specimen.
2. Tension loading simplified application of corrosive environment to the specimens.
3. The single-edge-notched tension specimens required less material and lower loads than many other types of tension specimens.

The importance of maintaining plane-strain conditions during stress-corrosion testing of high-strength ferrous alloys has been emphasized [1,9]. Therefore, it was important to design specimens of sufficient thickness to assure plane-strain loading. At the inception of this program, the specimen thickness recommended by ASTM[10] for maintaining plane strain was as follows:

$$B \geq 1.3\ (K_{Ic}/\sigma_{ys})^2$$

Where: B = specimen thickness - inch
K_{Ic} = plane-strain fracture toughness - psi$\sqrt{in}$
σ_{ys} = material yield strength - psi

Based upon this criterion, it appeared that a specimen thickness of 1/4 inch would provide plane-strain conditions and reasonable loading requirements for most of the program alloys. During the second year of this program, the ASTM thickness requirement was increased[11] as follows:

$$B \geq 2.5\ (K_{Ic}/\ \sigma_{ys})^2$$

Thus, the 1/4 inch-thick specimens became marginal for a number of program materials. The results of this program are discussed based upon the new ASTM thickness requirement. This thickness requirement is a general guideline, and actual thickness requirements may vary from alloy to alloy.

Single-edge-notched specimens identical to the stress-corrosion specimens were tested to determine plane-strain fracture toughness based upon stress intensity at pop-in (K_{Ic}) and based upon stress intensity at fracture (K_{Ix}).

TABLE IV

MATERIAL QUALIFICATION TESTS (1)

MATERIAL	CONDITION	ULTIMATE TENSILE STRENGTH (ksi)	YIELD STRENGTH AT 0.2% OFFSET (ksi)	PERCENT ELONGATION (%)	YOUNG'S MODULUS X10^6 (psi)	HARDNESS (ROCKWELL)
H-11 (Air Melt)	Tempered, 2 + 2 hrs. at 1000F	300.3	240.0	7.5	30.8	C 55.0
H-11 (Air Melt)	Tempered, 2 + 2 hrs. at 1100F	232.6	199.7	10.0	31.7	C 47.9
4340	Tempered 4 hrs. at 475F	267.2	225.9	7.5	29.5	C 52.0
4340	Tempered 4 hrs. at 800F	204.8	191.4	8.0	30.3	C 44
18Ni Maraging Steel (250 Grade)	Aged 3 hrs. at 900F	269.5	267.0	6.5	28.7	C 51
410 SS	Tempered 2 hrs. at 650F	197.0	174.5	11.0	32.0	C 43
410 SS	Tempered 2 hrs. at 1125F	128.8	110.8	14.0	33.0	C 27
AM355	SCT850	195.9	161.9	12.0	30.5	C 44
AM355	SCT1000	169.4	158.2	12.5	31.4	C 39
17-4PH	H900	202.4	191.6	10.5	29.3	C 45.4
17-4PH	H1150	151.6	148.5	13.8	31.0	C 35.0
304 SS	Annealed	84.0	34.7	60.7	32.0	B 82.3
304 SS	Sensitized 100 hrs. at 1100F	83.9	36.3	58.5	30.7	B 81.0
Inconel 718	1950F AC, 8 hrs. at 1350 + FC to 1200F for total time of 23 hrs.	189.6	167.2	15.5	29.8	C 43.5

(1) Tensile test values represent an average of two transverse tests.

This latter measure of fracture toughness was of value because it was much simpler to measure than the K_{Ic} which required sophisticated instrumentation to detect the load at pop-in. Also, the pop-in load was difficult to detect in some alloys whereas the fracture load was well defined.

Fracture toughness data for parent materials are summarized in Table V. Fracture modes of specimens are included to establish whether flat fractures (zero percent shear) occurred, indicating plane-strain conditions or if shear failures occurred indicating plane-stress conditions. Although some of the specimens required side notches to control the geometry of fatigue crack growth, fracture modes could not be established from side-notched specimens. Accordingly, all fracture modes listed in Table V were obtained from specimens without side notches. The thickness required to maintain plane strain, according to the most recent ASTM recommendations, is also included based upon calculations involving measured K_{Ic} values and the yield strength (σ_{ys}) values of Table IV. In cases where K_{Ic} and yield strength values were not measured, 0.9 K_{Ix} was used as an estimate of K_{Ic}, and literature values of yield strength were used to permit an estimate of thickness requirements for plane strain.

The ASTM thickness recommendation is that required for valid measurement of K_{Ic}, whereas stress-corrosion tests are generally conducted at lower stress intensities. Since specimen thickness was fixed in this program the ASTM thickness equation was rearranged to determine the maximum stress intensity that could be applied in stress-corrosion testing while still maintaining plane-strain conditions according to the following relationship:

$$K_I = \sqrt{\frac{B\,(\sigma_{ys})^2}{2.5}}$$

Where : K_I = maximum allowable initial stress intensity - ksi $\sqrt{in}$
B = specimen thickness - inch
σ_{ys} = material yield strength - psi

These values are included in Table V.

The results in Table V indicate that the specimens can be divided into three general groups as follows:

Group 1 - Specimens within this group essentially maintained plane-strain conditions up to K_{Ix} levels. Thus, fracture toughness as well as threshold stress intensity for stress corrosion (K_{ISCC}) could be determined under plane-strain conditions.

Group 2 - Specimens within this group maintained plane-strain conditions up to relatively high stress intensities but not up to K_{Ic} or K_{Ix} levels. Thus, measured fracture toughness values were approximate and somewhat higher than the true plane-strain fracture toughness values. However, there was excellent potential for obtaining true plane-strain K_{ISCC} values.

TABLE V

FRACTURE TOUGHNESS OF PARENT MATERIALS

MATERIAL AND CONDITION	B or B_N (in)	K_{Ic} (ksi $\sqrt{in}$)	K_{Ix} (ksi $\sqrt{in}$)	FAILURE MODE WITHOUT SIDE NOTCHES (% SHEAR)	(1) B or B_N RECOMMENDED BY ASTM (in)	(2) MAXIMUM ALLOWABLE K_{Ii} (ksi $\sqrt{in}$)
GROUP 1						
H-11(VM) 1000F	B = 0.230	28.5	28.5	0	~0.036	28.5
H-11(AM) 1000F	B = 0.230	27.6	31.9	0	0.033	31.9
H-11(AM) 1100F	B_N = 0.190	52.8	63.6	25	0.175	55.1
4340 475F	B_N = 0.190	43.7	46.6	27	0.094	46.6
17-4 H900	B = 0.250	52.7	55.6	5	0.189	55.6
AM355 SCT850	B = 0.250	38.6	47.8	10	0.142	47.8
AM355 SCT850(FH)	B = 0.250	55.5	62.4	0	~0.294	~51.2
GROUP 2						
4340 800F	B_N = 0.190	62.0	67.1	31	0.263	52.8
18Ni-250 900F	B_N = 0.190	105.0	111.3	65	0.387	73.6
410 650F	B_N = 0.210	-	91.3	60	~0.555	50.4
AM355 SCT1000	B_N = 0.210	-	101.0	65	~0.822	45.8
AM355 SCT1000(FH)	B_N = 0.250	-	117.5	-	~1.110	~50.0
GROUP 3						
410 1125F	B = 0.250	-	94.9	11	~1.488	35.0
17-4 H1150	B_N = 0.210	-	122.0	85	~1.362	42.9
304 SENS	B_N = 0.210	-	68.5	100	~7.220	10.5
304 ANN	B_N = 0.210	-	69.1	100	~8.040	10.0
INCONEL 718 SAA	B_N = 0.170	106.8	131.2	-	1.012	43.6

NOTES: (1) $B \geq 2.5\ (K_{Ic}/\sigma_{ys})^2$

(2) $K_{Ii} = \sqrt{\frac{B(\sigma_{ys})^2}{2.5}}$

B = overall specimen thickness - inch

B_N = net-section thickness of side-notched specimens - inch

K_{Ic} = plane-strain fracture toughness - ksi $\sqrt{in}$

K_{Ix} = stress intensity at fracture - ksi $\sqrt{in}$

K_{Ii} = initial stress intensity - ksi $\sqrt{in}$

σ_{ys} = yield strength - ksi

Group 3 - Specimens within this group maintained plane-strain conditions only at relatively low stress intensities. Thus, measured fracture toughness values were very approximate and substantially higher than the true plane-strain fracture toughness. True plane-strain K_{ISCC} values could not be obtained for these materials.

The failure modes of specimens generally showed increasing amounts of shear from Group 1 to Group 3 (Table V). However, several exceptions were noted. In Goup 1, 4340 475F and H-11 1100F exhibited significant amounts of shear even though specimen thicknesses met the ASTM recommendation for plane strain. In Group 3, the 410 1125F exhibited very little shear even though the specimen thickness was well below the ASTM recommendation for plane strain.

STRESS-CORROSION TESTING OF WELDMENTS

Since welding is frequently used for fabrication of structures, a test method for determining stress-corrosion susceptibility of weldments as well as parent materials is essential for assessing overall behavior of a material in a real structure.

Weldments contain varying microstructures from the fusion zone through the heat-affected zone. A valid stress-corrosion test method must (1) distinguish differences in stress-corrosion behavior as a function of weld microstructure and (2) establish which portion of a weldment is the controlling region with respect to stress corrosion.

The materials selected for development of an accelerated stress-corrosion test for weldments were 4340 (475F temper), 18Ni Maraging steel (aged three hours at 900F), and AM355 (SCT850 fully hardened). These alloys were selected for the following reasons:

1. Each material represents a distinctly different matrix. The 4340 represents a low-alloy medium-carbon martensitic matrix. Maraging steel represents a high-alloy, low-carbon martensitic matrix incorporating a precipitation hardening mechanism. The AM355 is a high-alloy, low-carbon martensitic matrix.

2. Each of these materials generally requires distinctly different welding and heat treating sequences.

Stress-corrosion testing of fusion zones was relatively straight-forward using single-edge-notched specimens similar to those used for parent materials. The only difference was that the fusion zone was located across the center of the specimen so crack growth would occur in a fusion zone of constant microstructure.

Stress-corrosion testing of heat-affected zones was more complicated because of the infinite variety of thermal cycles experienced by various regions in the zone. The problem in selecting thermal cycles for heat-affected-zone specimens was one of identifying which thermal cycles produce significant changes in stress-corrosion susceptibility. Such changes should be revealed in microstructural alterations that could not be predicted from a knowledge of thermal history and the appropriate equilibrium diagram because of the highly dynamic time-temperature conditions produced during welding.

Several investigators[12,13,14] have successfully employed Charpy V-notch and tensile specimens, exposed to representative synthetic heat-affected-zone thermal cycles, to establish the effects of thermal cycles on mechanical properties. Changes in these mechanical properties usually correlate with microstructural alterations and are expected to indicate differences in stress-corrosion susceptibility.

Synthetic heat-affected zones of 4340 steel were produced by exposing annealed specimens to various thermal cycles in a time-temperature controller (Gleeble), followed by reannealing, austentizing, oil quenching, and tempering four hours at 475F. Figure 8 shows that increasing peak temperatures from 1400F to 2500F produced no major effect upon impact strength, hardness, or microstructure.

At temperatures in the 1400F to 1800F range, impact values increased slightly with increasing peak temperatures. At lower peak temperatures within this range, the upper critical temperature was not reached under the dynamic heating conditions employed. Therefore, only partial grain refinement of the ferrite-austenite structure occurred during transformation of the austenite upon cooling. At higher peak temperatures in this range, complete austenization occurred accompanied by a greater degree of grain refinement during cooling. This grain refinement was probably responsible for the slightly higher impact values with peak temperatures approaching 1800F. At peak temperatures above 2000F, impact values decreased slightly with increasing temperature, an effect probably associated with grain coarsening.

Thermal cycles with peak temperatures of 2000F, 2300F, and 2500F were selected for stress-corrosion specimens representing typical microstructures of a heat-affected zone in a 4340 weldment.

Synthetic heat-affected zones of 18Ni Maraging steel were produced by exposing solution-annealed specimens to various thermal cycles followed by aging three hours at 900F. Figure 9 shows the effects of these peak temperatures on Charpy impact energy, microstructure, and hardness. Specimens exposed to a peak temperature of 900F closely approximated the structure and properties of unaffected parent material. The microstructure consisted of a martensitic matrix containing a small amount of retained austenite and some banding. As peak temperatures increased from 900F to 1250F, impact values increased and hardness decreased as a result of austenite reversion. As peak temperatures increased from 1250F to 1400F, the impact values decreased and hardness increased as a result of decreased austenite. The microstructure which experienced a peak temperature of 1400F closely resembled the microstructure of unaffected parent material. The impact strength remained constant from 1400F to 1700F. At peak temperatures from 1700F to 2400F, impact values increased substantially and hardness decreased. These changes reflected a coarsening of the prior austenite grains and the martensite plates.

Based upon these results, thermal cycles with peak temperatures of 1200F, 1400F, and 2400F were selected for stress-corrosion specimens representing typical microstructures of a heat-affected zone in an 18Ni Maraging steel weldment.

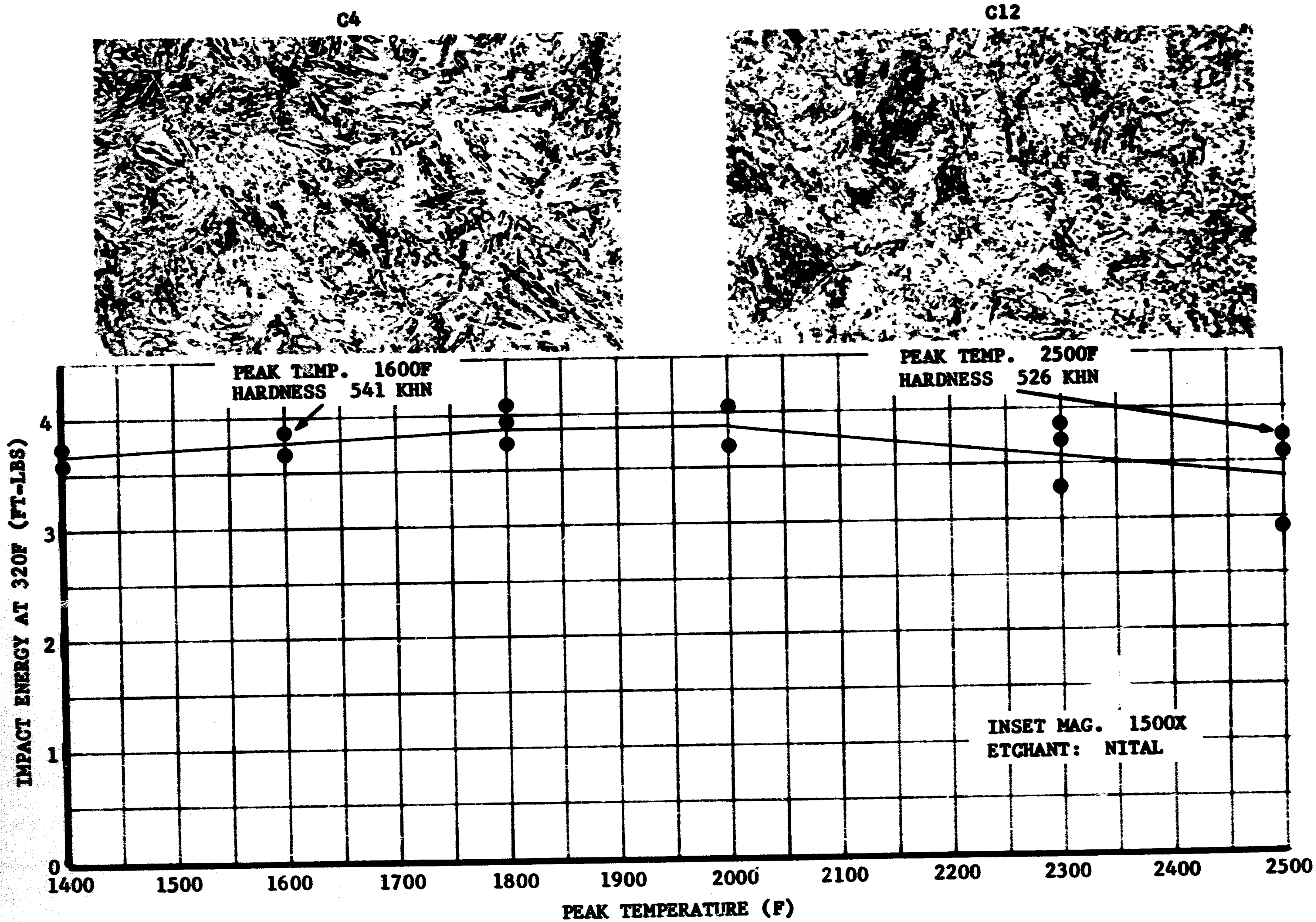

FIGURE 8 CHARPY V-NOTCH IMPACT RESISTANCE OF THE SYNTHETIC HEAT-AFFECTED-ZONE FOR 4340 - 475F TEMPER

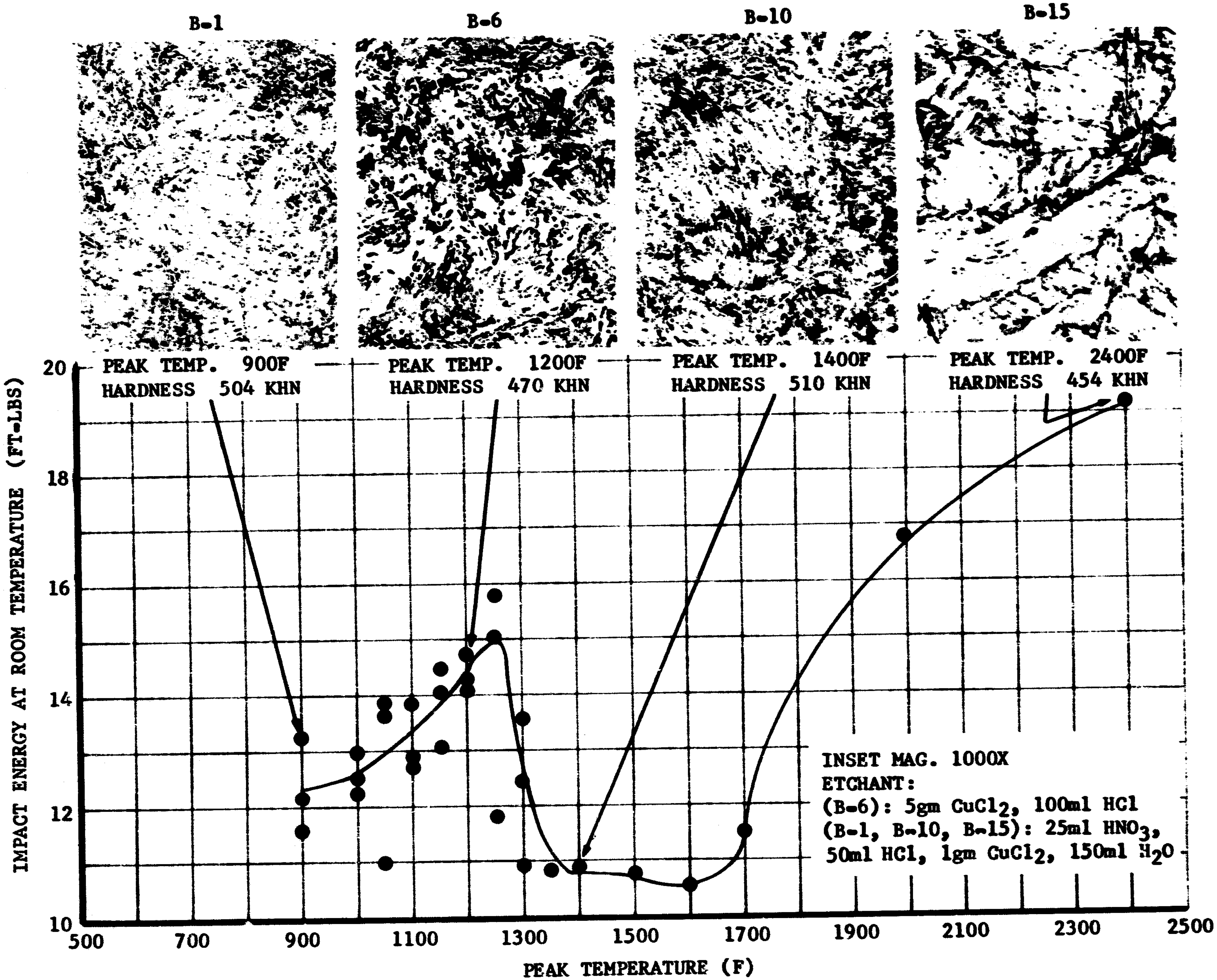

FIGURE 9 CHARPY V-NOTCH IMPACT RESISTANCE OF THE SYNTHETIC HEAT-AFFECTED-ZONE FOR 18Ni-250 MARAGING STEEL

Synthetic heat-affected zones of AM355 were produced by exposing solution-annealed specimens to various thermal cycles followed by heat treating to the fully hardened SCT850 condition as detailed previously in Appendix A. Figure 10 shows the effects of various peak temperatures on impact strength, hardness, and microstructure. Specimens exposed to a peak temperature of 1750F closely approximated the structure and properties of unaffected parent material. The microstructure consisted of a martensitic matrix containing a small amount of delta ferrite. Fine chromium carbides were well dispersed throughout the matrix, and coarse carbides were located predominately at interfaces between martensite and delta ferrite.

At a peak temperature of 1900F, most of the delta ferrite dissolved and a slight trend toward increased impact values was observed. At a peak temperature of 2000F, a significant amount of delta ferrite was re-formed with a corresponding reduction in impact energy. At peak temperatures from 2000F to 2400F, the amount of delta ferrite remained relatively constant, most of the coarse carbides dissolved, and impact values increased.

The microstructure produced by a peak temperature of 2480F consisted of a martensitic matrix with fine, well-dispersed chromium carbides and no delta ferrite. Grain-boundary melting occurred which impeded grain growth and also reduced impact values significantly. The absence or presence of delta ferrite at lower peak temperatures was explainable in terms of the Fe-Cr-Ni phase diagram [15]. However, the complete absence of delta ferrite at a peak temperature of 2480F was unexpected and is not yet understood.

Based upon these results, thermal cycles with peak temperatures of 2000F, 2400F, and 2480F were selected for stress-corrosion specimens representing typical microstructures of a heat-affected zone in an AM355 weldment.

Metallographic analysis, Charpy V-notch impact tests, and to a lesser extent, hardness measurements were helpful in establishing representative microstructural changes occurring across heat-affected zones in 18Ni Maraging steel, 4340, and AM355. For all three alloys, impact tests as a function of peak temperatures provided the best measure of microstructural changes. Metallographic analysis provided an insight into the specific microstructural changes responsible for changes in impact values. Hardness data provided the least sensitive measure of microstructural changes. In the case of 18Ni Maraging steel, hardness values were helpful, but for AM355, the hardness values were insensitive to changes in microstructure.

Fracture-toughness data for fusion zones and synthetic heat-affected zones are summarized in Table VI along with parent-material data for comparison. The thickness required to maintain plane strain and the maximum allowable stress intensity at which plane strain is maintained for the specimen thicknesses employed are also included. These values were calculated using yield strengths estimated from hardness measurements and the K_{Ic} values determined experimentally. In cases where a K_{Ic} value was not obtained, 0.9 K_{Ix} was used as an estimate of K_{Ic}.

All of the 4340 and AM355 specimens were essentially in a "Group 1" category, maintaining plane-strain conditions up to K_{Ix} levels. Thus, fracture toughness as well as threshold stress intensity for stress corrosion could be determined under plane-strain conditions. The 18Ni Maraging steel specimens

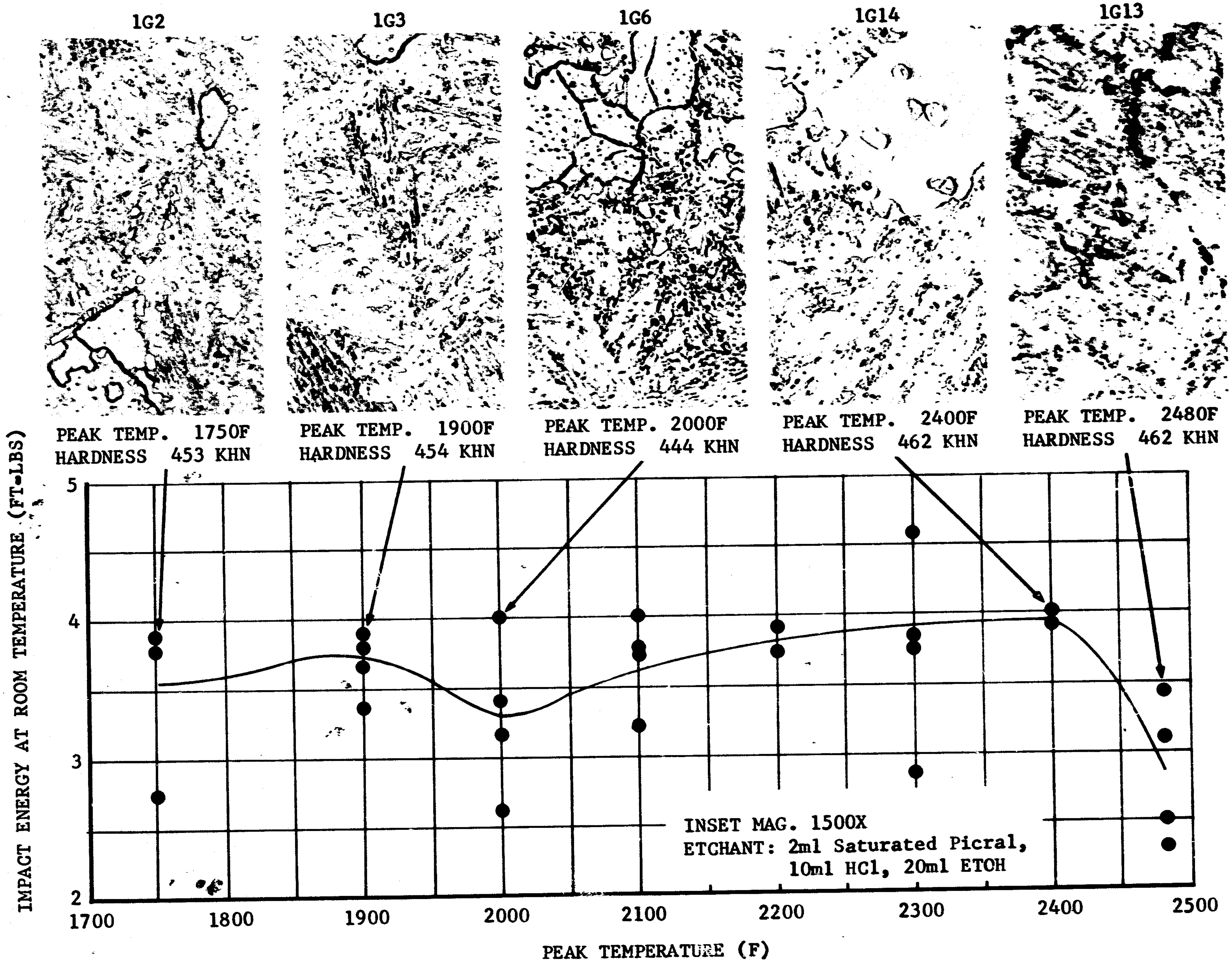

FIGURE 10 CHARPY V-NOTCHED IMPACT RESISTANCE OF THE SYNTHETIC HEAT-AFFECTED-ZONE FOR AM355-SCT 850 (FH)

TABLE VI

FRACTURE TOUGHNESS OF FUSION ZONES AND SYNTHETIC HEAT-AFFECTED ZONES

	B or B_N (in)	K_{Ic} (ksi $\sqrt{in}$)	K_{Ix} (ksi $\sqrt{in}$)	Microhardness (KHN)	Estimated σ_{ys} (ksi)	(1) B or B_N Recommended by ASTM (in)	(2) Maximum Allowable K_{Ii} (ksi $\sqrt{in}$)
4340 475F							
Fusion Zone	B_N = 0.210	48.3	50.3	550	225	0.114	50.3
Heat-Affected Zones							
2500F Peak Temp.	B_N = 0.210	57.2	60.2	526	220	0.169	60.2
2300F Peak Temp.	B_N = 0.210	55.5	60.5	530	220	0.159	60.5
2000F Peak Temp.	B_N = 0.210	55.8	59.1	540	225	0.154	59.1
Parent Material	B_N = 0.210	43.7	46.6	-	-	0.094	46.6
18 Ni(250) 900F							
Fusion Zone	B_N = 0.210	54.0	65.5	-	240	0.127	65.5
Heat-Affected Zones							
2400F Peak Temp.	B_N = 0.210	114.8	120.2	454	200	0.822	57.8
1400F Peak Temp.	B_N = 0.210	91.3	96.7	510	250	0.323	72.2
1200F Peak Temp.	B_N = 0.210	113.2	117.4	470	205	0.763	59.2
Parent Material	B_N = 0.190	105.0	111.3	-	-	0.387	73.6
AM355 SCT850(FH)							
Fusion Zone	B = 0.250		45.7	-	165	0.156	45.7
Heat-Affected Zones							
2480F Peak Temp.	B = 0.230	32.5	38.6	462	160	0.103	38.6
2400F Peak Temp.	B = 0.230		42.1	462	160	0.140	42.1
2000F Peak Temp.	B = 0.230	45.8	51.5	444	150	0.233	45.4
Parent Material	B = 0.250	55.5	62.4	-	-	0.294	51.2

NOTES: (1) $B \geq 2.5\,(K_{Ic}/\sigma_{ys})^2$

(2) $K_{Ii} = \sqrt{\frac{B(\sigma_{ys})^2}{2.5}}$

B = overall specimen thickness - inch

B_N = net-section thickness of side-notched specimens - inch

K_{Ic} = plane-strain fracture toughness - ksi $\sqrt{in}$

K_{Ix} = stress intensity at fracture - ksi $\sqrt{in}$

K_{Ii} = initial stress intensity - ksi $\sqrt{in}$

σ_{ys} = yield strength - ksi

were in a "Group 2" category. The specimens maintained plane-strain conditions up to relatively high stress intensities but not up to K_{Ic} or K_{Ix} levels. Thus, measured fracture-toughness values were probably somewhat higher than the true plane-strain fracture toughness. However, there was excellent potential for obtaining true plane-strain K_{ISCC} values.

The 4340 heat-affected zones exhibited high fracture toughness with a very slight trend toward decreasing toughness with increasing peak temperature. These results correlated well with Charpy impact data of Figure 8. The fusion zone exhibited somewhat lower toughness than the heat-affected zones, and the parent material exhibited the lowest toughness. The higher fracture toughness of the heat-affected and fusion zones may be associated with homogenization and grain refinement produced by the thermal exposures.

Fracture-toughness values for heat-affected zones of 18Ni Maraging steel followed the same trends obtained from Charpy impact tests. Toughness values for heat-affected zones were relatively high, but the fracture toughness of the fusion zone was quite low. Cox et al[16] suggested that low fusion-zone toughness is related to solid-state formation of Ti(C,N) particles in cell and dendrite boundary regions. Apparently, the amount of Ti(C,N) increases with higher welding-energy input.

Fracture-toughness values for heat-affected zones of AM355 exposed to peak temperatures of 2000F, 2400F, and 2480F generally followed the same trends obtained from the Charpy impact tests. However, the fracture toughness produced by a 2400F peak temperature was somewhat low compared to the Charpy data. The fracture-toughness specimens may have reached a peak temperature slightly above 2400F, which could account for this difference since toughness dropped rapidly in the narrow temperature range between 2400F and 2480F. The lowest fracture-toughness value was produced by the 2480F peak temperature as a result of partial melting in the grain boundaries.

SEACOAST STRESS-CORROSION TESTS OF PARENT MATERIALS

Detailed seacoast stress-corrosion test results for parent materials are included in Table BI of Appendix B. Many of the seacoast stress-corrosion failures occurred during the winter months when there were frequent periods of high moisture caused by dew, fog, or rain. Several failures of 4340-475F specimens actually coincided with the beginning of rain storms. These failures appeared to occur from the high humidity and not necessarily from direct impingement of rain on the specimens. During the drier summer months, the incidence of specimen failures decreased substantially. Thus, stress-corrosion failure times were highly dependent upon specific weather conditions existing during the test period. As a result, failure times exhibited a high degree of scatter and meaningful relationships could not be plotted between failure time and applied stress intensity. However, stress-corrosion behavior measured in terms of threshold loading conditions showed excellent consistency.

In some cases, general corrosion and stress-corrosion crack growth was greater on the windward or ocean side of the specimens than on the leeward side. Specimens of H-11, 4340, and 18Ni Maraging steel exhibited very heavy general corrosion on the surfaces. Of all the alloys tested, 410 specimens in both heat treatments were the only ones showing substantial general corrosion on the faces of the fatigue cracks. However, this effect did not affect stress-corrosion behavior in any significant manner.

Stress-corrosion crack growth was easily observed by visual examination of the fracture surfaces of most of the program alloys. In some specimens of H-11 1100F, 4340 800F, 18Ni Maraging steel, and 17-4 H900, it was difficult to ascertain stress-corrosion crack growth by visual examination alone, and fractographic analysis was essential. With the exception of 304 Sens., all of the program materials that failed by stress corrosion did so by growth of the fatigue crack. At high stress intensities, the 304 Sens. specimens showed nucleation and growth of new stress-corrosion cracks above and below the side notches as well as some stress-corrosion crack growth. At lower stress intensities, stress-corrosion cracks nucleated and grew above and below the side notches with no stress-corrosion crack growth from the fatigue crack. Thus, the fracture-mechanics approach to stress-corrosion testing is not applicable to the 304 alloy.

Examination of tested specimens showed that frequent reloading of a load train after specimen failures sometimes produced a small amount of low-cycle fatigue-crack growth in the remaining specimens. This region was seldom more than 0.010-inch, and it was readily distinguished from crack growth by stress corrosion. A review of the test results also showed no inconsistencies attributable to testing specimens in series where unloading and reloading was necessary as a result of specimen failures.

The data of Table BI of Appendix B was used to calculate the threshold stress intensity for stress corrosion (K_{ISCC}), which is defined as the stress intensity below which stress corrosion will not occur. The susceptibility of an alloy to stress corrosion may be noted in two manners based upon threshold stress intensity for stress corrosion. By rating materials based upon the threshold-stress-intensity ratio K_{ISCC}/K_{Ix}, differences in properties of different alloys are normalized. Thus, the ratio provides a measure of the degree to which the properties in the absence of a corrodent are degraded by a stress-corrosion environment.

Stress-corrosion susceptibility may also be rated on the basis of absolute K_{ISCC}. This value is important to the designer who must select the alloy that will permit the highest loading in a seacoast environment. Rating stress-corrosion susceptibility based upon K_{ISCC} rather than K_{ISCC}/K_{Ix} offers a distinct testing advantage. For alloys that show some degree of susceptibility to stress corrosion, K_{ISCC} will be less than K_{Ix}. Therefore, it is only necessary to maintain plane strain to a level of K_{ISCC} rather than K_{Ix}. In many cases, this results in a marked reduction in the specimen thickness and, thus, loading requirements needed to obtain a valid K_{ISCC} under plane-strain conditions.

The stress-corrosion susceptibilities of the program materials in the seacoast environment, based upon both K_{ISCC} and K_{ISCC}/K_{Ix}, are summarized in Table VII. The relative stress-corrosion susceptibility ratings of some of the alloys differ depending upon which criterion is used. The Inco 718, 304 Ann., and 17-4 H1150 alloys have the lowest stress-corrosion susceptibility according to both criteria, and 410 1125F, 4340 800F, and H-11(AM)

TABLE VII

STRESS-CORROSION SUSCEPTIBILITY OF PARENT MATERIALS IN SEACOAST TESTS

SUSCEPTIBILITY BASED ON K_{ISCC}

MATERIAL & CONDITION	K_{ISCC} (ksi $\sqrt{in}$)
Inco 718 SAA	>106
17-4 H1150	>93.9
(1) 18Ni(250) 900F	55.6 ± 7.6
304 ANN.	> 53.5
410 1125F	52.4 ± 7.5
(1) 4340 800F	48.3 ± 5.5
(1) H-11(AM) 1100F	39.5 ± 4.4
(1) 17-4 H900	<38.5 (38 est)
(1) AM355 SCT1000(FH)	33.1 ± 3.6
(1) AM355 SCT1000	24.5 ± 5.4
(1) 410 650F	22.0 ± 6.4
(1) H-11(AM) 1000F	16.7 ± 2.8
(1) 4340 475F	13.3 ± 2.0
(1) H-11(VM) 1000F	11.4 ± 5.6
(1) AM355 SCT850	<10.7
(1) AM355 SCT850(FH)	< 9.7
(1) 304 SENS.	< 8.5

INCREASING SUSCEPTIBILITY TO STRESS CORROSION

SUSCEPTIBILITY BASED ON K_{ISCC}/K_{Ix}

MATERIAL & CONDITION	K_{ISCC}/K_{Ix}
Inco 718 SAA	> 0.869
304 ANN.	> 0.774
17-4 H1150	> 0.771
4340 800F	0.720 ± 0.082
17-4 H900	< 0.694 (0.63 est)
H-11(AM) 1100F	0.621 ± 0.069
410 1125F	0.552 ± 0.080
H-11(AM) 1000F	0.522 ± 0.086
18Ni(250) 900F	0.500 ± 0.069
H-11(VM) 1000F	0.399 ± 0.198
4340 475F	0.286 ± 0.043
AM355 SCT1000(FH)	0.282 ± 0.031
AM355 SCT1000	0.242 ± 0.054
410 650F	0.241 ± 0.071
AM355 SCT850	< 0.223
AM355 SCT850(FH)	< 0.156
304 SENS.	< 0.124

K_{ISCC} = threshold stress intensity for stress corrosion - ksi $\sqrt{in}$

K_{Ix} = stress intensity at failure in absence of corrodent - ksi $\sqrt{in}$

(1) = valid plane-strain threshold value

1100F were also ranked high by both. The AM355 SCT850, AM355 SCT850(FH), and 304 Sens. materials showed the highest susceptibility according to both criteria. The remaining materials fell into two groups; those ranked considerabley better on an absolute than on a relative basis (18Ni(250) 900F, AM355 SCT1000(FH), AM355 SCT1000, and 410 650F) and those better in relative than absolute sensitivity (17-4 H900, H-11(AM) 1000F, H-11(VM) 1000F, and 4340 475F).

SEACOAST STRESS-CORROSION TESTS OF FUSION AND HEAT-AFFECTED ZONES

Detailed results for seacoast stress-corrosion tests of fusion zones and synethetic heat-affected zones are included in Table BII of Appendix B. Many of the comments made with regard to seacoast tests on parent materials also apply to these tests. The data of Table BII were used to calculate the threshold loading conditions for stress corrosion summarized in Table VIII. Results on parent materials are also included for comparison. All of the K_{ISCC} values are valid plane-strain values. The primary purpose of these results was to provide a basis for establishing the validity of the accelerated test results.

For 4340, Table VIII shows that the parent material exhibited the lowest threshold stress intensity for stress corrosion (K_{ISCC}) as well as the highest degree of degradation (lowest value of K_{ISCC}/K_{Ix}). Thus, stress corrosion of a 4340 weldment was controlled by the behavior of the parent material and not the fusion zone or the specific heat-affected zone which was tested.

For the 18Ni Maraging steel, the stress-corrosion susceptibility of a weldment was controlled by the low K_{ISCC} of the fusion zone. The data did not accurately define threshold conditions for the 1200F heat-affected zone, although it was estimated to behave similarly to the parent material. Conversely, the fusion zone of AM355 exhibited the highest K_{ISCC} and the least amount of degradation based upon K_{ISCC}/K_{Ix}. Therefore, the high stress-corrosion susceptibility of both the parent material and the heat-affected (2480F peak) zone were the limiting regions in a weldment of this alloy.

ACCELERATED STRESS-CORROSION TESTS OF PARENT MATERIALS

Detailed results of accelerated stress-corrosion tests on parent materials are tabulated in Table BIII of Appendix B. Many of the general comments made with regard to seacoast tests of parent materials also applied to accelerated tests. Stress-corrosion test results are plotted in Figures 11 through 19. These figures permit comparisons based upon stress-intensity ratios as well as actual stress intensity. The maximum initial-loading conditions allowable for maintaining plane strain are also indicated. As discussed earlier, a number of specimens would not maintain plane strain to failure. However, the K_{ISCC} values were sufficiently low so that they represented plane-strain values for most of the program materials.

TABLE VIII

STRESS-CORROSION SUSCEPTIBILITY OF FUSION ZONES AND SYNTHETIC HEAT-AFFECTED ZONES IN SEACOAST TESTS

MATERIAL, CONDITION, AND DESCRIPTION	K_{ISCC} (ksi$\sqrt{in}$)	K_{Ix} (ksi$\sqrt{in}$)	$\frac{K_{ISCC}}{K_{Ix}}$
4340 Tempered at 475F			
Fusion Zone	23.3 ± 3.8	50.3	0.463 ± 0.075
Heat-Affected Zone (2500F Peak Temp)	24.0 ± 6.0	60.2	0.400 ± 0.100
Parent Material	13.3 ± 2.0	46.6	0.286 ± 0.043
18Ni Maraging Steel (250 Grade) Aged at 900F			
Fusion Zone	27.8 ± 7.3	65.5	0.424 ± 0.112
Heat-Affected Zone (1200F Peak Temp)	< 54.1	117.4	< 0.461
Parent Material	55.6 ± 7.6	111.3	0.500 ± 0.069
AM355 SCT850 (Fully Hardened)			
Fusion Zone	> 27.1	45.7	> 0.594
Heat-Affected Zone (2480F Peak Temp)	< 8.6	38.6	< 0.223
Parent Material	< 9.7	62.4	< 0.156

K_{ISCC} = threshold stress intensity for stress corrosion - ksi $\sqrt{in}$

K_{Ix} = stress intensity at failure in absence of corrodent for each individual zone - ksi $\sqrt{in}$

The only exceptions being:

1. 410 1125F
2. 17-4 H1150
3. 304 ANN
4. Inco 718 SAA

In general, Figures 11 through 19 show consistent relationships between loading conditions and failure times. In a few cases, failure times showed scatter that was probably attributable to a change in the experimental test method. During the first year of this program, specimens were stressed before application of corrodent. Thus crack blunting could occur by creep, particularly at high stress intensities, and produce longer failure times. Subsequently, the corrodent was applied prior to stressing to eliminate this problem, and failure times at a given stress intensity were shorter in some cases.

The stress-corrosion behavior of H-11 steel is shown in Figure 11. For the 1000F temper, the vacuum-melted material shows somewhat less susceptibility to stress corrosion than air-melted material based upon either K_{ISCC} or K_{ISCC}/K_{Ix} values. Early stress-corrosion tests on H-11 tempered at 1100F were conducted using specimens side-notched to a depth of 0.020 inch. Examination of failed specimens showed that stress corrosion took place by nucleation and growth of cracks from the side notches as well as by growth of the fatigue crack. This problem was eliminated by reducing the side-notch depth to 0.010 inch, and specimens of this configuration were tested in the vicinity of the threshold value to establish it without question.

The stress-corrosion behavior of 4340 steel is shown in Figure 12. The threshold-stress-intensity ratio for stress corrosion of 4340 tempered at 475F is 0.237 ± 0.022, which corresponds to a stress-intensity threshold of 11.1 ± 1.1 ksi $\sqrt{in}$. The effects of side-notch depth observed for H-11 tempered at 1100F were also seen on 4340 tempered at 800F, and the problem was solved in the same manner. The threshold-stress-intensity ratio for 4340 tempered at 800F was 0.442 ± 0.022, which corresponded to a stress-intensity threshold of 29.7 ± 1.5 ksi $\sqrt{in}$.

The stress-corrosion behavior of the 18Ni Maraging steel is shown in Figure 13. The threshold-stress-intensity ratio for stress corrosion is 0.655 ± 0.036, which corresponds to a stress-intensity threshold of 71.0 ± 4.8 ksi $\sqrt{in}$. Rolfe, Novak, and Gross[17] determined the stress-corrosion behavior of a similar material in synthetic sea water by using fatigue-cracked cantilever beam specimens. Their results indicated a threshold-stress-intensity ratio of 0.68, which corresponded to a stress intensity of 49 ksi $\sqrt{in}$. While their stress-intensity ratio was in good agreement with the value obtained in this program, there was a significant difference in stress-intensity values. However, the K_{Ic} of their material was 72 ksi $\sqrt{in}$ compared to an approximate K_{Ic} of 105 ksi $\sqrt{in}$ for material used in this program.

The stress-corrosion behavior of 410 stainless steel is shown in Figure 14. The material tempered at 1125F exhibited a stress-corrosion threshold higher than the allowable loading for plane strain. Therefore, the K_{ISCC} is not a plane-strain threshold.

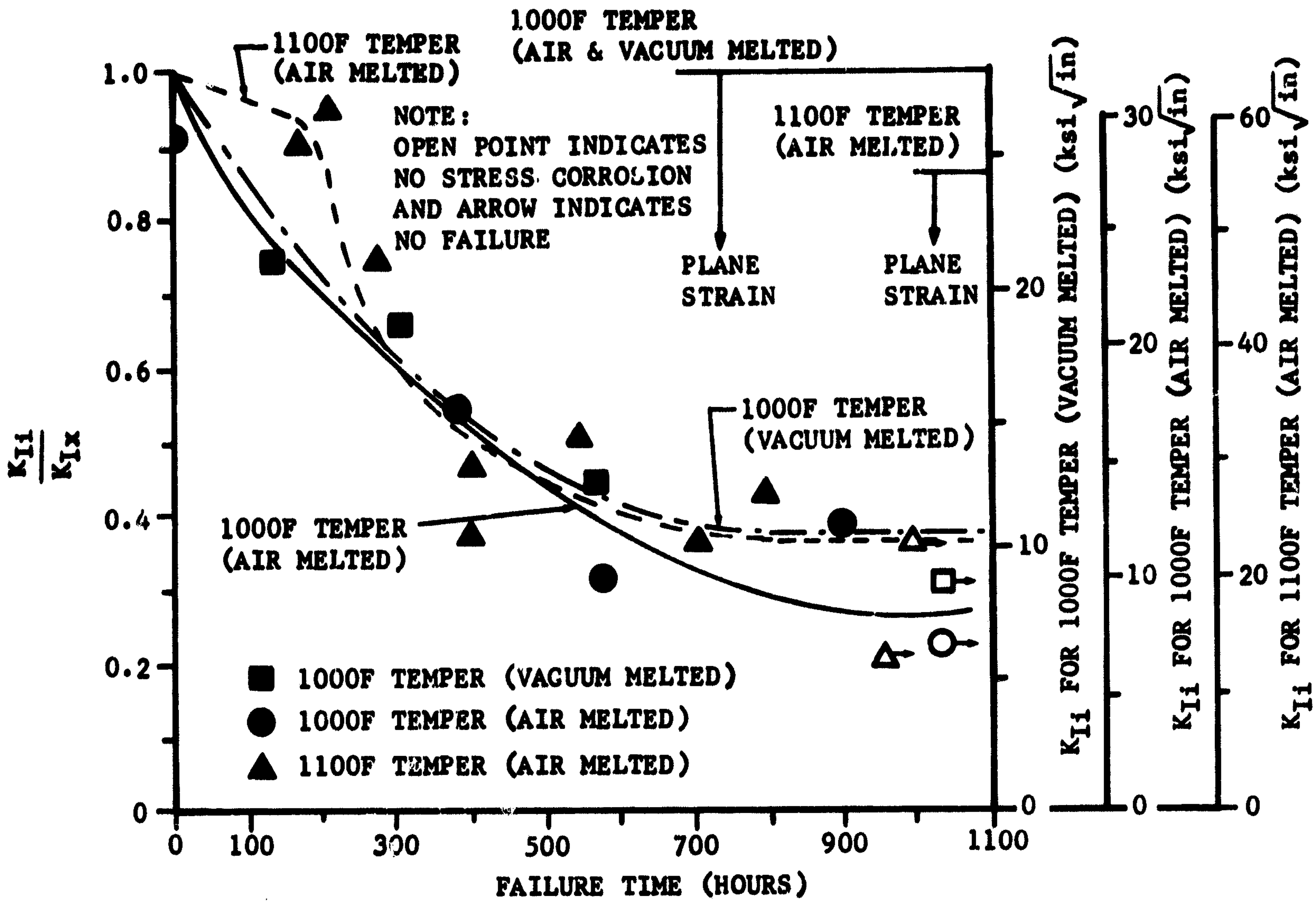

FIGURE 11 STRESS-CORROSION BEHAVIOR OF H-11 - ACCELERATED TEST

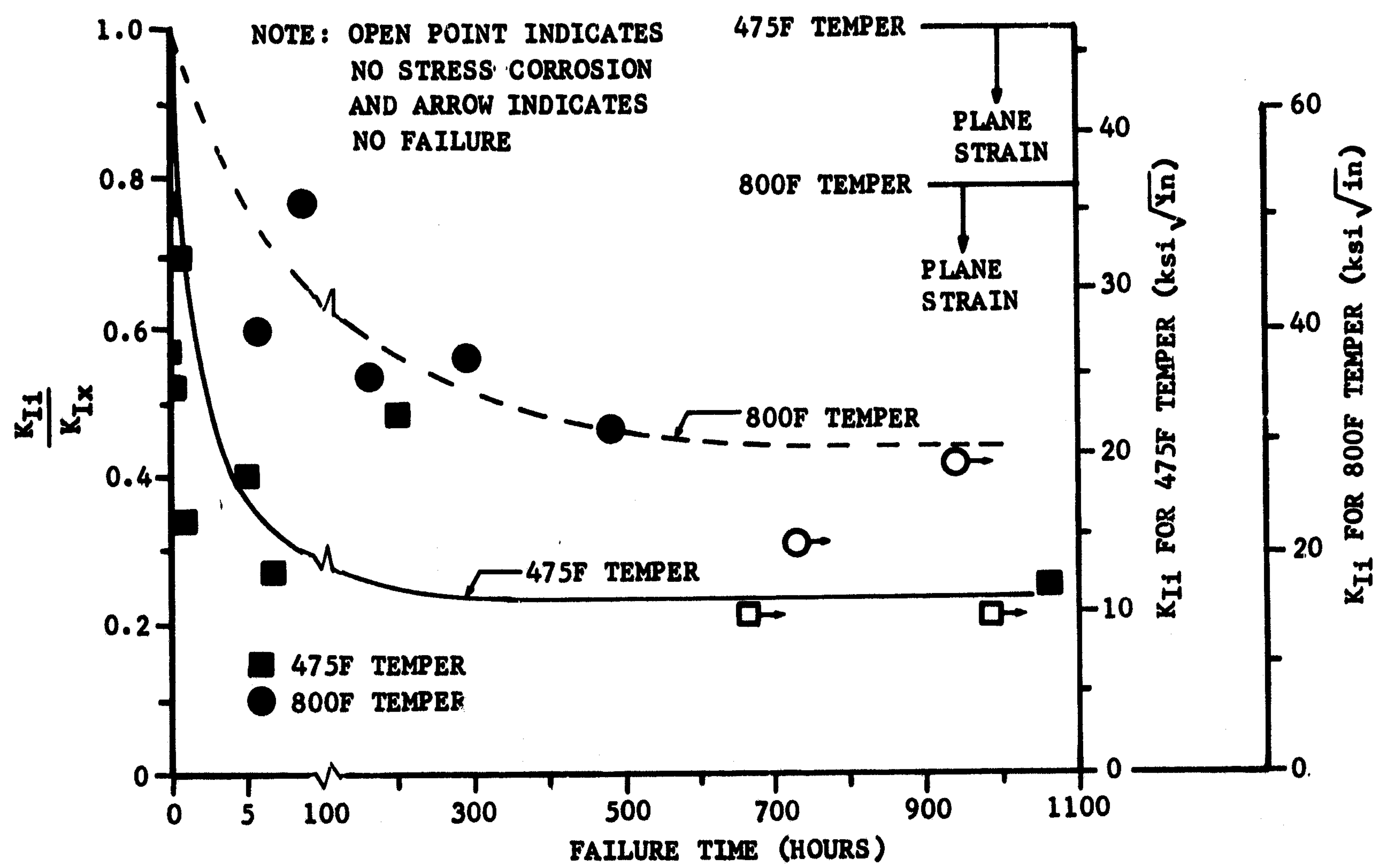

FIGURE 12 STRESS-CORROSION BEHAVIOR OF 4340 - ACCELERATED TEST

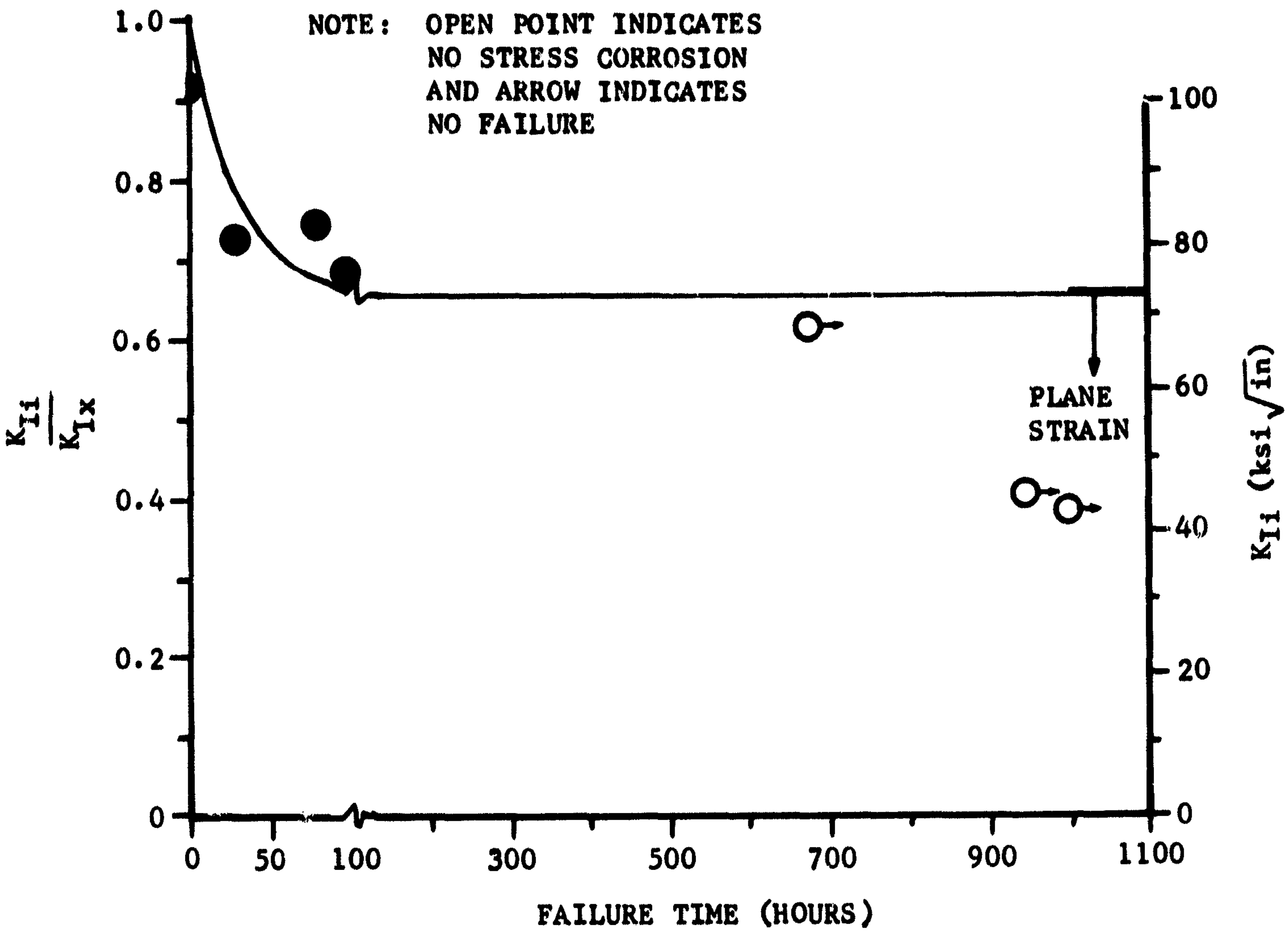

FIGURE 13 STRESS-CORROSION BEHAVIOR OF 18Ni MARAGING STEEL (250 GRADE) - ACCELERATED TEST

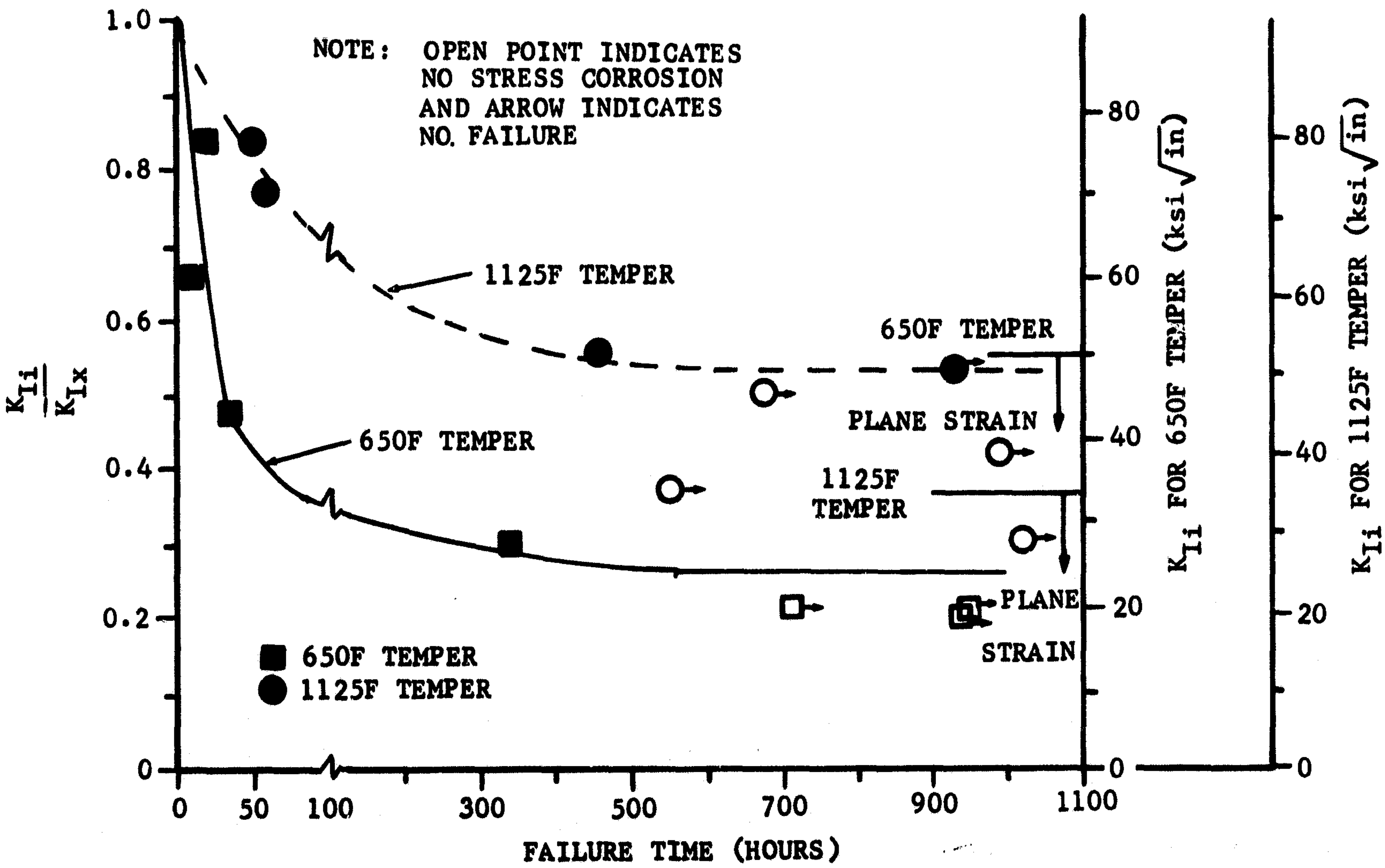

FIGURE 14 STRESS-CORROSION BEHAVIOR OF 410 - ACCELERATED TEST

The stress-corrosion behavior of 17-4 stainless steel is shown in Figure 15. The curve for 17-4 H1150 material was based primarily upon specimens loaded to stress-intensity ratios of approximately 0.76 and 0.8. Although these specimens failed during test, fractographic analysis showed overload failures with no evidence of stress corrosion. The threshold level for this H1150 material was far above the allowable stress intensity for plane strain.

The stress-corrosion behavior of AM355 stainless steel is shown in Figures 16 and 17 for the standard and fully hardened heat treatments respectively. On the basis of either K_{ISCC} or K_{ISCC}/K_{Ix} values, the SCT850(FH) heat treatment produced the highest susceptibility to stress corrosion. The SCT1000(FH) heat treatment produced the lowest susceptibility on the basis of K_{ISCC}, and SCT850 the lowest based on K_{ISCC}/K_{Ix}.

The stress-corrosion behavior of 304 stainless steel is shown in Figure 18. Material in the annealed condition exhibited low susceptibility to stress corrosion, whereas sensitized material was highly susceptible. The behavior of sensitized material was unique among the materials studied in this program. It was the only material in which a 1000-hour test time did not appear to be sufficient to establish threshold loading conditions. Also, stress corrosion occurred by nucleation and growth of new stress-corrosion cracks at regions well removed from the fatigue crack as well as by growth of the fatigue crack. In all other program materials, tested as smooth or properly side-notched specimens, stress corrosion occurred solely by growth of the fatigue crack. Therefore, a fracture mechanics approach to stress-corrosion testing of 304 is not applicable.

The stress-corrosion behavior of Inconel 718, shown in Figure 19, indicated that this material exhibited excellent resistance to stress corrosion.

The stress-corrosion susceptibilities of parent materials in the accelerated test are summarized in Table IX, based upon K_{ISCC} as well as K_{ISCC}/K_{Ix} values.

Eleven of the seventeen materials rank essentially the same according to either criterion. Inconel 718, 17-4 H1150, 304 annealed, and 18Ni(250) 900F show low sensitivities to stress corrosion; 410 1125F, 4340 800F, and H-11(AM) 1100F moderate sensitivities; and 4340 475F, H-11(AM) 1000F, 304 sensitized, and AM355 SCT850(FH) high sensitivities. The materials ranking considerably better on an absolute rather than a relative basis are AM355 SCT1000(FH), AM355 SCT1000, and 410 650F; those better on a relative basis are 17-4 H900, AM355 SCT850, and H-11(VM) 1000F.

ACCELERATED STRESS-CORROSION TESTS OF FUSION AND SYNTHETIC HEAT-AFFECTED ZONES

Detailed results of accelerated stress-corrosion tests on fusion and synthetic-heat-affected zones are tabulated in Table BIV of Appendix B. Threshold K_{ISCC} and K_{ISCC}/K_{Ix} values calculated from these results are summarized in Table X. For 4340, the parent material exhibited the highest susceptibility to stress corrosion based upon K_{ISCC} or K_{ISCC}/K_{Ix} values. In 18Ni Maraging steel, the parent material exhibited the lowest susceptibility to stress corrosion. The AM355 results show that the fusion zone exhibited the lowest susceptibility, with the parent material and heat-affected zones exhibiting similar and high susceptibility.

NOTE: OPEN POINT INDICATES NO STRESS
CORROSION AND ARROW INDICATES NO FAILURE

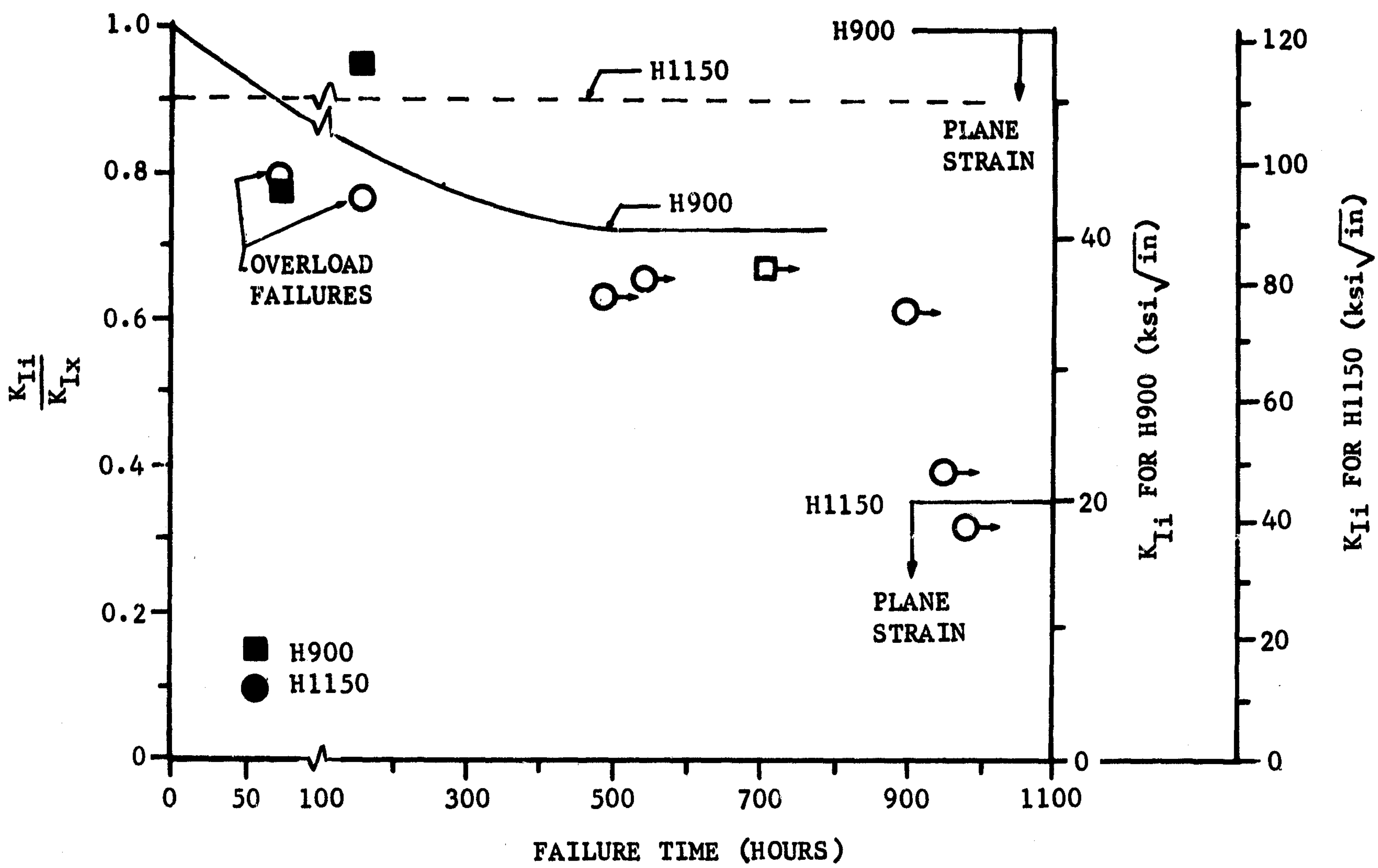

FIGURE 15 STRESS-CORROSION BEHAVIOR OF 17-4 - ACCELERATED TEST

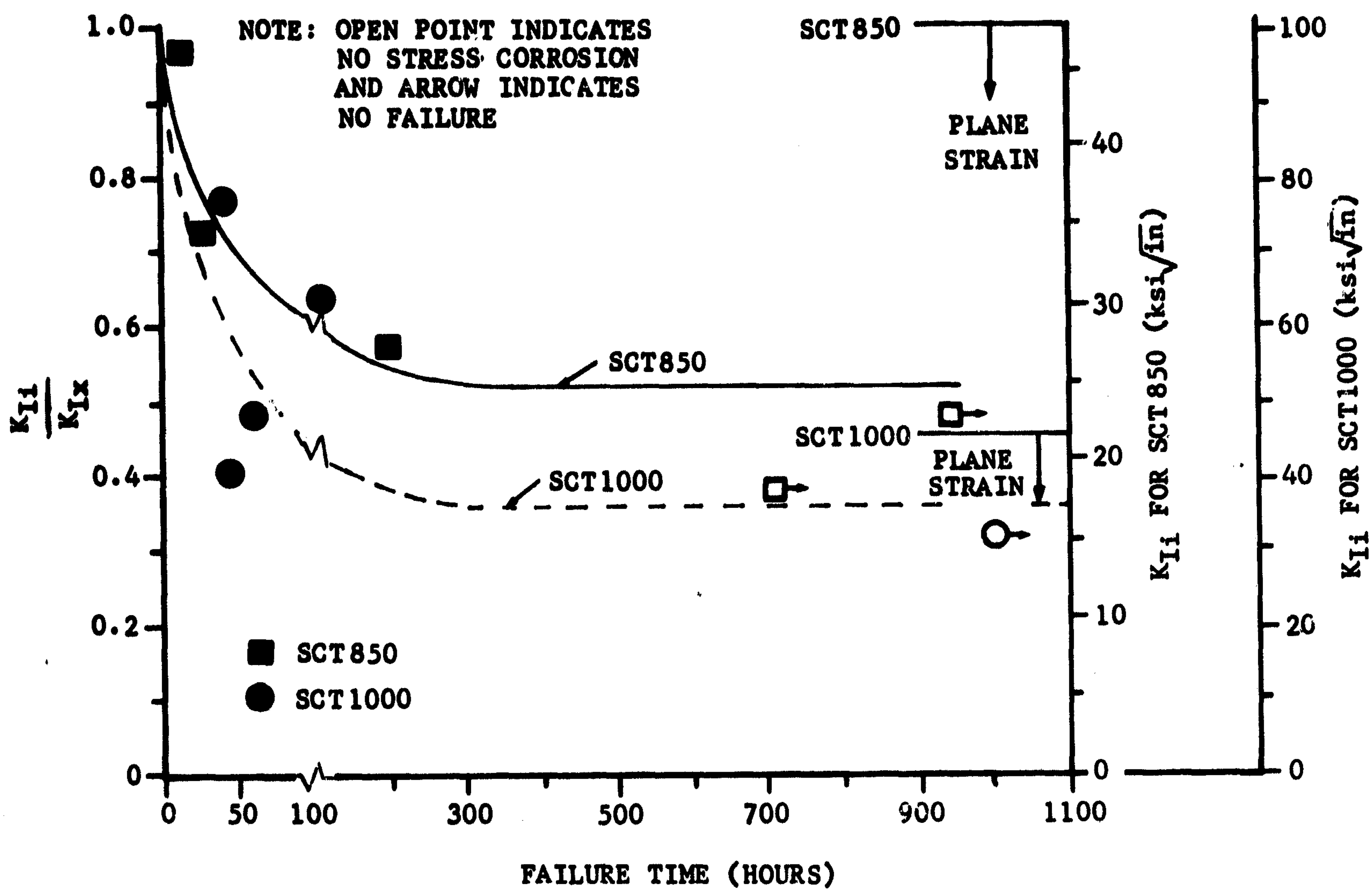

FIGURE 16 STRESS-CORROSION BEHAVIOR OF AM355 - ACCELERATED TEST

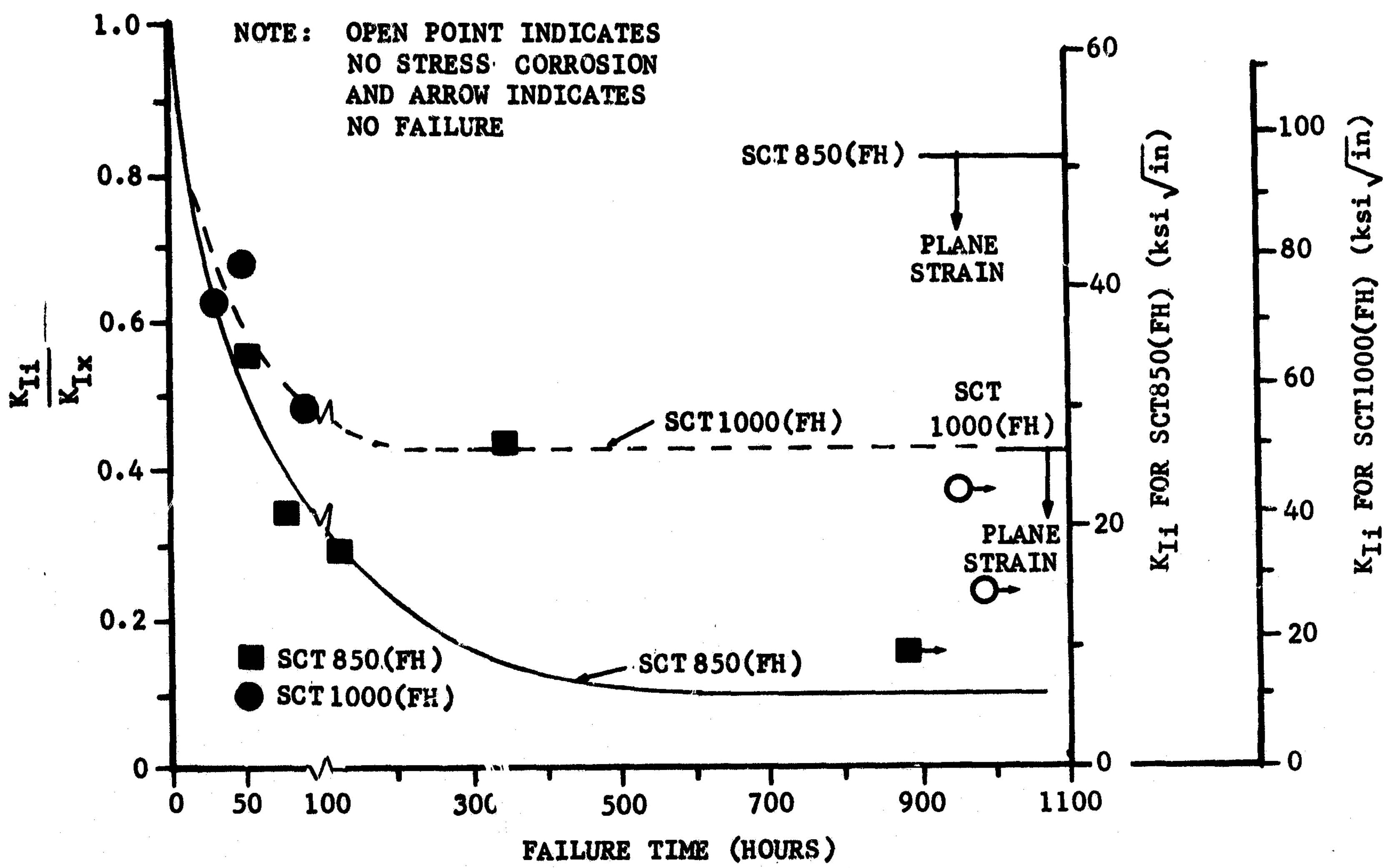

FIGURE 17 STRESS-CORROSION BEHAVIOR OF FULLY HARDENED AM355 - ACCELERATED TEST

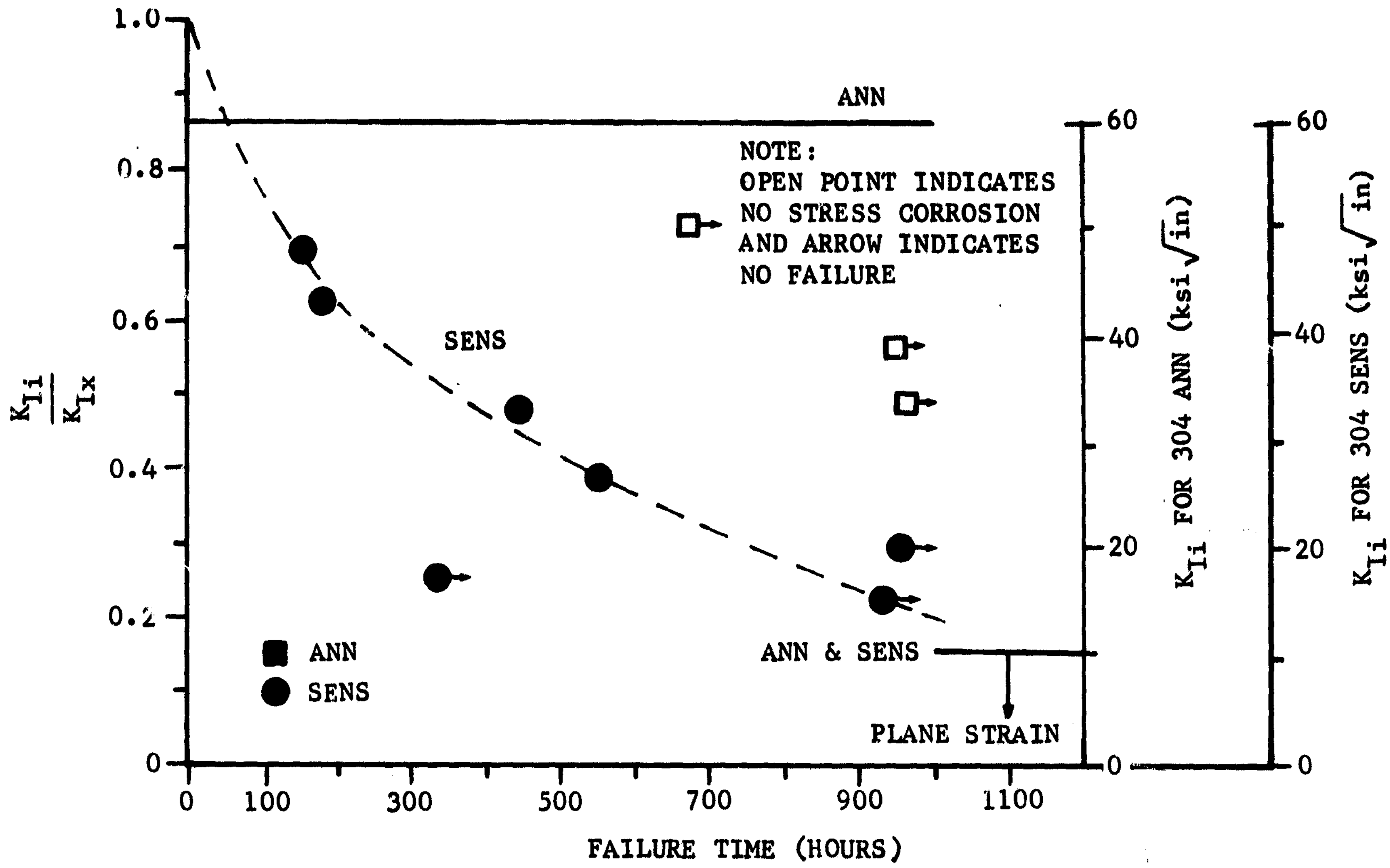

FIGURE 18 STRESS-CORROSION BEHAVIOUR OF 304 - ACCELERATED TEST

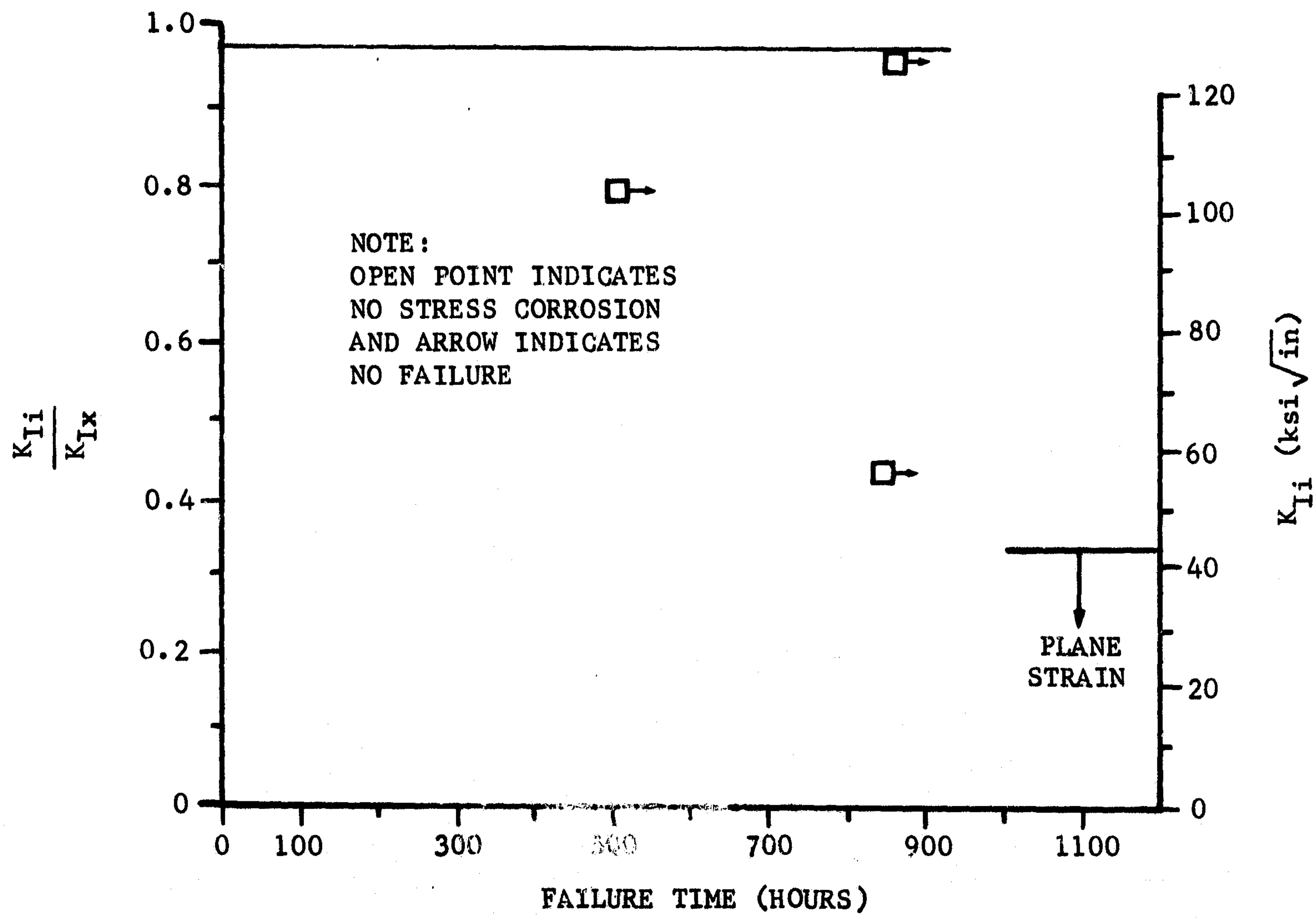

FIGURE 19 STRESS-CORROSION BEHAVIOR OF INCONEL 718 - ACCELERATED TEST

TABLE IX

STRESS-CORROSION SUSCEPTIBILITY OF PARENT MATERIALS IN ACCELERATED TESTS

SUSCEPTIBILITY BASED ON K_{ISCC}

MATERIAL & CONDITION	K_{ISCC} (ksi $\sqrt{in}$)
Inco 718 SAA	130 ± 1.0
17-4 H1150	110 ± 12.0
(1) 18Ni(250) 900F	72.9 ± 4.0
304 ANN.	59.7 ± 9.4
(1) AM355 SCT1000(FH)	50.3 ± 6.7
410 1125F	49.6 ± 1.9
(1) 17-4 H900	40.3 ± 2.8
(1) AM355 SCT1000	36.7 ± 4.0
(1) 4340 800F	29.7 ± 1.5
(1) AM355 SCT850	24.9 ± 2.1
(1) 410 650F	23.8 ± 3.9
(1) H-11(AM) 1100F	23.2 ± 0.2
(1) 4340 475F	11.1 ± 1.1
(1) H-11(VM) 1000F	10.8 ± 1.9
(1) H-11(AM) 1000F	8.6 ± 1.4
304 SENS.	<15.2
(1) AM355 SCT850(FH)	~ 6.2

Increasing susceptibility to stress corrosion

SUSCEPTIBILITY BASED ON K_{ISCC}/K_{Ix}

MATERIAL & CONDITION	K_{ISCC}/K_{Ix}
Inco 718 SAA	0.981 ± 0.019
17-4 H1150	0.894 ± 0.106
304 ANN.	0.865 ± 0.135
17-4 H900	0.724 ± 0.050
18Ni(250) 900F	0.655 ± 0.036
410 1125F	0.524 ± 0.020
AM355 SCT850	0.521 ± 0.044
4340 800F	0.442 ± 0.022
AM355 SCT1000(FH)	0.428 ± 0.057
H-11(VM) 1000F	0.378 ± 0.068
H-11(AM) 1100F	0.365 ± 0.003
AM355 SCT1000	0.363 ± 0.039
H-11(AM) 1000F	0.270 ± 0.044
410 650F	0.261 ± 0.043
4340 475F	0.237 ± 0.022
304 SENS	< 0.222
AM355 SCT850(FH)	~ 0.100

K_{ISCC} = threshold stress intensity for stress corrosion - ksi $\sqrt{in}$

K_{Ix} = stress intensity at failure in absence of corrodent - ksi $\sqrt{in}$

(1) = valid plane-strain threshold value

TABLE X

STRESS-CORROSION SUSCEPTIBILITY OF FUSION ZONES AND SYNTHETIC HEAT-AFFECTED ZONES IN ACCELERATED TESTS

MATERIAL, CONDITION, AND DESCRIPTION	K_{ISCC} (ksi $\sqrt{in}$)	K_{Ix} (ksi $\sqrt{in}$)	$\frac{K_{ISCC}}{K_{Ix}}$
4340 Tempered at 475F			
Fusion Zone	14.8 ± 4.0	50.3	0.296 ± 0.079
Heat-Affected Zones			
2500F Peak Temp	16.7 ± 0.1	60.2	0.278 ± 0.002
2300F Peak Temp	17.4 ± 1.8	60.5	0.288 ± 0.030
2000F Peak Temp	13.0 ± 6.6	59.1	0.219 ± 0.111
Parent Material	11.1 ± 1.1	46.6	0.237 ± 0.022
18Ni Maraging Steel (250 Grade) Aged at 900F			
Fusion Zone	23.4 ± 4.5	65.5	0.358 ± 0.069
Heat-Affected Zones			
2400F Peak Temp	40.1 ± 7.3	120.2	0.334 ± 0.061
1400F Peak Temp	38.5 ± 4.4	96.7	0.396 ± 0.047
1200F Peak Temp	61.6 ± 8.0	117.4	0.525 ± 0.068
Parent Material	72.9 ± 4.0	111.3	0.655 ± 0.036
AM355 SCT850 (Fully Hardened)			
Fusion Zone	> 33.5	45.7	> 0.733
Heat-Affected Zones			
2480F Peak Temp	7.0 ± 1.8	38.6	0.180 ± 0.048
2400F Peak Temp	< 4.5	42.1	< 0.107
2000F Peak Temp	7.0 ± 2.2	51.5	0.135 ± 0.042
Parent Material	~ 6.2	62.4	~ 0.100

K_{ISCC} = threshold stress intensity for stress corrosion - ksi $\sqrt{in}$

K_{Ix} = stress intensity at failure in absence of corrodent for each individual zone - ksi $\sqrt{in}$

STRESS-CORROSION BEHAVIOR USING WOL SPECIMENS

As the specimen thickness required for plane strain increases above approximately 1/2-inch, loads required for single-edge-notched (SEN) specimens become impractically high ($>$ 35,000 lbs) for some of the materials studied in this program. The wedge-opening-loading (WOL) specimen[2] was selected as an alternate coupon for evaluating stress-corrosion susceptibility of materials that require a comparatively large thickness to maintain plane strain. WOL specimens could be tested in a series load train at loads that are approximately one-quarter of the loads required for SEN specimens of equivalent thickness.

Transverse WOL specimens of the IT type (1 inch thick) were prepared from AM355 heat treated to the SCT1000 condition. The measurement capacity of this specimen was reported[2] to be $K_I/\sigma_{ys} = 0.79$. Since the yield strength of the material was 158 ksi, this corresponded to a maximum allowable K_I for plane strain of 125 ksi $\sqrt{in}$. Based upon the latest ASTM recommendation[11], the maximum allowable K_I for plane strain was 100 ksi $\sqrt{in}$. Fracture-toughness tests yielded an average K_{Ic} of 106 ksi $\sqrt{in}$ and an average K_{Ix} of 151 ksi $\sqrt{in}$. These values were higher than the values obtained on the 1/4-inch thick SEN specimens (Table V). Also, the fractured specimens exhibited approximately 25 percent shear, which was unexpected for this thickness.

Figure 20 shows a comparison of accelerated stress-corrosion behavior determined from WOL specimens and SEN specimens. The WOL specimens provided a K_{ISCC} of 33.8 $\pm$ 2.1 ksi $\sqrt{in}$ compared to 36.7 $\pm$ 4.0 ksi $\sqrt{in}$ for the SEN specimens. Thus the K_{ISCC} values were in excellent agreement. Test times required to establish threshold values were somewhat longer for WOL specimens than SEN specimens as a result of the greater amount of crack growth necessary to produce failures in WOL specimens.

The WOL specimen provided very clear pop-in indications and thus clearly defined K_{Ic} values, and it was for this application that the specimen was designed. Several general comments are in order concerning the use of these specimens for stress-corrosion tests. WOL specimens are more difficult to machine than SEN specimens. Also testing is complicated by the large clevice needed to load the specimen, particularly in a corrosive environment. The high degree of eccentric loading requires a strong and stiff loading train to prevent bending of load train components. This eccentricity also leads to large movements of the lever arm as crack growth proceeds, so that frequent leveling is required. Also it was necessary to apply the corrodent to the crack before attaching the clevice, which restricts access considerably.

The SEN specimen was significantly less expensive and easier to work with in stress-corrosion testing. Therefore, the WOL specimen is recommended only for materials requiring large thickness and, thus, high loads that are impractical with SEN specimens. The WOL specimen is also advantageous for tests ir the short transverse direction of heavy plate whose thickness is not enough for a SEN specimen to be cut parallel to that dimension.

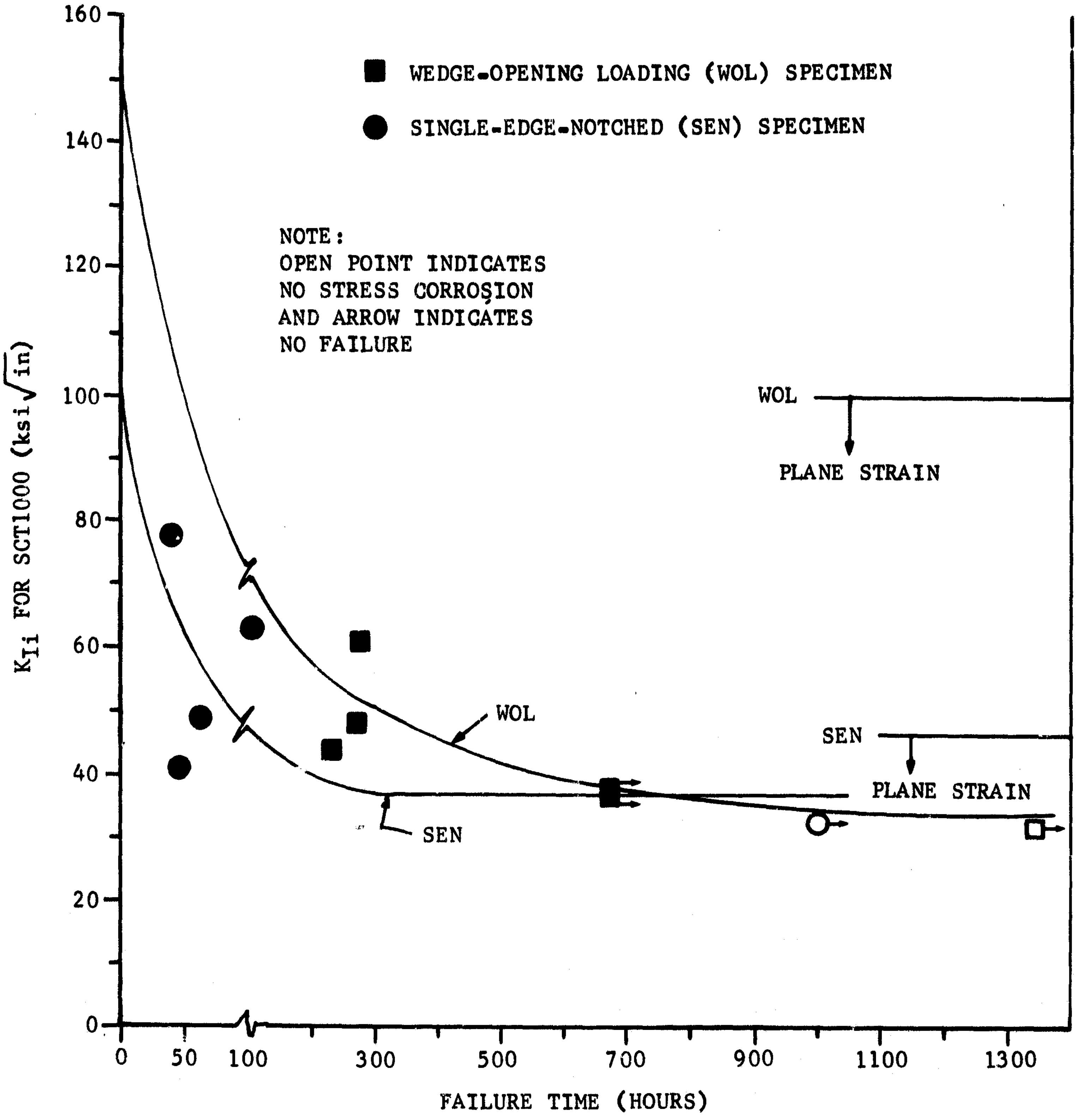

FIGURE 20 ACCELERATED STRESS-CORROSION BEHAVIOR OF AM355 SCT1000 DETERMINED FROM SEN AND WOL SPECIMENS

FRACTOGRAPHIC ANALYSES

In some specimens that showed crack extension after testing, it was difficult to establish the reason for this growth by visual examination of fracture surfaces. Fractographic analysis was an invaluable tool for separating crack growth produced by stress corrosion from crack growth produced by fatigue or overload.

In stress-corrosion testing of martensitic matrices, there is always a question whether the environmental failure mechanism is hydrogen embrittlement or an anodic stress-corrosion process. The fracture appearance is similar for both mechanisms in many martensitic matrices so that fractography cannot identify conclusively which mechanism prevails. Therefore, in cases where seacoast- and accelerated-test fractures agreed, this did not provide conclusive proof that the failure mechanisms were identical for both test types. Conversely, if fracture appearances in the seacoast and accelerated tests were different, then the failure mechanisms in each case were clearly different.

Fractographic analyses were conducted utilizing the two-stage plastic-replica technique. Figure 21 shows electron fractographs of seacoast and accelerated-stress-corrosion failures of air-melted H-11 tempered at 1000F. These fractographs were taken in the stress-corrosion regions of crack growth. Both environments produced identical intergranular fracture modes. In both instances, the exposed grain facets were extremely pitted and corroded. Specimens of H-11 tempered at 1100F were also examined, and they showed similar intergranular stress-corrosion fractures for the seacoast and accelerated tests.

Typical fractographs of 4340 specimens tempered at 475F are shown in Figure 22. Intergranular fracture was observed in both cases, as evidenced by the pyramidal grain-facet morphology. Some corrosion products and pitting caused by general corrosion of the fracture surface after stress-corrosion failure were observed on the specimen tested in the laboratory.

Electron fractographs of 18Ni Maraging steel are shown in Figure 23. The seacoast specimen had a semi-featureless topology which was intergranular in nature. The smooth grain-like facets and grain boundaries were not as well defined as in classical examples whereas the stress-corrosion zone of the accelerated test specimen revealed a well defined, intergranular mode of propagation. Grain boundaries were very evident, and a small amount of corrosion product was visible as particles on the grain faces.

Figure 24 shows fractographs of 410 tempered at 650F and tested at stress intensities well above both threshold values and allowable plane-strain loading conditions. Seacoast specimens revealed only intergraular stress-corrosion fracture, as evidenced by the sharp pyramidal facets. Very slight corrosion of the fracture facets was noticed. Analysis of the accelerated-test specimen revealed a mixed-mode fracture. Both intergranular and transgranular cleavage fracture were found. The relative proportion of intergranular-to-cleavage mode was approximated at 4:1. Hydrogen embrittlement generally produces a quasi-cleavage fracture mode in 410 tempered at 650F-700F;[18] the presence of cleavage in the accelerated-test specimen suggested that hydrogen embrittlement may have contributed to failure.

1775

SPECIMEN A38 SEACOAST TEST

$K_{Ii} = 26.7 \text{ ksi} \sqrt{\text{in}}$

1778

SPECIMEN A40 ACCELERATED TEST

$K_{Ii} = 29.2 \text{ ksi} \sqrt{\text{in}}$

FIGURE 21 ELECTRON FRACTOGRAPHS OF STRESS-CORROSION FRACTURES OF AIR-MELTED H-11 (1000F TEMPER)

SPECIMEN C9 SEACOAST TEST

$K_{Ii} = 43.2$ ksi $\sqrt{in}$

SPECIMEN C13 ACCELERATED TEST

$K_{Ii} = 35.9$ ksi $\sqrt{in}$

FIGURE 22 ELECTRON FRACTOGRAPHS OF STRESS-CORROSION FRACTURES OF 4340 (475F TEMPER)

1739

SPECIMEN B5 SEACOAST TEST

$K_{Ii} = 93.8$ ksi $\sqrt{in}$

1745

SPECIMEN B14 ACCELERATED TEST

$K_{Ii} = 82.5$ ksi $\sqrt{in}$

FIGURE 23 ELECTRON FRACTOGRAPHS OF STRESS-CORROSION FRACTURES OF 18Ni-250 (900F) MARAGING STEEL

1715

SPECIMEN E5 SEACOAST TEST

$K_{Ii} = 76.0$ ksi $\sqrt{in}$

1719

INTERGRANULAR FRACTURE REGION

1722

TRANSGRANULAR CLEAVAGE REGION

SPECIMEN E21 ACCELERATED TEST

$K_{Ii} = 59.9$ ksi $\sqrt{in}$

FIGURE 24 ELECTRON FRACTOGRAPHS OF STRESS-CORROSION FRACTURES OF 410 (650F TEMPER) AT HIGH STRESS INTENSITIES

Figure 25 shows fractographs of 410 tempered at 650F and tested at stress intensities close to K_{ISCC} values and within plane-strain loading allowables. In this case, the seacoast-and accelerated-test specimens show similar intergranular fractures. However, the overload region of the seacoast specimen showed an intergranular fracture whereas the accelerated specimen showed a normal dimpled (ductile) overload region. The reason for this anomaly is not understood.

Several specimens of 410 tempered at 1125F were also examined to compare fracture modes. The stress-corrosion regions of seacoast- and accelerated-test specimens showed similar intergranular failure modes with many areas of "mud cracking" (intergranular corrosion products). However, some discrepancies between seacoast and accelerated fractures were found in the overload regions where mixtures of intergranular, quasi-cleavage, and ductile overload fractures were observed. A routine fracture-toughness specimen was examined and the mode of overload failure was a mixture of quasi-cleavage and overload dimples. The expected fracture should have been an area of notch-induced quasi-cleavage followed by ductile overload. Two additional stress-corrosion specimens were examined. The accelerated-test specimen showed intergranular fracture over the entire fracture, whereas the seacoast-test specimen showed intergranular stress corrosion followed by mixed cleavage and dimple structure in the overload region. The reason for these differences in overload-failure modes is not now understood.

Electron fractographs taken from the fracture surface of the 17-4 seacoast specimen showed an intergranular mode of fracture with isolated areas of transgranular cleavage failure. Grain facets were mottled and corroded as shown in Figure 26. Analysis of the accelerated specimen also revealed a mixed-mode fracture with both intergranular and cleavage type fracture. The relative amount of cleavage fracture was slightly higher in the laboratory specimen. A high degree of secondary cracking was also noted in both specimens. Since the reported mode of stress-corrosion failure of this material is intergranular, the cleavage areas could have resulted from a notch-induced type propagation or possibly hydrogen embrittlement. Nevertheless, both seacoast and laboratory specimens were similar in fracture topography.

Figure 27 shows typical electron fractographs taken from the stress-corrosion propagation zone of AM355 heat treated to the SCT850 condition. Fracture was found to be intergranular in both the seacoast-and accelerated-test specimens. This was evidenced by the smooth grain facets observed in both fractographs. The accelerated-test specimen G27 did, however, show isolated areas of quasi-cleavage type transgranular fracture. Specimens G5, loaded to a K_{Ii} of 35.4 ksi $\sqrt{in.}$ in the seacoast environment, and G28, loaded to a K_{Ii} of 34.7 ksi $\sqrt{in.}$ in the accelerated test, also were examined fractographically. At this higher stress intensity, the seacoast specimen still exhibited an intergranular fracture mode. The fracture mode of the accelerated-test specimen changed from essentially intergranular fracture to approximately 80-percent transgranular quasi-cleavage and 20-percent intergranular fracture. However, the results on specimens of Figure 27 were considered to be more significant because K_{Ii} values were closer to the K_{ISCC} value.

Fractographic analyses were also performed on 304 (sensitized) specimens, but it was difficult to obtain good photographs because of extensive deformation in the samples. Nevertheless, the seacoast and accelerated-test specimens both exhibited similar intergranular fractures.

2699

SPECIMEN E27 SEACOAST SPECIMEN

$K_{Ii} = 28.4$ ksi $\sqrt{in}$

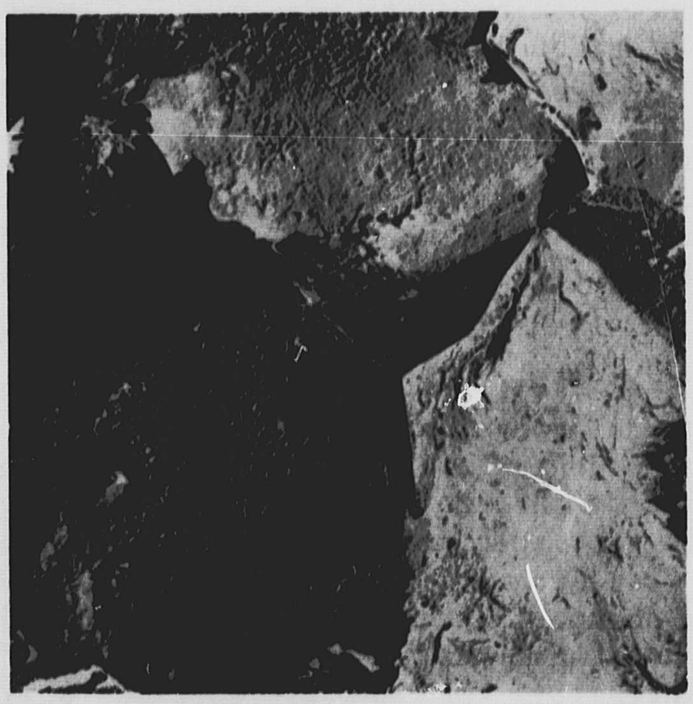

2702

SPECIMEN E26 ACCELERATED TEST

$K_{Ii} = 27.7$ ksi $\sqrt{in}$

FIGURE 25 ELECTRON FRACTOGRAPHS OF STRESS-CORROSION FRACTURES OF 410 (650F TEMPER) AT LOW STRESS INTENSITIES

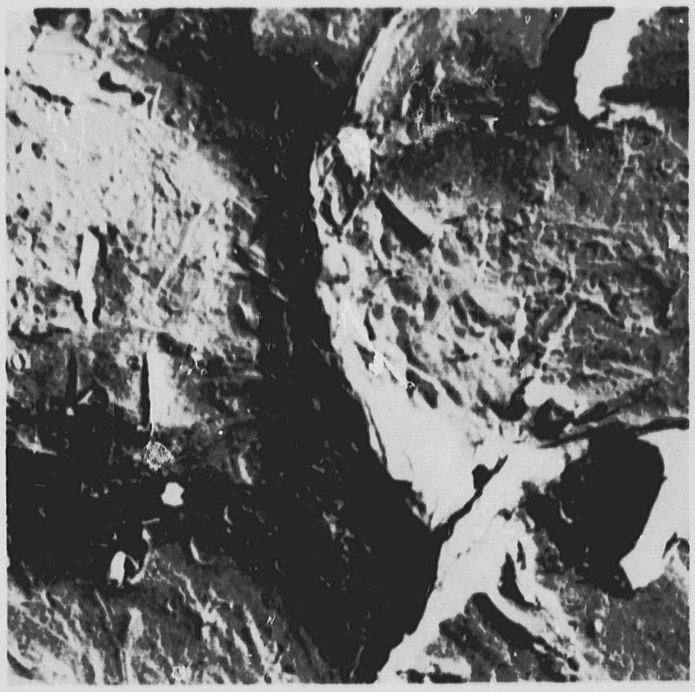

2217

INTERGRANULAR FRACTURE REGION

2208

TRANSGRANULAR FRACTURE REGION

SPECIMEN F7 SEACOAST TEST

$K_{Ii} = 44.1 \text{ ksi} \sqrt{\text{in}}$

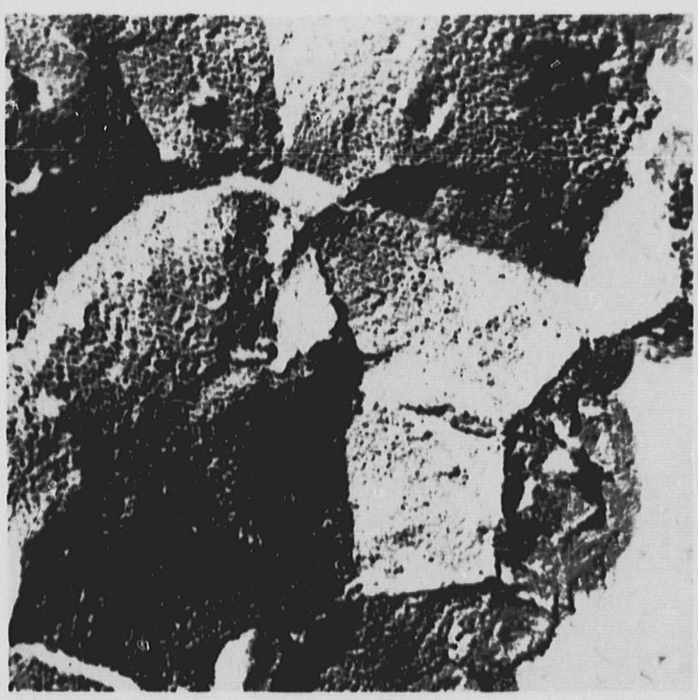

1773

INTERGRANULAR FRACTURE REGION

1769

TRANSGRANULAR FRACTURE REGION

SPECIMEN F29 ACCELERATED TEST

$K_{Ii} = 43.0 \text{ ksi} \sqrt{\text{in}}$

FIGURE 26 ELECTRON FRACTOGRAPHS OF STRESS-CORROSION FRACTURES OF 17-4 (H900)

1724

SPECIMEN G4 SEACOAST TEST
$K_{Ii} = 28.7$ ksi $\sqrt{in}$

1767

INTERGRANULAR FRACTURE REGION

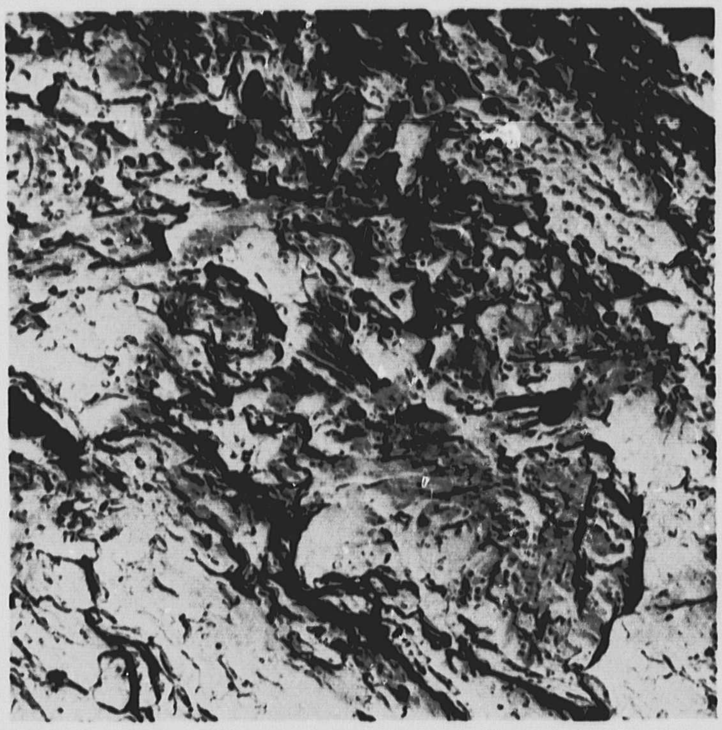

1768

QUASI-CLEAVAGE TRANSGRANULAR REGION

SPECIMEN G27 ACCELERATED TEST
$K_{Ii} = 27.0$ ksi $\sqrt{in}$

FIGURE 27 ELECTRON FRACTOGRAPHS OF STRESS-CORROSION FRACTURES OF AM355 (SCT850)

Electron fractographs of the fusion zone of 18Ni Maraging steel are shown in Figure 28. Both the seacoast and laboratory specimens showed a "pseudo"-intergranular fracture mode. The grain boundaries did not appear sharp and well defined as in other materials. the grain facets were mottled and slightly extended in appearance. This was probably related to the nature of the microstructure within the fusion zone. However, both seacoast and laboratory specimens were very similar in fracture topography.

In summary, some of the fractographic comparisons showed anomalies between seacoast-and accelerated-test specimens. However, none of these anomalies were observed in the stress-corrosion regions of specimens tested near threshold stress intensities. Therefore, fractography showed no definite differences in stress-corrosion failure mode for seacoast and accelerated tests. On the other hand, fractography did not prove that failure mechanisms were identical in both types of tests.

VALIDITY OF THE ACCELERATED TEST

Table XI shows a comparison of K_{ISCC} values obtained in the seacoast and accelerated tests on parent materials. The 17 conditions of material and heat treatment fell into three basic groups. Ten of these combinations were in Group A where K_{ISCC} values obtained in the accelerated test were essentially equivalent to those obtained at the seacoast. Four fell in Group B where K_{ISCC} values were in good agreement for seacoast and accelerated tests. The H-11(AM) 1100F, 4340 800F, and AM355 SCT850 in Group C exhibited significant differences in seacoast and accelerated K_{ISCC} values.

The reasons for the differences in seacoast and accelerated K_{ISCC} values for the Group C materials are not clearly known at present. However, the H-11 and 4340 alloys, which had higher K_{ISCC} values in seacoast tests, required long test times at the seacoast, and the specimen surfaces corroded severely. It is possible that the corrosion products restricted entry of corrodent into the crack thereby leading to a high apparent K_{ISCC}. It is also possible that failure modes in the seacoast and accelerated environments were different for these materials. Accelerated stress-corrosion tests conducted under anodic and cathodic polarization might provide some answer to the mechanism, particularly if polarization changed the K_{ISCC} to the same value observed at the seacoast.

The AM355 SCT850 in Group C exhibited a lower K_{ISCC} in the seacoast test than in the accelerated test. This disagreement was surprising in as much as all the other heat treatments applied to AM355 showed good-to-excellent agreement between seacoast- and accelerated- tests. The fractographic analyses showed some differences in failure modes at high stress intensities but not at lower stress intensities near the threshold values. Additional accelerated and seacoast tests are needed to check these results. Again, accelerated tests conducted under polarization would help to reveal reasons for the difference in K_{ISCC} values.

Stress-corrosion susceptibility of the parent materials in the seacoast and accelerated tests are compared in Table XII on the basis of K_{ISCC} values. With the exception of the above mentioned discrepancies for Group C materials, the relative ratings from the accelerated test were in good agreement with those of the seacoast test.

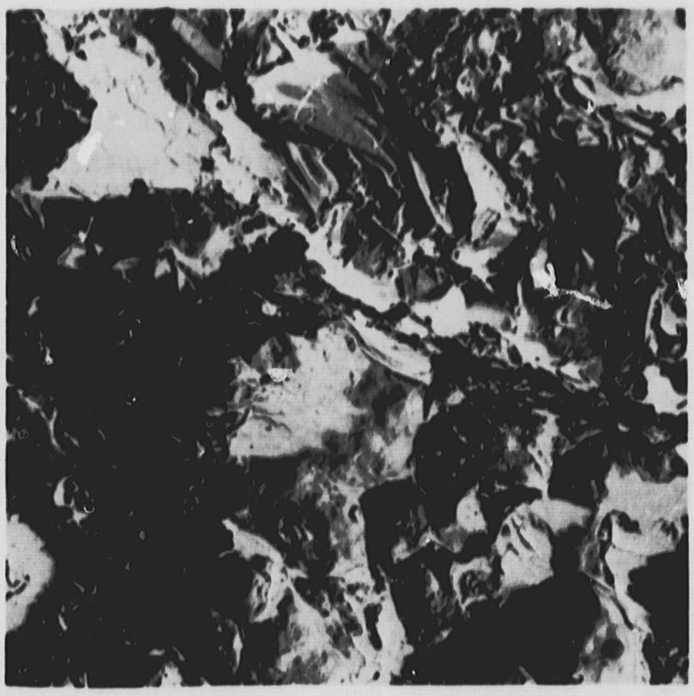

2516

SPECIMEN 2WB7 SEACOAST TEST

$K_I = 59.8 \text{ ksi} \sqrt{\text{in}}$

2693

SPECIMEN 2WB10 ACCELERATED TEST

$K_{Ii} = 51.2 \text{ ksi} \sqrt{\text{in}}$

FIGURE 28 ELECTRON FRACTOGRAPHS OF STRESS-CORROSION FRACTURES IN 18Ni-250 (900F) FUSION ZONES

TABLE XI

COMPARISON OF K_{ISCC} VALUES FOR SEACOAST AND ACCELERATED TESTS OF PARENT MATERIALS

MATERIAL & CONDITION	SEACOAST TEST K_{ISCC} (ksi$\sqrt{in}$)	ACCELERATED TEST K_{ISCC} (ksi$\sqrt{in}$)
Group A		
(1) H-11(VM) 1000F	11.4 ± 5.6	10.8 ± 1.9
(1) 4340 475F	13.3 ± 2.0	11.1 ± 1.1
(1) 410 650F	22.0 ± 6.4	23.8 ± 3.9
- 410 1125F	52.4 ± 7.5	49.6 ± 1.9
(1) 17-4 H900	< 38.5 (38 est)	40.3 ± 2.8
- 17-4 H1150	> 93.9	110 ± 12.0
(1) AM355 SCT850(FH)	< 9.7	~ 6.2
(1) 304 SENS.	< 8.5	< 15.2
- 304 ANN.	> 53.5	59.7 ± 9.4
- Inco 718 SAA	> 106	130 ± 1.0
Group B		
(1) H-11(AM) 1000F	16.7 ± 2.8	8.6 ± 1.4
(1) 18Ni(250) 900F	55.6 ± 7.6	72.9 ± 4.0
(1) AM355 SCT1000	24.5 ± 5.4	36.7 ± 4.0
(1) AM355 SCT1000(FH)	33.1 ± 3.6	50.3 ± 6.7
Group C		
(1) H-11(AM) 1000F	39.5 ± 4.4	23.2 ± 0.2
(1) 4340 800F	48.3 ± 5.5	29.7 ± 1.5
(1) AM355 SCT850	< 10.7	24.9 ± 2.1

K_{ISCC} = threshold stress intensity for stress corrosion - ksi$\sqrt{in}$

(1) = valid plane-strain threshold value

TABLE XII

STRESS-CORROSION SUSCEPTIBILITY OF PARENT MATERIALS

SEACOAST TEST		ORDER OF INCREASING SUSCEPTIBILITY TO STRESS CORROSION	ACCELERATED TEST	
K_{ISCC} (ksi $\sqrt{in}$)	MATERIAL & CONDITION		MATERIAL & CONDITION	K_{ISCC} (ksi $\sqrt{in}$)
> 106	Inco 718 SAA	1	Inco 718 SAA	130 ± 1.0
> 93.9	17-4 H1150	2	17-4 H1150	110 ± 12.0
55.6 ± 7.6	(1) 18Ni(250) 900F	3	(1) 18Ni(250) 900F	72.9 ± 4.0
> 53.5	304 ANN.	4	304 ANN.	59.7 ± 9.4
52.4 ± 7.5	410 1125F	5	(1) AM355 SCT1000(FH)	50.3 ± 6.7
48.3 ± 5.5	(1) 4340 800F	6	410 1125F	49.6 ± 1.9
39.5 ± 4.4	(1) H-11(AM) 1100F	7	(1) 17-4 H900	40.3 ± 2.8
< 38.5(38 est)	(1) 17-4 H900	8	(1) AM355 SCT1000	36.7 ± 4.0
33.1 ± 3.6	(1) AM355 SCT1000(FH)	9	(1) 4340 800F	2917 ± 1.5
24.5 ± 5.4	(1) AM355 SCT1000	10	(1) AM355 SCT850	24.9 ± 2.1
22.0 ± 6.4	(1) 410 650F	11	(1) 410 650F	23.8 ± 3.9
16.7 ± 2.8	(1) H-11(AM) 1000F	12	(1) H-11(AM) 1100F	23.2 ± 0.2
13.3 ± 2.0	(1) 4340 475F	13	(1) 4340 475F	11.1 ± 1.1
11.4 ± 5.6	(1) H-11(VM) 1000F	14	(1) H-11(VM) 1000F	10.8 ± 1.9
< 10.7	(1) AM355 SCT850	15	(1) H-11(AM) 1000F	8.6 ± 1.4
< 9.7	(1) AM355 SCT850(FH)	16	304 SENS.	< 15.2
< 8.5	(1) 304 SENS.	17	(1) AM355 SCT850(FH)	~ 6.2

K_{ISCC} = threshold stress intensity for stress corrosion - ksi $\sqrt{in}$

(1) = valid plane-strain threshold value

Table XIII shows a comparison of K_{ISCC} values obtained in the seacoast and accelerated tests on weldments. For the 4340 fusion zone and heat-affected zone, K_{ISCC} values for seacoast tests were slightly higher than K_{ISCC} values for accelerated tests. Nevertheless, the results were in good agreement and well within Group B. Threshold values for the fusion zone of 18Ni Maraging steel were in excellent agreement as were values for the fusion and heat-affected zones of AM355. The correlation between seacoast and accelerated results on the heat-affected zone of the Maraging steel is somewhat inconclusive but is estimated to be within Group B. The results of Table XIII indicate a good overall agreement between threshold levels for the weldments.

TABLE XIII

COMPARISON OF K_{ISCC} VALUES FOR SEACOAST AND ACCELERATED TESTS ON WELDMENTS

MATERIAL, CONDITION, AND DESCRIPTION	SEACOAST TEST K_{ISCC} (ksi $\sqrt{in}$)	ACCELERATED TEST K_{ISCC} (ksi $\sqrt{in}$)
<u>4340 Tempered at 475F</u>		
Fusion Zone	23.3 ± 3.8	14.8 ± 4.0
Heat-Affected Zone (2500F Peak Temp)	24.0 ± 6.0	16.7 ± 0.1
<u>18Ni Maraging Steel (250 Grade) Aged at 900F</u>		
Fusion Zone	27.8 ± 7.3	23.4 ± 4.5
Heat-Affected Zone (1200F Peak Temp)	< 54.1	61.6 ± 8.0
<u>AM355 SCT850 (Fully Hardened)</u>		
Fusion Zone	> 27.1	> 33.5
Heat-Affected Zone (2480F Peak Temp)	< 8.6	7.0 ± 1.8

K_{ISCC} = threshold stress intensity for stress corrosion - ksi $\sqrt{in}$

CONCLUSIONS

1. An accelerated, laboratory, stress-corrosion test was developed for high-strength, ferrous and nickel alloys based upon use of single-edge-notched and fatigue-cracked specimens tension-loaded in plane strain in a corrodent consisting of 200 gm. NaCl/liter of distilled water at room temperature.

2. A nominal specimen thickness of 1/4 inch was adequate for determining threshold stress intensities for stress corrosion under plane strain of all program materials except 410 1125F, 17-4 H1150, 304SS, and Inconel 718.

3. The accelerated test required a maximum test time of 1000 hours. Test times were one to three orders of magnitude shorter than test times required for similar specimens in a seacoast environment. The reduction in test time was produced by the aggressive corrodent, the presence of a crack, and the plane-strain loading conditions.

4. The test method was applicable to weldments and parent materials with the exception of 304 stainless steel. The 304 alloy failed by nucleation and growth of new stress-corrosion cracks rather than growth of the existing crack.

5. Twenty-three combinations of material, heat treatment, and welding were tested in a seacoast environment and compared to accelerated-test results. Threshold stress intensities for stress corrosion were in good-to-excellent agreement for 20 of these combinations. Only H-11(AM) 1000F, 4340 800F, and AM355 SCT850 showed discrepancies. Additional tests are needed to resolve the reasons for these discrepancies.

6. The applicability of a wedge-opening-loading specimen for stress-corrosion testing was confirmed. This specimen offers the advantage of reduced loading requirements. However, the single-edge-notched specimen is preferable to the wedge-opening-loading specimen where loading requirements are not an overriding consideration.

REFERENCES

1. Brown, B. F., "A New Stress-Corrosion Cracking Test for High-Strength Alloys," Materials Research and Standards, Volume VI, No. 3, pp. 129-133, March 1966

2. Wessel, E. T., State of the Art of the WOL Specimen for K_{Ic} Fracture Toughness Testing, Research Report 67-1D6-BTLFR-R1, Westinghouse Research Laboratories, Pittsburgh, Pennsylvania, March 22, 1967.

3. Freedman, A. H., Development of an Accelerated Stress-Corrosion Test for Ferrous and Nickel Alloys, NOR 67-12, Contract No. NAS 8-20333, Northrop Corporation, Norair Division, Hawthorne, California, February 1967.

4. Srawley, J. E., and Brown, W. F., "Fracture Toughness Testing," NASA TN D-2599, January 1965.

5. Payne, W. W., "Practical Specimens for K_{Ic} Measurement," Second Annual Workshop in Fracture Mechanics, Denver University (Denver, Colorado), August 1965.

6. Srawley, J. E., Jones, M. H., and Gross, B., "Experimental Determination of the Dependence of Crack Extension Force on Crack Length for a Single-Edge-Notched Tension Specimen," Proposed NASA Technical Note (Draft No. E-2392).

7. Freed, C. N., and Krafft, J. M., "Effect of Side Grooving on Measurements of Plane-Strain Fracture Toughness," text prepared for ASTM Fracture Testing Committee (E-24), May 1965.

8. Wilson, W. K., Optimization of WOL Brittle Fracture Test Specimen, Westinghouse Research Report 66-B40-BTLFR-R1, January 4, 1966.

9. Brown, S. F., "Stress-Corrosion Cracking and Corrosion Fatigue in High-Strength Steels," DMIC Report No. 210, Problems in the Load-Carrying Applications of High-Strength Steels, October, 1964.

10. "Fracture Toughness Testing and its Applications," ASTM STP 381, Am. Soc. Testing Mats., 1965.

11. Brown, W. F. Jr., Srawley, J. E., "Plane-Strain Crack-Toughness Testing of High-Strength Metallic Materials," ASTM STP 410, Am. Soc. Testing Mats., December 1967.

12. Wu, K. C., "A Study of the Weld Heat-Affected Zone of Centrifically Cast 5% Chromium Steel," Welding Journal, Research Supplement (42), page 392S, September 1963.

13. Wu, K. C., A Study of the Weld Heat-Affected Zones in Modified 4340 and 5% Chromium Steels, Watervliet Arsenal Report WVT-R1-6110-R, December 1961.

REFERENCES
(Continued)

14. Peterson, W. A., "Weld Heat-Affected Zone of 18% Nickel Maraging Steel," Welding Journal, Research Supplement (43), page 428S, September 1964.

15. Clark, D. S., Varney, W. R., Physical Metallurgy for Engineers, page 268, D. Van Nostrand Company, Inc., 1952.

16. Cox, P. H. S., Birkle, A. J., Reisdorf, B. G., and Pellissier, G. E., An Investigation of the Mechanical Properties and Microstructures of 18Ni(250) Maraging Steel Weldments, ASM Trans. Quarterly, Vol. 60, No. 2, June 1967.

17. Rolfe, S. T., Novak, S. R., and Gross, J. H., "Stress-Corrosion Testing of Ultraservice Steels Using Fatigue-Cracked Specimens," Paper No. 90 presented at the 69th annual meeting of the ASTM, Atlantic City, N. J., 27 June - 1 July, 1966.

18. Phillips, A., Kerlins, V., and Whiteson, B. V., Electron Fractography Handbook, 2 Volumes, TR ML-TDR-64-461, 1965.

APPENDIX A

SPECIMEN PREPARATION PROCEDURES

TABLE AI

PREPARATION PROCEDURES FOR PARENT MATERIAL SPECIMENS

I H-11

Annealed Condition

Machining

Enveloping

Encapsulate specimens in evacuated stainless steel sheet envelope.

Austenitizing

1. Preheat to 1150-1600F for 30 min.
2. Heat to 1850 ± 25F for 30 min.

Quenching

Rapid air cool below 150F

Tempering

280-300 ksi

Double temper 2 + 2 hrs. at 1000 ± 10F

220-240 ksi

Double temper 2 + 2 hrs. at 1100 ± 10F

Envelope Removal

Finish Machining

1. Surface grind ~ 0.010 inch from faces to finish at 0.230 ± 0.002 inch thickness.
2. Sand edges to remove oxide.
3. Side notch 220-240 ksi specimens.

Tension-Tension Fatigue-Cracking

280-300 ksi

Cycle 1000-4200 lb @ 3600 cpm (1000-4400 lb @ 1800 cpm) to start crack and 1000-3400 lb at either rate to grow crack.

220-240 ksi

Cycle 1000-4600 lb @ 3600 cpm to start crack and 1000-4000 lb to grow it. Or, at 1800 cpm use 1000-5300 lb and 1000-4600 lb.

II 4340

Annealed Condition

Machining

Enveloping

Encapsulate specimens in evacuated stainless steel sheet envelope.

Austenitizing

15 Min. at 1575 ± 20F

Quenching

Oil quench

Tempering

260-280 ksi

4 hrs. at 475 ± 10F

200-220 ksi

4 hrs. at 800 ± 10F

Envelope Removal

Finish Machining

1. Surface grind ~ 0.010 inch from faces to finish at 0.230 ± 0.002 inch thickness.
2. Sand edges to remove oxide.
3. Side notch specimens.

Tension-Tension Fatigue-Cracking

260-280 ksi

Cycle 1000-4600 lb @ 3600 cpm to start crack and 1000-4000 lb to grow it. Or, at 1800 cpm cycle 1000-4800 lb to start and grow.

200-220 ksi

Cycle 1000-4400 lb @ 3600 cpm or 1000-4900 lb @ 1800 cpm.

TABLE AI (Continued)

III 18Ni Maraging Steel

Solution Annealed Condition

Finish Machining

1. Surface grind ~ 0.010 inch from faces to finish at 0.230 ± 0.002 inch thickness.
2. Side notch.

Aging

Age 3 hrs. at 900 ± 10F in air and sand surfaces.

Tension-Tension Fatigue-Cracking

Cycle 1000-4000 lb @ 3600 cpm or 1000-4800 lb @ 1800 cpm.

IV 410 SS

Annealed Condition

Machining

Enveloping

Encapsulate specimens in evacuated stainless steel sheet envelope.

Austenitizing

23 ± 8 min. at 1750 ± 10F

Quenching

Rapid air cool

Tempering

2 hrs. at 650 ± 10F

2 hrs. at 1125 ± 10F

Envelope Removal

Finish Machining

1. Surface grind ~ 0.010 inch from faces to finish at 0.250 ± 0.002 inch thickness.
2. Side-notch those specimens tempered at 650F.
3. Sand edges to remove oxide.

Tension-Tension Fatigue-Cracking

650F Temper

Cycle 1000-4500 lb @ 3600 cpm or 1000-4700 lb @ 1800 cpm.

1125F Temper

Cycle 1000-5000 lb @ 3600 cpm or 1000-5300 lb @ 1800 cpm.

TABLE AI (Continued)

V 17-4PH

Condition A (Solution Treated)

Machining

Aging

H900

900 ± 10F for
1 hr. in air

H1150

1150 ± 10F for
4 hrs. in air

Finish Machining

1. Surface grind ~ 0.010 from faces to to finish at .250 ± .002 inch thickness.
2. Sand edges to remove oxide.
3. Side notch H1150 specimens.

Tension-Tension Fatigue-Cracking

H900

Cycle 1000-5000 lb
@ 3600 cpm.

H1150

Cycle 1000-5000 lb
@ 3600 or 1800 cpm.

VI AM355

Solution Annealed Condition

Machining

Austenite Conditioning

15 min. at 1750 ± 25F in vacuum followed by argon cool and refrigeration at -100F for 3 hrs. min.

Aging

SCT 850

3 hrs. at
850 ± 10F in air

SCT 1000

3 hrs. at
1000 ± 10F in air

Finish Machining

1. Surface grind ~ 0.010 inch from faces to finish at 0.250 ± 0.002 inch thickness.
2. Side notch SCT 1000 specimens.
3. Sand edges to remove oxide.

Tension-Tension Fatigue-Cracking

SCT 850

Cycle 1000-5000 lb
@ 3600 cpm or 1000-5700 lb @ 1800 cpm.

SCT 1000

Cycle 1000-5000 lb
@ 3600 cpm or 1000-5500 lb @ 1800 cpm.

TABLE AI (Continued)

VII AM355

Solution Annealed Condition

Machining

Sub-Zero Cooling

3 hrs. at -100F

Enveloping

Encapsulate specimens in evacuated envelope of stainless-steel foil.

Austenite Conditioning

15 min. at 1750 ± 25F followed by rapid air cool and refrigeration at -100F for 3 hours.

Aging

SCT850 (Fully Hardened)	SCT1000 (Fully Hardened)
3 hrs. at 850 ± 10F	3 hrs. at 1000 ± 10F

Envelope Removal

Finish Machining

1. Surface grind ~0.10 inch from faces to finish at 0.250 ± 0.002 inch thickness.
2. Side notch SCT 1000 specimens to a depth of 0.009 ± 0.001 inch.

Tension-Tension Fatigue-Cracking

Cycle 1000-5700 lb @ 1800 cpm.

TABLE AI (Continued)

VIII 304 SS

Annealed Condition

Sensitization

100 hrs. at 1100 ±10F in air

Finish Machining

1. Surface grind ~ 0.010 inch from faces to finish at 0.250 ± 0.002 inch thickness.
2. Side notch.

Tension-Tension Fatigue-Cracking

Cycle 1000-4100 lb @ 3600 cpm.

IX INCONEL 718

Solution Annealed Condition

1950F, air cool

Finish Machining

1. Surface grind 0.010 inch from faces to finish at 0.210 ± 0.002 inch thickness.
2. Side notch.

Aging

8 hrs. at 1350 ± 10F, furnace cool to 1200F for a total time of 23 hrs. in air, and sand surfaces to remove oxide.

Tension-Tension Fatigue-Cracking

Cycle 1000-5400 lb @ 1800 or 3600 cpm.

TABLE AII

PREPARATION PROCEDURES FOR FUSION AND HEAT-AFFECTED-ZONE SPECIMENS

4340 STEEL

Annealed Condition

Fusion-Zone Specimens

TIG Welding

1. Preheat to 400F-500F.
2. Post-heat for one hour at 600F.

X-Ray

Enveloping

Encapsulate specimens in evacuated envelope of stainless-steel foil.

Annealing

One-half hour at 1500F ± 25F, furnace cool.

Envelope Removal

Machining

1. Dress weld flush with parent material.
2. Machine to a width of 0.750 ± 0.002 inch.
3. Edge notch 0.100 ± 0.002 inch deep.

Enveloping

Encapsulate specimens in evacuated envelope of stainless-steel foil.

Heat Treating

1. Austenitize 15 min. at 1575 ± 25F.
2. Oil quench.
3. Temper 4 hrs. at 475F ± 10F.

Envelope Removal

Finish Machining

1. Surface grind ~ 0.010 inch from faces to finish at 0.230± 0.002 inch thickness.
2. Side notch 0.009 ± 0.001 inch deep.

Tension-Tension Fatigue-Cracking

Cycle 1000-4800 lb @ 1800 cpm.

Synthetic Heat-Affected-Zone Specimens

Machine Blanks

Thermal-Cycling Exposure

Enveloping

Encapsulate specimens in evacuated envelope of stainless-steel foil.

Annealing

One-half hour at 1500F ± 25F, furnace cool.

Envelope Removal

Machining

Edge notch 0.110 ± 0.002 inch deep.

Enveloping

Encapsulate specimens in evacuated envelope of stainless-steel foil.

Heat Treating

1. Austenitize 15 min. at 1575F ± 25F.
2. Oil quench.
3. Temper 4 hrs. at 475F.

Envelope Removal

Finish Machining

1. Surface grind ~ 0.010 inch from edges and faces to finish at a thickness of 0.230 ± 0.002 inch and a width of 0.750 ± .002 inch.
2. Side notch to a depth of 0.009 ± 0.001 inch.

Tension-Tension Fatigue-Cracking

For peak temps. of 2500F and 2300F, cycle 1000-2800 lb @ 1800 cpm. For 2000F peak temperature use 1000-4800 lb at 1800 cpm.

TABLE AII (Continued)

18Ni Maraging Steel

Solution Annealed Condition

Fusion-Zone Specimens

TIG Welding

X-Ray

Finish Machining

1. Dress weld flush with parent material.
2. Surface grind ~0.010 inch from faces to finish at 0.230 ± 0.002 inch thickness.
3. Edge notch 0.100 ± 0.002 inch deep.
4. Side notch 0.009 ± 0.001 inch deep.

Enveloping

Encapsulate specimens in evacuated envelope of stainless-steel foil.

Aging

Age 3 hrs. at 900 ± 10F.

Envelope Removal

Tension-Tension Fatigue-Cracking

Cycle 1000-4600 lb @ 1800 cpm.

Synthetic Heat-Affected-Zone Specimens

Machine Blanks

Thermal-Cycling

Finish Machining

1. Surface grind ~0.010 inch from edges and faces to finish at a thickness of 0.230 ± 0.002 inch and a width of 0.750 ± 0.002 inch.
2. Edge notch 0.100 ± 0.002 inch deep.
3. Side notch 0.009 ± 0.001 inch deep.

Enveloping

Encapsulate specimens in evacuated envelope of stainless-steel foil.

Aging

Age 3 hrs. at 900 ± 10F.

Envelope Removal

Tension-Tension Fatigue-Cracking

Cycle 1000-5100 lb @ 1800 cpm.

TABLE AII (Continued)

AM355 (FULLY HARDENED)

Solution Annealed Condition

Fusion-Zone Specimens

TIG Welding

X-Ray

Machining

1. Dress weld flush with parent material.
2. Machine to a width of 0.750 ± 0.002 inch.
3. Edge notch 0.100 ± 0.002 inch deep.

Sub-Zero Cooling

3 hrs. at -100F

Enveloping

Encapsulate specimens in evacuated envelope of stainless-steel foil.

Austenite Conditioning

15 min. at 1750F ± 25F followed by rapid air cool and refrigeration at -100F for 3 hours.

Aging (SCT 850)

3 hrs. at 850F ± 10F

Envelope Removal

Finish Machining

1. Surface grind ~ 0.010 from faces to finish at 0.250 ± 0.002 inch thickness.

Tension-Tension Fatigue-Cracking

Cycle 1000-5700 lb @ 1800 cpm.

Synthetic Heat-Affected-Zone Specimens

Machine Blanks

Thermal Cycling Exposure

Machining

Edge notch 0.110 ± 0.002 inch deep.

Sub-Zero Cooling

3 hrs. at -100F

Enveloping

Encapsulate specimens in evacuated envelope of stainless-steel foil.

Austenite Conditioning

15 min. at 1750F ± 25F followed by rapid air cool and refrigeration at -100F for 3 hours.

Aging (SCT 850)

3 hrs. at 850F ± 10F

Envelope Removal

Finish Machining

1. Surface grind ~ 0.010 inch from edges and faces to finish at a thickness of 0.230 ± 0.002 inch and a width of 0.750 ± 0.002 inch.

Tension-Tension Fatigue-Cracking

Cycle 1000-5200 lb @ 1800 cpm.

APPENDIX B

SEACOAST AND ACCELERATED STRESS-CORROSION TESTS

TABLE BI

SEACOAST STRESS-CORROSION TESTS OF PARENT MATERIALS

SPEC NO	W (in)	B (in)	B_N (in)	a_o (in)	a_f (in)	P (lbs)	$t^{(1)}$ (hrs)	K_{Ii} (ksi$\sqrt{in}$)	$\frac{K_{Ii}}{K_{Ix}}$	NOTES
H-11 (Air Melted) Tempered at 1000F										
A15	0.751	0.230	-	0.272	0.272	3000	305	30.6	0.959	Sm.local SC region
A38	0.750	0.231	-	0.245	0.325	3000	714F	26.7	0.837	
A33	0.750	0.230	-	0.261	0.363	2000	506F	19.4	0.608	
A41	0.750	0.230	-	0.197	0.197	2000	7627	13.9	0.436	No SC
A45	0.750	0.230	-	0.210	0.210	1010	5225	7.5	0.236	No SC
H-11 (Vacuum Melted) Tempered at 1000F										
D9	0.750	0.230	-	0.232	0.462	2030	4203F	17.0	0.597	
D23	0.749	0.230	-	0.159	0.159	1000	5059	5.7	0.201	No SC
H-11 (Air Melted) Tempered at 1100F										
A6	0.750	0.229	0.187	0.255	0.288	6000	1279F	65.9	1.03	
A47	0.750	0.230	0.215	0.276	0.276	4000	4676	43.9	0.690	Local SC verified by fractography
A4	0.750	0.230	0.185	0.266	0.266	3000	11495	35.1	0.551	No SC
A46	0.749	0.230	0.211	0.316	0.316	2030	7627	27.4	0.430	No SC
A25	0.750	0.209	0.188	0.217	0.217	2000	3572	18.4	0.289	No SC
A26	0.750	0.209	0.191	0.205	0.205	1000	4000	8.5	0.134	No SC
4340 Tempered at 475F										
C6	0.749	0.229	0.181	0.255	0.386	4000	49F	45.1	0.968	Failures occurred during rain periods
C9	0.750	0.230	0.190	0.254	0.338	4000	224F	43.2	0.928	
C5	0.749	0.232	0.184	0.237	0.359	3000	305F	30.4	0.653	
C31	0.750	0.230	0.187	0.258	0.430	2000	4748F	22.3	0.478	
C46	0.750	0.229	0.212	0.201	0.452	2030	190F	15.3	0.329	
C32	0.750	0.230	0.193	0.265	0.265	1000	8818	11.3	0.242	No SC
4340 Tempered at 800F										
C19	0.750	0.232	0.190	0.256	0.343	6000	978F	65.2	0.972	
C18	0.749	0.232	0.196	0.258	0.330	5000	2009F	53.8	0.802	
C17	0.750	0.232	0.195	0.256	0.256	4000	9460	42.7	0.637	No SC verified by fractography
C16	0.750	0.232	0.190	0.230	0.230	3000	12843	28.6	0.426	No SC
C57	0,750	0.229	0.208	0.280	0.280	2030	7627	23.3	0.347	No SC
18Ni Maraging Steel (250 Grade) Aged at 900F										
B6	0.749	0.229	0.185	0.275	-	8000	4208F	98.1	0.884	
B5	0.749	0.229	0.188	0.245	0.335	9000	1774F	93.8	0.844	SC verified by fractography
B19	0.749	0.229	0.185	0.247	-	8000	4040F	85.3	0.768	
B16	0.749	0.229	0.187	0.251	-	6000	7202	64.8	0.584	SC verified by fractography
B23	0.749	0.229	0.212	0.209	0.298	8000	4130F	63.2	0.569	
B3	0.749	0.229	0.187	0.228	0.228	5000	11657	47.9	0.431	No SC

TABLE BI (Cont'd)

SPEC NO	W (in)	B (in)	B_N (in)	a_o (in)	a_f (in)	P (lbs)	$t^{(1)}$ (hrs)	K_{Ii} (ksi$\sqrt{in}$)	K_{Ii}/K_{Ix}	NOTES
410 Tempered at 650F										
E6	0.750	0.250	0.206	0.280	-	8000	1659F	90.5	0.992	
E5	0.748	0.250	0.208	0.304	0.350	6000	1594F	76.0	0.834	
E4	0.750	0.250	0.211	0.268	0.435	5000	5002F	52.4	0.574	
E28	0.748	0.250	0.204	0.239	0.435	4000	3584F	37.3	0.409	
E27	0.748	0.250	0.203	0.241	0.530	3000	5706F	28.4	0.312	
E29	0.749	0.250	0.203	0.250	0.250	2000	4887	15.5	0.169	No SC
410 Tempered at 1125F										
E15	0.750	0.251	-	0.266	0.266	9000	2544	81.9	0.864	Sm.local SC region
E37	0.750	0.250	-	0.284	0.284	6000	5004	59.9	0.632	Intergranular SC verified by fractography
E16	0.750	0.251	-	0.263	0.263	5000	4923	44.8	0.472	No SC
E14	0.750	0.251	-	0.274	0.274	4000	9437	37.9	0.399	No SC
E39	0.750	0.250	-	0.248	0.248	3000	3425	25.0	0.264	No SC
17-4 H900										
F10	0.749	0.251	-	0.262	0.262	6000	2407	53.6	0.965	Sm.local SC region
F7	0.749	0.252	-	0.260	-	5000	4849F	44.1	0.794	SC verified by fractography
F2	0.741	0.251	-	0.273	0.437	4000	9460	38.5	0.694	
17-4 H1150										
F19	0.749	0.251	0.199	0.258	0.258	9000	2544	93.9	0.771	No SC
F18	0.749	0.251	0.210	0.262	0.262	8000	9844	81.7	0.670	No SC
F17	0.749	0.251	0.202	0.230	0.230	4000	4831	35.7	0.293	No SC
F16	0.749	0.251	0.196	0.244	0.244	3000	11581	29.5	0.242	No SC
AM355 SCT850										
G7	0.751	0.249	-	0.265	0.305	5000	488F	45.5	0.952	
G5	0.752	0.249	-	0.260	0.390	4000	1857F	35.4	0.741	SC verified by fractography
G4	0.750	0.250	-	0.275	0.487	3000	1379F	28.7	0.601	
G32	0.750	0.251	-	0.232	0.427	3000	1103F	23.0	0.482	
G34	0.750	0.251	-	0.205	0.537	2000	1297F	13.3	0.279	
G35	0.750	0.251	-	0.299	0.439	1000	4530	10.7	0.223	
AM355 SCT1000										
G16	0.751	0.251	0.212	0.262	0.262	9000	2544	90.9	0.900	No SC
G15	0.751	0.251	0.211	0.247	0.247	8000	4208F	75.2	0.746	Local SC region
G14	0.752	0.251	0.215	0.283	0.379	6000	3268F	66.3	0.647	
G39	0.749	0.251	0.231	0.250	0.451	5000	2553F	44.8	0.444	
G20	0.751	0.251	0.207	0.227	0.473	5000	5254F	43.0	0.426	
G13	0.751	0.251	0.209	0.223	0.464	4000	7668F	33.4	0.331	
G42	0.750	0.251	0.230	0.215	0.546	4000	1847F	29.9	0.296	
G43	0.750	0.251	0.232	0.263	0.263	2000	2323	19.0	0.188	No SC

TABLE BI (Cont'd)

SPEC NO	W (in)	B (in)	B_N (in)	a_o (in)	a_f (in)	P (lbs)	$t^{(1)}$ (lbs)	K_{Ii} (ksi$\sqrt{in}$)	$\frac{K_{Ii}}{K_{Ix}}$	NOTES
AM355 SCT850 (Fully Hardened)										
1G4	0.750	0.249	-	0.252	0.410	5000	647F	42.7	0.686	
1G3	0.748	0.249	-	0.267	0.479	4000	980F	37.1	0.596	
1G7	0.750	0.249	-	0.247	0.516	3000	859F	25.0	0.401	
1G6	0.749	0.250	-	0.239	0.562	2030	4099F	16.2	0.260	
1G12	0.750	0.250	-	0.278	0.393	1000	4530	9.7	0.156	
AM355 SCT1000 (Fully Hardened)										
1G18	0.751	0.250	0.233	0.302	0.383	8000	1522F	91.5	0.799	
1G15	0.751	0.250	0.232	0.264	0.455	6000	3211F	57.2	0.487	
1G17	0.750	0.250	0.232	0.191	0.400	8000	2004F	52.5	0.446	
1G16	0.751	0.250	0.232	0.256	0.448	4000	2984F	36.7	0.313	
1G24	0.750	0.250	0.233	0.270	0.270	3000	4405	29.5	0.251	No SC
304 Sensitized										
H4	0.749	0.254	0.214	0.222	0.262	6000	804F	49.1	0.718	New SC cracks formed above and below side notches and fatigue crack grew by SC
H3	0.749	0.253	0.214	0.240	0.240	5000	3610F	44.9	0.655	
H7	0.749	0.254	0.214	0.228	-	3000	4627F	25.3	0.370	
H26	0.751	0.250	0.209	0.225	-	2000	5043F	16.9	0.247	New SC cracks formed above and below side notches - no growth of fatigue crack by SC
H28	0.750	0.250	0.206	0.223	0.223	1000	2323	8.5	0.124	
304 Annealed										
H15	0.742	0.254	0.203	0.228	0.228	6000	4530	53.5	0.774	No SC
H14	0.741	0.254	0.212	0.198	0.198	5000	9599	36.9	0.534	No SC
Inconel 718 Solution Annealed and Aged										
I4	0.749	0.211	0.166	0.270	0.270	8000	9844	106.	0.869	No SC
I16	0.749	0.210	0.164	0.264	0.264	8000	6883	104.	0.852	No SC
I5	0.749	0.211	0.170	0.243	0.243	9000	2544	102.	0.835	No SC
I3	0.749	0.211	0.168	0.264	0.264	5000	4782	63.7	0.523	No SC

NOTE: (1) F after test time denotes failure of specimen.

TABLE BII

SEACOAST STRESS-CORROSION TESTS OF FUSION ZONES AND SYNTHETIC HEAT-AFFECTED ZONES

SPEC NO	W (in)	B (in)	B_N (in)	a_o (in)	a_f (in)	P (lbs)	$t^{(1)}$ (hrs)	K_{Ii} ksi$\sqrt{in}$	$\frac{K_{Ii}}{K_{Ix}}$	NOTES
4340 Tempered at 475F										
Fusion Zone										
2WC15	0.750	0.231	0.213	0.236	0.397	3000	1108F	27.1	0.538	
3WC3	0.750	0.230	0.215	0.252	0.252	2000	5486	19.5	0.387	No SC
3WC13	0.750	0.231	0.217	0.190	0.190	2000	5222	14.0	0.278	No SC verified by fractography
3WC8	0.750	0.230	0.210	0.241	0.241	1000	5469	9.4	0.186	No SC
3WC12	0.750	0.230	0.214	0.145	0.145	1010	5225	5.7	0.113	No SC
Heat-Affected Zone - 2500F Peak Temp.										
GC23	0.750	0.230	0.215	0.257	-	3000	1404F	30.0	0.500	
GC24	0.750	0.230	0.214	0.236	0.236	2000	3632	18.0	0.299	No SC
GC25	0.750	0.230	0.213	0.207	0.207	1000	4530	7.8	0.129	No SC
18Ni Maraging Steel (250 Grade) Aged at 900F										
Fusion Zone										
2WB5	0.749	0.229	0.211	0.303	0.397	5000	861F	63.6	0.970	
2WB7	0.749	0.229	0.212	0.254	-	6000	646F	59.8	0.913	
2WB12	0.751	0.228	0.210	0.259	0.288	4000	4634	41.1	0.627	Definite SC
2WB13	0.750	0.228	0.206	0.282	0.300	3000	4205	35.1	0.536	SC
2WB11	0.750	0.229	0.208	0.256	0.256	2000	3632	20.4	0.311	No SC
Heat-Affected Zone - 1200F Peak Temp.										
GB11	0.750	0.230	0.211	0.248	0.277	8000	2323	77.4	0.659	
GB10	0.749	0.230	0.211	0.219	0.241	8000	4044	66.8	0.569	
GB8	0.749	0.230	0.204	0.255	0.302	6000	3940	61.8	0.527	SC verified by fractography
GB9	0.749	0.230	0.207	0.267	0.278	5000	3821	54.1	0.461	Definite SC
AM355 SCT850 (Fully Hardened)										
Fusion Zone										
1W1G4	0.752	0.250	-	0.265	0.460	3000	1224F	27.1	0.594	No intergranular SC verified fractographically - failure may be from H embrittlement.
2W1G13	0.753	0.251	-	0.248	0.248	2000	3472	16.5	0.361	No SC
1W1G9	0.752	0.248	-	0.258	0.258	1010	5225	8.9	0.195	No SC
Heat-Affected Zone - 2480F Peak Temp.										
G1G4	0.750	0.230	-	0.256	0.450	3000	843F	28.3	0.731	
G1G5	0.750	0.230	-	0.249	0.452	2000	1295F	18.2	0.471	
G1G6	0.750	0.230	-	0.238	0.679	1000	1414F	8.6	0.223	

NOTE: (1) F after test time denotes failure of specimen.

TABLE BIII

ACCELERATED STRESS-CORROSION TESTS OF PARENT MATERIALS

SPEC NO	W (in)	B (in)	B_N (in)	a_o (in)	a_f (in)	P (lbs)	$t^{(1)}$ (hrs)	K_{Ii} (ksi$\sqrt{in}$)	$\frac{K_{Ii}}{K_{Ix}}$	Notes
H-11 (Vacuum Melted) Tempered at 1000F										
D7	0.750	0.230	-	0.230	0.296	3000	137F	24.8	0.745	
D4	0.750	0.230	-	0.253	0.353	2000	307F	18.6	0.653	
D6	0.750	0.230	-	0.179	0.371	2000	570F	12.7	0.446	
D2	0.750	0.230	-	0.243	0.243	1000	1031	8.8	0.310	No SC
H-11 (Air Melted) Tempered at 1000F										
A40	0.750	0.230	-	0.262	0.332	3000	4.05F	29.2	0.915	Intergranular SC verified by fractography
A19	0.751	0.230	-	0.242	0.360	2000	373F	17.5	0.549	
A42	0.750	0.230	-	0.174	-	2000	899F	12.3	0.386	
A36	0.750	0.231	-	0.268	0.506	1000	579F	10.0	0.313	
A18	0.751	0.230	-	0.205	0.205	1000	1031	7.2	0.227	NO SC
H-11 (Air Melted) Tempered at 1100F										
A8	0.750	0.229	0.191	0.242	0.406	6000	207F	60.7	0.954	
A7	0.750	0.229	0.179	0.258	0.444	5000	163F	57.6	0.906	Intergranular SC verified by fractography
A48	0.746	0.230	0.215	0.292	-	4000	275F	47.9	0.753	
A49	0.750	0.230	0.211	0.269	-	3000	522F	32.3	0.508	
A9	0.750	0.229	0.188	0.234	0.510	3000	398F	29.5	0.464	
A24	0.750	0.209	0.185	0.290	0.509	2000	795F	26.9	0.423	
A10	0.748	0.229	0.188	0.135	0.519	4000	400F	23.6	0.371	
A27	0.750	0.209	0.191	0.187	-	3000	702F	23.4	0.367	
A29	0.750	0.209	0.190	0.262	0.262	2000	995F	23.0	0.362	No SC
A50	0.749	0.230	0.212	0.169	-	2000	958	12.8	0.207	No SC verified by fractography
4340 Tempered at 475F										
C13	0.750	0.230	0.186	0.226	0.321	3780	0.26F	35.9	0.770	
C28	0.751	0.230	0.190	0.255	0.388	3000	0.83F	32.4	0.695	
C50	0.751	0.230	0.211	0.177	0.326	4000	0.2F	26.7	0.573	
C49	0.751	0.230	0.213	0.117	0.338	5000	0.1F	24.5	0.525	
C27	0.749	0.230	0.194	0.265	0.454	2000	200F	22.5	0.483	
C47	0.750	0.229	0.211	0.241	0.427	2000	5.0F	18.7	0.401	
C51	0.750	0.229	0.211	0.134	0.401	3000	0.9F	16.1	0.345	
C54	0.751	0.230	0.212	0.168	0.418	2000	6.9F	12.7	0.273	
C48	0.751	0.230	0.210	0.157	0.542	2000	1062F	12.1	0.259	
C26	0.748	0.230	0.191	0.239	0.239	1000	670	10.0	0.215	No SC
C56	0.751	0.230	0.212	0.176	0.176	1500	989	9.9	0.213	No SC

TABLE BIII (Cont'd.)

SPEC NO	W (in)	B (in)	B_N (in)	a_o (in)	a_f (in)	P (lbs)	$t^{(1)}$ (hrs)	K_{Ii} (ksi$\sqrt{in}$)	$\frac{K_{Ii}}{K_{Ix}}$	NOTES
4340 Tempered at 800F										
C22	0.749	0.232	0.186	0.241	0.360	5000	8.7F	51.3	0.765	
C25	0.748	0.232	0.185	0.241	0.328	4000	7-19F	41.3	0.615	
C20	0.749	0.232	0.189	0.237	0.306	4000	5.8F	39.7	0.592	
C39	0.750	0.210	0.188	0.221	0.368	4000	295F	37.5	0.559	
C21	0.749	0.232	0.184	0.270	0.389	3000	162F	36.0	0.537	
C40	0.750	0.210	0.186	0.239	0.358	3000	488F	31.2	0.464	
C38	0.745	0.210	0.188	0.219	0.219	3000	940	28.2	0.420	No SC
C24	0.749	0.232	0.184	0.244	0.244	2000	712	21.0	0.313	No SC
18Ni Maraging Steel (250 Grade) Aged at 900F										
B9	0.749	0.229	0.187	0.261	0.280	9000	4.2F	102.0	0.917	Similar textures
B14	0.750	0.229	0.185	0.241	0.263	8000	77.2F	82.5	0.741	in SC and over-
B21	0.750	0.229	0.213	0.257	-	8000	25.4F	80.5	0.723	load regions
B22	0.750	0.229	0.209	0.245	0.431	8000	98.7F	76.8	0.690	
B15	0.750	0.229	0.186	0.263	0.263	6000	677	68.9	0.619	No SC verified by
B13	0.749	0.229	0.187	0.217	0.217	5000	950	45.2	0.406	No SC fractography
B12	0.749	0.229	0.184	0.246	0.246	4000	1000	42.6	0.383	No SC
410 Tempered at 650F										
E25	0.749	0.250	0.202	0.243	0.359	8000	18.1F	76.5	0.838	
E21	0.749	0.250	0.204	0.253	0.342	6000	11.5F	59.9	0.656	
E24	0.748	0.250	0.202	0.267	0.451	4000	32.3F	43.3	0.474	
E26	0.749	0.250	0.205	0.238	0.493	3000	340F	27.7	0.303	
E32	0.749	0.250	0.235	0.273	0.273	2000	958	19.9	0.218	No SC
E23	0.749	0.250	0.204	0.248	0.248	2000	712	19.5	0.213	No SC
E31	0.750	0.250	0.236	0.186	0.186	3000	939	18.9	0.207	No SC
410 Tempered at 1125F										
E19	0.751	0.251	-	0.260	0.395	9000	47.2F	79.3	0.835	Mixed-mode SC
E18	0.750	0.251	-	0.266	0.349	8000	66.4F	72.8	0.767	
E41	0.750	0.250	-	0.259	0.428	6000	460F	52.9	0.558	
E40	0.749	0.250	-	0.235	0.281	6600	935	51.5	0.543	
E20	0.749	0.250	-	0.238	0.269	6000	677	47.7	0.502	No SC
E38	0.749	0.250	-	0.243	0.264	5000	992	40.8	0.429	No SC
E17	0.750	0.251	-	0.260	0.260	4000	552	35.3	0.372	No SC
E42	0.750	0.250	-	0.223	0.243	4000	1020	29.3	0.309	No SC
17-4 H900										
F35	0.741	0.251	-	0.255	-	6000	157F	52.8	0.950	
F29	0.750	0.251	-	0.255	0.320	5000	72F	43.0	0.773	SC verified
F26	0.750	0.251	-	0.272	-	4000	710	37.5	0.674	No SC

TABLE BIII (Cont'd)

SPEC NO	W (in)	B (in)	B_N (in)	a_o (in)	a_f (in)	P (lbs)	$t^{(1)}$ (hrs)	K_{Ii} (ksi$\sqrt{in}$)	$\frac{K_{Ii}}{K_{Ix}}$	NOTES
17-4 H1150										
F25	0.749	0.229	0.206	0.290	0.290	8000	70.5F	97.4	0.798	No SC - overload failure verified by fractography
F23	0.749	0.251	0.208	0.288	0.288	8000	152F	93.6	0.767	
F21	0.749	0.251	0.209	0.235	0.235	9000	549	80.4	0.659	No SC
F38	0.746	0.251	0.233	0.264	0.264	8000	484	77.0	0.631	No SC
F20	0.749	0.251	0.210	0.246	0.246	8000	900	75.4	0.618	No SC
F22	0.749	0.251	0.209	0.250	0.250	5000	950	48.3	0.396	No SC
F15	0.749	0.251	0.209	0.252	0.252	4000	976	39.0	0.320	No SC
AM355 SCT850										
G22	0.751	0.250	-	0.268	0.440	5000	7.9F	46.0	0.962	
G28	0.751	0.250	-	0.256	0.473	4000	24.5F	34.7	0.726	SC verified by fractography
G27	0.750	0.250	-	0.263	0.509	3000	194F	27.0	0.565	
G33	0.751	0.251	-	0.231	0.231	3000	939	22.8	0.477	No SC
G26	0.750	0.250	-	0.266	0.266	2000	712	18.3	0.383	No SC
AM355 SCT1000										
G19	0.751	0.251	0.209	0.251	0.417	8000	37.5F	77.3	0.765	
G18	0.750	0.250	0.212	0.270	0.434	6000	105F	63.3	0.626	
G40	0.751	0.251	0.232	0.268	0.472	5000	61.4F	48.6	0.481	
G41	0.751	0.250	0.233	0.233	0.452	5000	45.3F	40.6	0.402	
G17	0.751	0.251	0.215	0.223	0.223	4000	1001	32.7	0.324	No SC
AM355 SCT850 Fully Hardened										
1G1	0.750	0.250	-	0.256	0.516	4000	52.7F	34.7	0.557	
1G2	0.750	0.250	-	0.264	0.530	3000	350F	27.1	0.435	
1G10	0.750	0.249	-	0.218	0.550	3000	77.2F	21.5	0.345	
1G11	0.750	0.250	-	0.265	0.571	2000	128F	18.2	0.292	
1G13	0.750	0.250	-	0.281	0.381	1000	885	9.8	0.158	Definite SC crack growth
AM355 SCT1000 Fully Hardened										
1G13	0.750	0.250	0.229	0.270	0.365	8000	49.9F	79.6	0.677	
1G22	0.750	0.250	0.230	0.254	0.412	8000	32.9F	73.2	0.623	
1G23	0.751	0.250	0.232	0.263	0.509	6000	88.6F	57.0	0.485	
1G21	0.751	0.250	0.230	0.245	0.245	5000	950	43.6	0.371	No SC
1G14	0.751	0.251	0.231	0.253	0.253	3000	983	27.1	0.231	No SC

TABLE BIII (Cont'd)

SPEC NO	W (in)	B (in)	B_N (in)	a_o (in)	a_f (in)	P (lbs)	$t^{(1)}$ (hrs)	K_{Ii} (ksi$\sqrt{in}$)	$\frac{K_{Ii}}{K_{Ix}}$	NOTES
304 Sensitized 100 hrs. at 1100F										
H9	0.748	0.254	0.208	0.245	0.354	5000	157F	47.2	0.690	New SC cracks formed above and below side notches and fatigue crack grew by SC
H22	0.749	0.248	0.209	0.226	0.355	5000	180F	42.8	0.624	
H25	0.751	0.250	0.207	0.216	0.400	4000	448F	32.5	0.474	
H24	0.749	0.249	0.204	0.226	0.407	3000	551F	26.1	0.[illegible]81	
H10	0.746	0.254	0.199	0.253	0.253	2000	958	20.4	0.298	New SC cracks formed above and below side notches--no growth of fatigue crack by SC
H23	0.750	0.249	0.208	0.227	0.227	2000	336	17.2	0.252	
H27	0.750	0.249	0.206	0.123	0.123	3000	939	15.2	0.222	
304 Annealed										
H17	0.749	0.254	0.204	0.220	0.220	6000	677	50.4	0.729	No SC
H16	0.740	0.254	0.200	0.200	0.200	5000	950	39.1	0.566	No SC
H18	0.749	0.254	0.215	0.230	0.230	4000	968	34.0	0.492	No SC
Inconel 718 Solution Annealed and Aged										
I14	0.749	0.208	0.167	0.311	0.311	8000	862	129	0.962	No SC
I10	0.749	0.210	0.164	0.246	0.246	9000	509	107	0.797	No SC
I6	0.746	0.209	0.171	0.291	0.291	4000	847	58.0	0.433	No SC

NOTE: (1) F after test time denotes failure of specimen.

TABLE BIV

ACCELERATED STRESS-CORROSION TESTS OF FUSION ZONES & SYNTHETIC HEAT-AFFECTED ZONES

SPEC NO	W (in)	B (in)	B_N (in)	a_o (in)	a_f (in)	P (lbs)	$t^{(1)}$ (hrs)	K_{Ii} (Ksi$\sqrt{in}$)	$\frac{K_{Ii}}{K_{Ix}}$	NOTES
4340 Tempered at 475F										
Fusion Zone										
3WC6	0.750	0.230	0.213	0.279	0.450	2000	18.3F	22.4	0.446	
2WC16	0.749	0.231	0.214	0.244	0.447	2000	40F	18.8	0.374	
3WC14	0.750	0.231	0.218	0.143	0.143	2000	988	10.9	0.217	No SC
3WC5	0.749	0.230	0.212	0.222	0.222	1000	967	8.5	0.169	No SC
Heat-Affected Zone -2500F Peak Temp.										
GC26	0.751	0.230	0.211	0.197	0.417	3000	1.5F	22.2	0.369	
GC32	0.751	0.230	0.213	0.144	0.394	3000	2.1F	16.8	0.280	
GC27	0.751	0.230	0.214	0.221	0.221	2000	1055	16.6	0.276	No SC
GC28	0.751	0.230	0.213	0.206	0.206	1000	959	7.7	0.128	No SC
Heat-Affected Zone - 2300F Peak Temp.										
GC11	0.750	0.230	0.212	0.236	0.374	3000	0.4F	27.2	0.450	
GC12	0.750	0.230	0.215	0.249	0.468	2000	515F	19.2	0.317	
GC17	0.750	0.230	0.214	0.302	0.302	1250	1005	15.6	0.258	No SC
GC14	0.750	0.230	0.212	0.232	0.232	1000	959	8.9	0.147	No SC
Heat-Affected Zone - 2000F Peak Temp.										
GC2A	0.750	0.229	0.213	0.259	0.368	3000	0.4F	30.5	0.517	
GC3	0.750	0.230	0.214	0.252	0.447	2000	71F	19.5	0.330	
GC7	0.750	0.230	0.211	0.124	0.124	1250	1005	6.4	0.108	No SC
GC6A	0.750	0.230	0.215	0.161	0.161	1000	959	6.1	0.103	No SC
18Ni Maraging Steel (250 Grade) Aged at 900F										
Fusion Zone										
2WB10	0.750	0.288	0.210	0.258	-	5000	112F	51.2	0.782	Intergranular SC verified by fractography
2WB4	0.750	0.228	0.210	0.264	0.339	4000	189F	42.2	0.645	
2WB6	0.749	0.229	0.209	0.238	0.516	3000	104F	27.9	0.426	
2WB14	0.750	0.229	0.213	0.245	-	2000	936	18.9	0.289	No SC
2WB15	0.750	0.228	0.211	0.171	0.171	2000	936	13.0	0.198	No SC
Heat-Affected Zone - 2400F Peak Temp.										
GB29	0.750	0.230	0.211	0.240	-	8000	36.2F	74.3	0.617	
GB30	0.749	0.230	0.207	0.248	0.376	6000	792F	59.0	0.491	
GB32	0.749	0.230	0.209	0.242	0.261	5000	1006	47.4	0.394	
GB34	0.749	0.230	0.210	0.215	0.215	4000	959	32.8	0.273	No SC
GB33	0.749	0.230	0.210	0.217	0.217	3000	985	24.9	0.207	No SC

TABLE BIV (Cont'd)

SPEC NO	W (in)	B (in)	B_N (in)	a_o (in)	a_f (in)	P (lbs)	$t^{(1)}$ (hrs)	K_{Ii} (Ksi$\sqrt{in}$)	$\frac{K_{Ii}}{K_{Ix}}$	NOTES
18Ni Maraging Steel (250 Grade) Aged at 900F (Cont'd)										
Heat-Affected Zone - 1400F Peak Temp.										
GB19	0.749	0.230	0.211	0.247	0.304	8000	30F	77.2	0.799	
GB20	0.750	0.230	0.211	0.216	-	6000	192F	49.2	0.509	
GB24	0.749	0.230	0.209	0.223	-	5000	248F	42.9	0.443	
GB23	0.750	0.230	0.213	0.225	0.225	4000	959	34.1	0.349	No SC
GB21	0.750	0.230	0.216	0.170	0.170	5000	1052	31.7	0.328	No SC
GB22	0.749	0.231	0.211	0.227	0.227	3000	985	26.1	0.270	No SC
Heat-Affected Zone - 1200F Peak Temp.										
GB6	0.749	0.230	0.211	0.227	0.227	8000	941	69.6	0.593	Very local, small SC region
GB5	0.749	0.230	0.208	0.230	0.230	6000	982	53.6	0.457	No SC
GB7	0.750	0.230	0.212	0.228	0.228	5000	1052	43.5	0.370	No SC
AM355 SCT850 (Fully Hardened)										
Fusion Zone										
2WIG15	0.753	0.250	-	0.250	0.487	4000	532F	33.5	0.733	No intergranular SC verified fractographically-failure may be from H embrittlement
2WIG11	0.753	0.250	-	0.219	0.219	4000	1005	28.5	0.624	No SC
1WIG 5	0.753	0.250	-	0.226	0.226	3000	1007	22.2	0.486	No SC
1WIG8	0.753	0.250	-	0.274	0.274	2000	958	18.9	0.414	No SC
2WIG14	0.753	0.250	-	0.207	0.207	2000	958	13.4	0.294	No SC
Heat-Affected Zone - 2480F Peak Temp.										
GIG7	0.750	0.230	-	0.259	0.435	3000	11.3F	28.8	0.747	
GIG8	0.750	0.230	-	0.248	0.511	2000	85.6F	18.1	0.469	
GIG10	0.750	0.230	-	0.243	0.304	1000	1079	8.8	0.228	Local SC
GIG12	0.750	0.229	-	0.253	0.253	550	1003	5.1	0.132	No SC
Heat-Affected Zone - 2400F Peak Temp.										
GIG17	0.750	0.230	-	0.247	0.441	3000	33.8F	27.1	0.644	
GIG18	0.750	0.230	-	0.239	0.507	2000	119F	17.3	0.411	
GIG19	0.750	0.230	-	0.259	0.351	1000	1079	9.6	0.228	SC
GIG23	0.750	0.230	-	0.228	0.228	550	1003	4.5	0.107	Very small, local SC region
Heat-Affected Zone - 2000F Peak Temp.										
GIG27	0.750	0.230	-	0.263	0.507	3000	15.3F	23.3	0.569	
GIG28	0.750	0.230	-	0.254	0.550	2000	78.2F	18.7	0.363	
GIG31	0.750	0.230	-	0.248	0.328	1000	1006	9.1	0.177	
GIG33	0.750	0.230	-	0.242	0.242	550	1003	4.8	0.093	No SC

NOTE: (1) F after test time denotes failure of specimen.